

ON THE TURBULENT FLOW OF DILUTE POLYMER SOLUTIONS

Thesis by

Myles Walsh, III

In Partial Fulfillment of the Requirements

for the Degree of

Doctor of Philosophy

California Institute of Technology

Pasadena, California

1967

ACKNOWLEDGEMENTS

The author would like to express his gratitude to Dr. Paul J. Blatz for his continuous advice and encouragement. He would also like to thank Dr. J. W. Hoyt for suggesting the problem and for generously providing experimental data and facilities. Discussions with Dr. Philip G. Saffman were very useful in interpreting some of the results. The excellent handling of the manuscript and drawings is due to Mrs. Elizabeth Fox, whose patience is much appreciated.

The partial support of this research under Contract No. AF04(611)-9572 and Contract No. F-04611-67-C-0057 for the Air Force Rocket Propulsion Laboratory, Edwards Air Force Base, Edwards, California is gratefully acknowledged.

ABSTRACT

This paper is concerned with the problem of explaining the anomalous decrease in turbulent skin friction observed in the turbulent flow of very dilute polymer solutions.

The experimental evidence for dilute solutions is summarized.

The polymer molecule in solution is examined from a theoretical point of view, using the Rouse model. It is found that the model predicts that the molecule will locally store energy as a function of the local strain rate of the solution.

The experimental evidence is reexamined and it is concluded that the anomalous decrease in turbulent momentum transport results because the molecules manage to alter the energy balance of the small disturbances at the edge of the viscous sublayer. By slightly altering this balance the molecules allow viscous dissipation to destroy disturbances which would have had sufficient energy to grow had the molecules not been present. By decreasing the number of small disturbances which grow per unit area and time and move out from the edge of the viscous sublayer, the addition of polymer molecules ultimately changes the structure of the turbulence in the outer part of the boundary layer. This change results in lower Reynolds stresses and hence lower turbulent momentum transport.

With the help of the relation for local energy storage derived from the Rouse model, parameters are developed to characterize the phenomenon. These parameters appear to be useful in understanding the experimental evidence to date.

TABLE OF CONTENTS

PART	TITLE	PAGE
	ACKNOWLEDGEMENTS	ii
	ABSTRACT	iii
	TABLE OF CONTENTS	iv
I.	SUMMARY	
	I-1 Introduction	1
	I-2 Method of Approach	1
	I-3 Results	2
	I-4 Recommendations	2
II.	INTRODUCTION	
	II-1 Definition of a Dilute Solution	3
	II-2 The Problem	4
	II-3 Previous Experimental Investigations	6
	II-4 Previous Theoretical Investigations	19
	II-5 The Object of this Thesis	20
III.	THEORY OF ENERGY STORAGE AND DISSIPATION	
	III-1 Introduction - Some Definitions	22
	III-2 Rouse's Theory for Dissipation	23
	III-3 Extension of Rouse's Theory to Include Energy Storage	37
	III-4 Possible Mechanism for Degradation	44
	III-5 Qualitative Approach Using Dimensional Analysis	49
	III-6 Discussion of the Validity of the Results	51
	III-7 Qualitative Extension to Large Strain Rate	57

TABLE OF CONTENTS (Cont'd)

PART	TITLE	PAGE
IV.	EFFECT OF POLYMERS ON THE TURBULENT ENERGY BALANCE	
	IV-1 Introduction	60
	IV-2 A Constitutive Law - Two Assumptions	61
	IV-3 The Toms Effect: A Wall Phenomenon	64
	IV-4 A Qualitative Explanation	66
	IV-5 A Quantitative Explanation of the Toms Effect	68
	IV-6 An Estimate of H	72
V.	COMPARISON OF THEORY WITH EXPERIMENT	
	V-1 Discussion of Theory	78
	V-2 Comparison of Theory with Experiment	85
	V-3 Conclusion	92
VI.	LARGE H	
	VI-1 Discussion	94
	VI-2 A Law of the Wall for Large H	95
	VI-3 Velocity Defect Law	96
	VI-4 A Resistance Law for Large H	97
	VI-5 Comparison of Theory with Existing Data	100
VII.	THE TOMS EFFECT USING POLYELECTROLYTES	
	VII-1 An Experiment	107
VIII.	APPENDICES	
	A The Rouse Matrix	114
	B Solution of (42)	117

TABLE OF CONTENTS (Cont'd)

PART	TITLE	PAGE
C	Evaluation of P_m	122
D	Evaluation of $\Delta\bar{F}$	124
E	Autoxidation and Biological Degradation	125
REFERENCES		128

I. SUMMARY

I-1 Introduction

The reduction of turbulent skin-friction drag may very well represent the key to substantial improvements in the performance of our existing ships and submarines.

Experimentally it has been observed that the drag of bodies may be substantially reduced by injecting into the body's boundary layer small amounts of high-molecular-weight material. To date, this phenomenon has not been understood. No theory has been suggested which can predict this effect.

Thus, if one wishes to determine whether a dilute aqueous solution of locust bean gum will be effective in reducing the drag of a torpedo, one has first to mix a solution and then squirt this solution into the turbulent boundary layer of the rapidly moving torpedo. If the torpedo goes faster, then locust bean gum works. This practical approach to the problem is typical of much of the current research on drag reduction.

I-2 Method of Approach

In this thesis we have approached the problem from a different point of view. We have first summarized the existing experimental evidence relating to the behavior of dilute polymer solutions in turbulent flows. Then we take the existing theory for dilute polymer solutions and show that this theory implies that polymer molecules can locally store energy. Under certain restrictive conditions the magnitude of this energy may be exactly calculated. Thirdly, we

examine the experimental evidence and conclude that in order to explain the effect one must study the way in which the turbulence is generated. This conclusion differs somewhat from that of previous investigators. Fourthly, we perform an estimate of the magnitudes of the terms involved in the energy balance of the turbulence. From this estimate we develop parameters suitable for characterizing the observed effect. Then finally we demonstrate that this theory predicts the observed phenomena.

I-3 Results

This theory predicts not only if an additive will be effective, but also how much of an effect will take place. All one needs to know is the concentration and temperature of the solution at the edge of the viscous sublayer, the polymer's molecular weight and distribution, the turbulent wall stress expected, and the "intrinsic viscosity" of the solution.

Furthermore, this thesis sheds some light on the related problems of shear degradation in turbulent flows and the effect of wall conditions on the structure of wall turbulence.

I-4 Recommendations

It is suggested that careful experiments be performed using fractionated samples in an apparatus similar to that used by Shin (1965). The existing data is suggestive but more careful measurements are needed to really test this theory over a variety of Reynolds numbers and polymer solutions.

II. INTRODUCTION

II-1 Definition of a Dilute Solution

Staudinger (1930) was the first to characterize polymer solutions using viscosity measurements. Viscosity measurements are relatively easy to make and provide the experimenter with much useful information about the physics of polymer solutions.

Throughout this thesis references will be made to "the intrinsic viscosity" of a polymer solution. High-molecular-weight polymer molecules possess the ability to increase greatly the viscosity of the solvent in which they are dissolved. This is a manifestation of the voluminous character of randomly coiled long chain molecules. The intrinsic viscosity represents the capacity of a given polymer to enhance the viscosity of a solution. It is defined as:

$$[\eta] = \lim_{c \rightarrow 0} \left(\frac{\eta_s - \eta_o}{c \eta_o} \right) \quad (1)$$

where η_s is the viscosity of the solution, η_o is the viscosity of the solvent and c is the weight concentration of the solution.

By a "dilute solution" we mean that the polymer molecules may be considered to exist as long chains separated extensively from each other by pure solvent. We arbitrarily define a dilute solution as one for which the ratio of the total effective volume of the molecules to the total volume of the solution is less than one hundredth. It is assumed that polymer-polymer interaction and/or entanglement does not occur.

This is a restriction on the volume concentration of the

solution. In practice, one needs a restriction on the weight concentration of a solution. An estimate of the restriction on the weight concentration of a "dilute solution" may be made by noting that according to the Einstein viscosity relation (A. Einstein, 1906),

$$c[\eta] = 2.5\phi \quad (2)$$

Here ϕ is the small ratio of the total effective volume of the molecules to the total volume of the solution. Thus throughout this thesis we mean by a "dilute solution" a high-molecular-weight linear polymer solution for which

$$c[\eta] < 2.5 \times 10^{-2} \quad (3)$$

We consider solutions as concentrated when (3) does not hold.

For example, at 25°C an aqueous solution of poly(ethylene oxide) of six million molecular weight has an intrinsic viscosity of $2 \times 10^{-3} (\text{ppmw})^{-1}$. Thus an aqueous solution of this polymer with a concentration of only 100ppmw would by our definition be considered concentrated. A 10ppmw solution would be considered dilute.

II-2 The Problem

Measurements made over the last eighteen years indicate that turbulent momentum transport may be greatly decreased by the addition of minute quantities of high-molecular-weight polymer molecules to Newtonian solvents. This decrease in turbulent momentum transport at a given Reynolds number is customarily measured as a decrease in the turbulent skin coefficient.

Investigators have noted reductions in skin friction of as much as eighty percent for a great variety of wall turbulence experiments. Simultaneously no non-Newtonian effects have been observed for these same solutions in the wakes of grids and in the mean velocity profile of a round jet.

When dilute polymer solutions are tested in laminar flow by conventional viscometry it is noted that non-Newtonian fluid properties are not evident within the accuracy of the experiment. Further, if anything, the measured steady state viscosity of the solution actually increases. The density of these dilute solutions is, to many significant figures, identical with that of the solvents used.

Since hydrodynamicists normally regard density and viscosity as the only relevant properties of a fluid, it seems paradoxical that turbulent flows of dilute solutions can behave so differently from their solvents.

In the last eighteen years formidable mathematical talents have been employed in order to attempt to explain, even qualitatively, this paradox. Yet there has been little progress. The reason for this is evident. On one hand, the "simple" Newtonian turbulent boundary layer problem is many times older and yet it defies exact analysis. On the other hand, the properties of dilute polymer solutions are not well understood. Exact constitutive laws do not exist for these dilute solutions. Even if they did, they are likely to be very complicated and defy experimental checks. The combination of these two difficult problems is the problem under consideration.

Turbulent momentum transport in Newtonian fluids is primarily an inertial phenomenon. Thus once a turbulent motion is established, it is the large scale disturbances which determine the rate of momentum transport. These large scale disturbances, once formed, are relatively unaffected by the viscosity of the fluid.

The major problem inherent in explaining the paradox lies in reconciling two readily measurable facts, namely, momentum transport in wall turbulence is drastically reduced and this change is accomplished by only slightly changing the effective viscosity of the fluid, a quantity which, in itself, appears to play only a minor role in turbulent momentum transport.

II-3 Previous Experimental Investigations of the Turbulent Flow of Dilute Solutions

Toms (1948) appears to have been the first to quantitatively measure the anomalous behavior of dilute solutions in turbulent pipe flow. He measured the flow rates of solutions of poly(methylmethacrylate) in monochlorobenzene through a variety of straight tubes. These flow rates were plotted versus polymer concentration at different pressure gradients. The nature of the flow régime prevailing under particular conditions was found by a simple modification of Reynolds's color-filament experiment.

By carefully distinguishing between the laminar and turbulent flow régimes, Toms noted that the addition of polymer to monochlorobenzene always resulted in a decrease of flow rate in laminar

flow. However, in turbulent flow at a constant pressure gradient, the flow rate increased with polymer concentration up to a certain optimum concentration after which it started to gradually decrease.

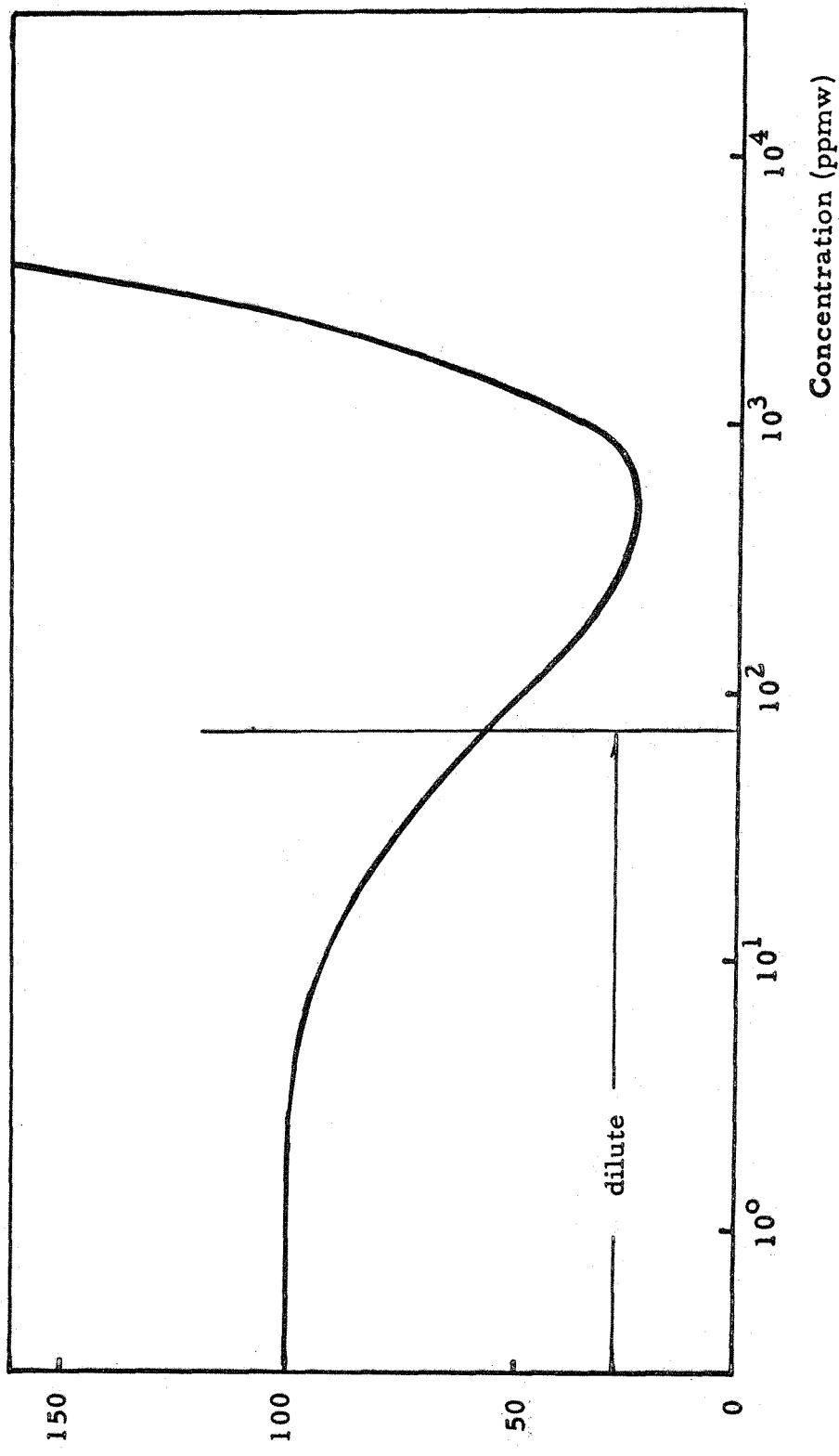
In recognition of Toms's pioneering research this anomalous behavior will in the rest of this thesis be referred to as "the Toms Effect".

Toms's remarkable result was not given the recognition it deserved until the Office of Naval Research became interested in the problem in 1962. With their assistance, scientists from a variety of fields have investigated the Toms Effect.

Since this thesis is primarily concerned with the behavior of dilute solutions, the notable work of Dodge and Metzner (1959), Shaver and Merrill (1959), Ripken and Pilch (1963), Savins (1964), and Metzner and Park (1964) will not be discussed. All of these scientists have performed turbulent pipe flow experiments with a variety of very concentrated solutions. In general, they have found that substantial reductions in wall stress are possible due to polymer addition until the increase in the "viscosity" of the solution gets so large that gains made due to the Toms Effect are lost again due to the higher dissipation of the solution. Thus if a solution is pumped through a pipe at constant turbulent flow rate and the pressure gradient required to maintain this flow rate measured and plotted versus concentration, then one finds a curve of the shape shown in Figure 1.

Most of the points shown in Figure 1 are for concentrated solutions. Thus the data in Figure 1 are of little interest to us. We assume that it is understood why the Toms Effect eventually

Pressure Drop Per Unit Length of Pipe at Constant Flow Rate



Typical Relationship Between Concentration and Turbulent Pressure Drop

Figure 1

disappears as the concentration is raised. We are primarily interested in how and why the Toms Effect arises; Shin's thesis (1965) is recommended for those interested in a full discussion of the disappearance of the Toms Effect.

Pruitt and Crawford (1963), Fabula (1963), and Hoyt and Fabula (1964) deserve much credit for calling attention to the fact that the Toms Effect can be observed (indeed, becomes most prominent) at polymer concentrations for which the solutions are truly dilute. They also demonstrated that the Toms Effect is not restricted to solutions of a few polymers in a few solvents. Rather the Toms Effect may be observed in any dilute polymer solution provided only the molecular weight of the polymer is large.

Of the many polymers they tried, they found that poly(ethylene oxide) manufactured commercially by Union Carbide under the trade name of Polyox produced the most striking results. Experimenters since 1964 have tended to use Polyox in preference to other polymers for this reason. Further since the U. S. Navy has supported most of the research on the Toms Effect, the solvent has tended to be water or sea water.

By 1965 it had become apparent to most investigators that the molecular parameters of the polymer samples being used, the concentration of the solution and, in some mysterious way, the wall stress are important parameters in the Toms Effect. It was further suspected by many that the Toms Effect might well be associated with wall turbulence.

Thus in 1965 Pruitt and Crawford published a report titled:

"Effect of Molecular Weight and Segmental Constitution on the Drag Reduction of Water Soluble Polymers". Despite the title, they never actually measured the molecular weights of the samples they used. Neither did they fractionate their samples to determine the effect of the molecular weight distribution on the Toms Effect. Thus most of their results must be considered to some extent preliminary and qualitative. The molecular weights they give are, with one exception, those given by the manufacturer.

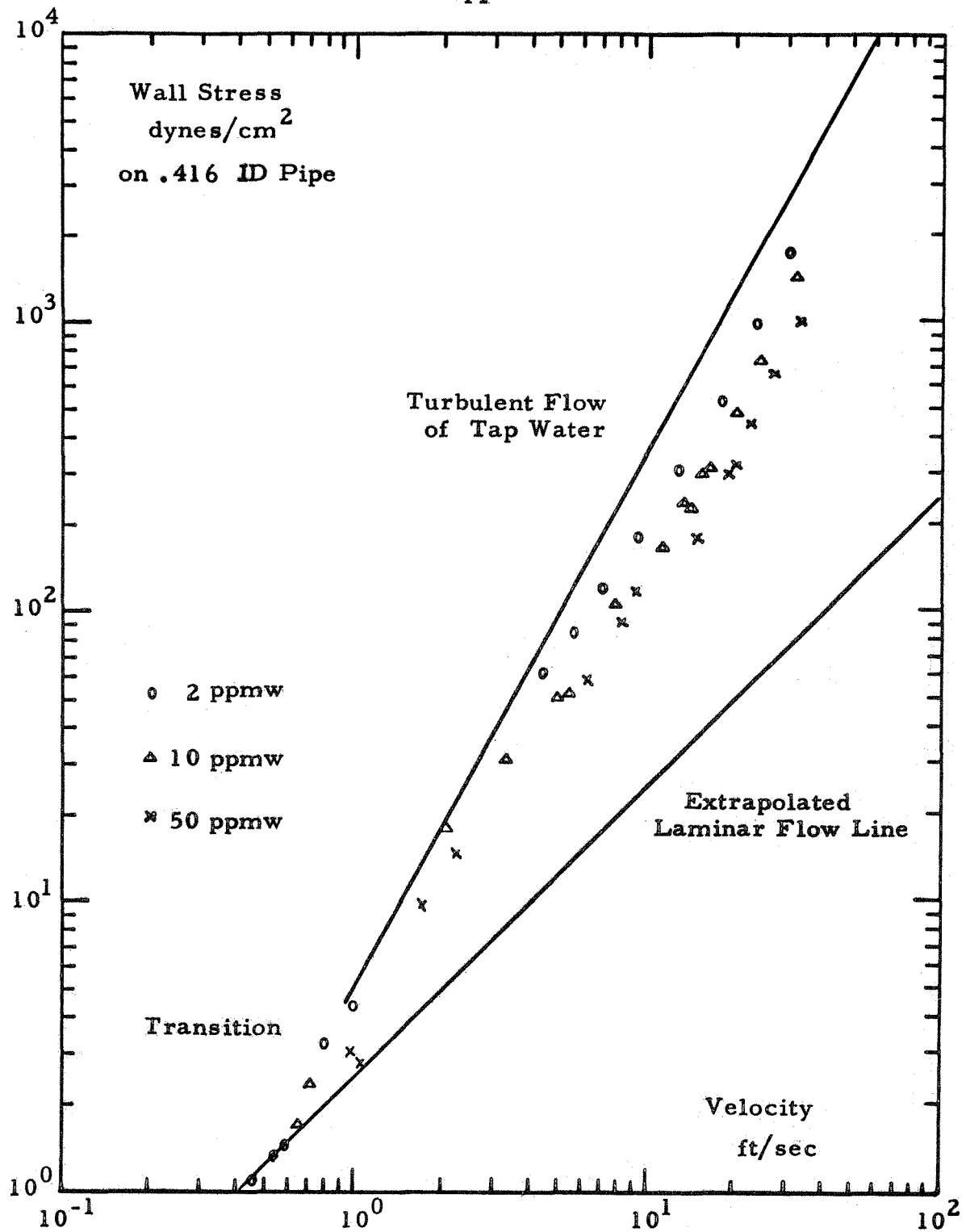
Their report includes pipe flow data on some 16 polymer samples. All of these were dissolved in tap water. A typical curve from this data is reproduced in Figure 2.

In Figure 2, the black line is the curve for the turbulent wall stress in a .416 inch ID smooth pipe due to the turbulent flow of tap water in that pipe. The circles represent the behavior of a 2 ppmw Polyox WSR-301. The solution behaves just like water until an "onset" wall stress, τ^* , of 60 dynes/cm^2 .

At this wall stress the Toms Effect begins to take place. As the wall stress becomes larger the Toms Effect appears to get larger up to a point. Then it appears to decrease again.

The triangles represent the behavior of a 10 ppmw solution of the same polymer. Once again an onset wall stress is observed, this time at about 15 dynes/cm^2 . As the wall stress becomes larger the Toms Effect appears to get larger up to a point. Then it appears to begin to disappear.

For a 50 ppmw solution, however, there appears to be no onset wall stress. In other words, transition and the Toms Effect



Flow Study of Solutions of 1.6 Million Molecular Weight Polyox

Pruitt and Crawford (1965), p. 41

Figure 2

take place simultaneously.

Pruitt and Crawford (1965) noted that the actual molecular weight of the sample "may have been less than one half the value" of four million given by the manufacturer. They base this statement on intrinsic viscosity data. Thus we assign a value of $1.6 \pm 1 \times 10^6$ to the sample of Polyox WSR-301 Pruitt and Crawford used.

For higher molecular weight Polyox at moderate wall stresses, Pruitt and Crawford (1965) observed substantial shear degradation of the molecules. By this it is meant that the results depended on the number of times the solutions are pumped through the pipe.

Many observers have noted this effect in turbulent flows of dilute polymer solutions. This effect is of some interest especially since it is customarily not observed in laminar flows. This effect will be treated in some detail in Chapter III. The important point here is that the results of the higher molecular weight material are suspect because the manufacturer's molecular weight may bear little relationship to the actual molecular weight of the polymer molecules in the experiment.

Table 1 presents a list of onset wall stresses for the two lowest molecular weights of the Polyox Pruitt and Crawford (1965) tested.

It should be noted that for a given sample, the product of the onset stress times the solution's concentration is approximately constant. This experimental result escaped Pruitt and Crawford. The far right hand column in Table 1 may be ignored for the present.

TABLE 1

Data for the Onset of the Toms Effect in Turbulent Pipe Flow from Pruitt and Crawford

Molecular Weight of Polyox Sample	Onset Stress in dynes/cm ²	Concentration of Solution in ppmw	H _{critical}
500,000	600	2	.017
500,000	120	10	.017
500,000	24	50	.017
1,600,000	60	2	.018
1,600,000	15	10	.022

The maximum reduction in wall stress possible would occur if laminar flow were maintained at all Reynolds numbers. In practice, the turbulent wall stress measured in the flow of a dilute solution, τ_s , at a given Reynolds number is somewhat greater than the extrapolated laminar wall stress, τ_l , but less than the turbulent wall stress measured in the flow of the solvent, τ_o . Thus as a measure of the effectiveness of an additive at a given Reynolds number we define "the percent approach to laminar flow", L, as:

$$L = \left(\frac{\tau_o - \tau_s}{\tau_o - \tau_l} \right) \times 100\% \quad (4)$$

constant Reynolds number

Metzner and Park (1963), Metzner and Park (1964), Pruitt and Crawford (1965), and Shin (1965) have all called this function by different symbols and names and have used it to quantitatively characterize the Toms Effect.

For a variety of polymers in water Pruitt and Crawford (1965) found that the maximum value of L that could be obtained was, within 5%, 80%. This remarkable result is apparently independent of polymer, pipe size or Reynolds number for a pipe flow Reynolds number range of 3,000 to 100,000. This result was also found independently by Hoyt and Fabula (1964).

Shin (1965) tested a variety of aqueous Polyox solutions and poly(isobutylene) solutions in a narrow-gap Couette viscometer. The outer cylinder was spun rapidly enough to insure fully developed turbulent flow. Torques on the inner cylinder were electronically measured and plotted versus time by a recorder.

Thus Shin (1965) was able to study the behavior of small volumes of dilute solution subjected to turbulent flow. By extrapolating the torque readings back to zero time and by using new sample solutions whenever appreciable mechanical degradation was suspected, Shin was able to eliminate the effects of mechanical degradation due to turbulent shear from his data.

Shin (1965) emphasized the great importance of molecular weight in his thesis. The molecular weights of the samples used were measured using light scattering techniques. Simultaneously, Shin measured the intrinsic viscosity of his samples.

He found that for aqueous Polyox solutions at 25°C

$$[\eta] = 1.03 \times 10^{-4} \overline{M}_w^{0.78} \text{ dl/gm} \quad (5)$$

and for poly(isobutylene), PIB, in cyclohexane at 25°C

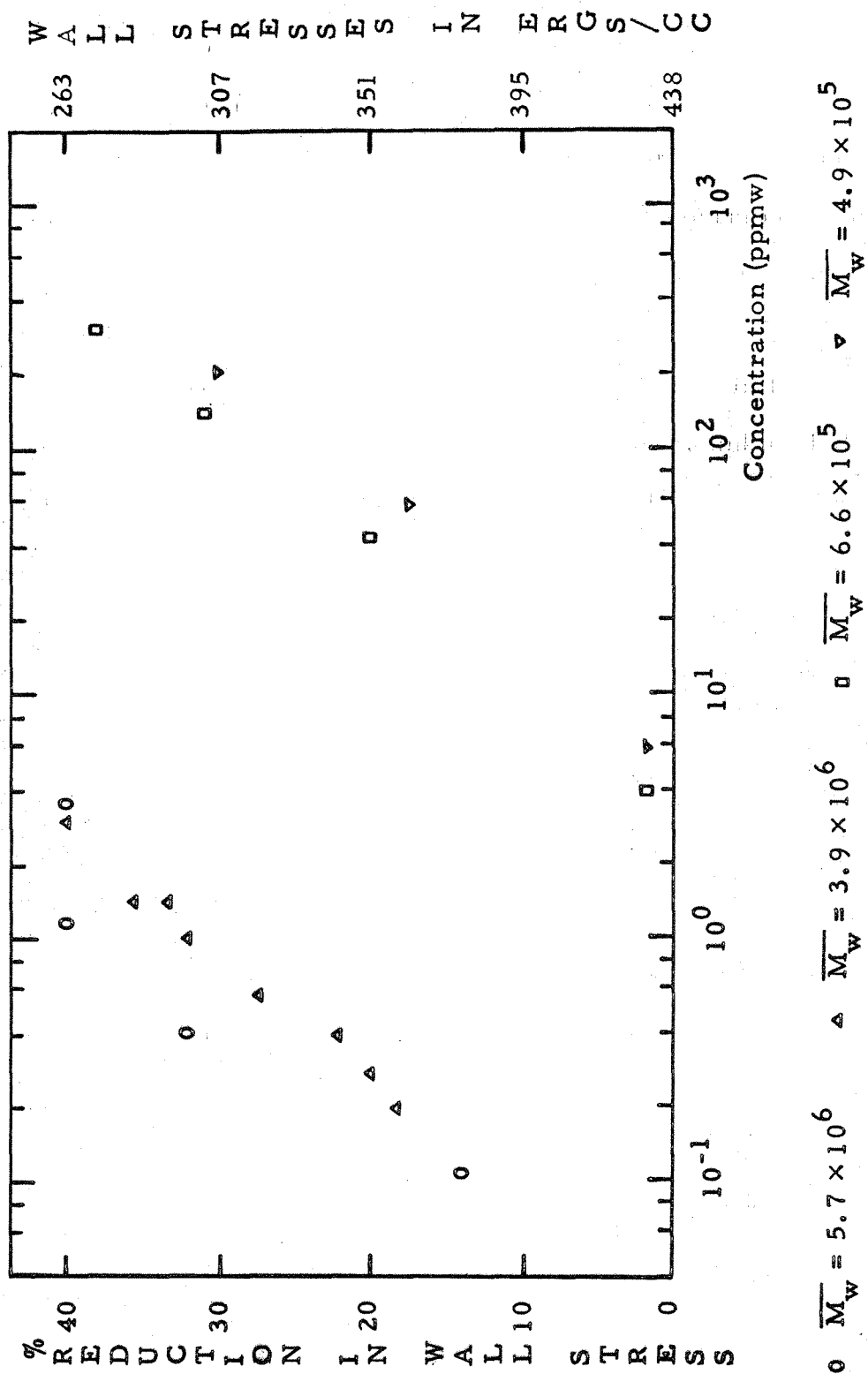
$$[\eta] = 2.65 \times 10^{-4} \overline{M}_w^{0.69} \text{ dl/gm.} \quad (6)$$

where \overline{M}_w is the weight average molecular weight of the sample.

These measurements agree well with previous investigations.

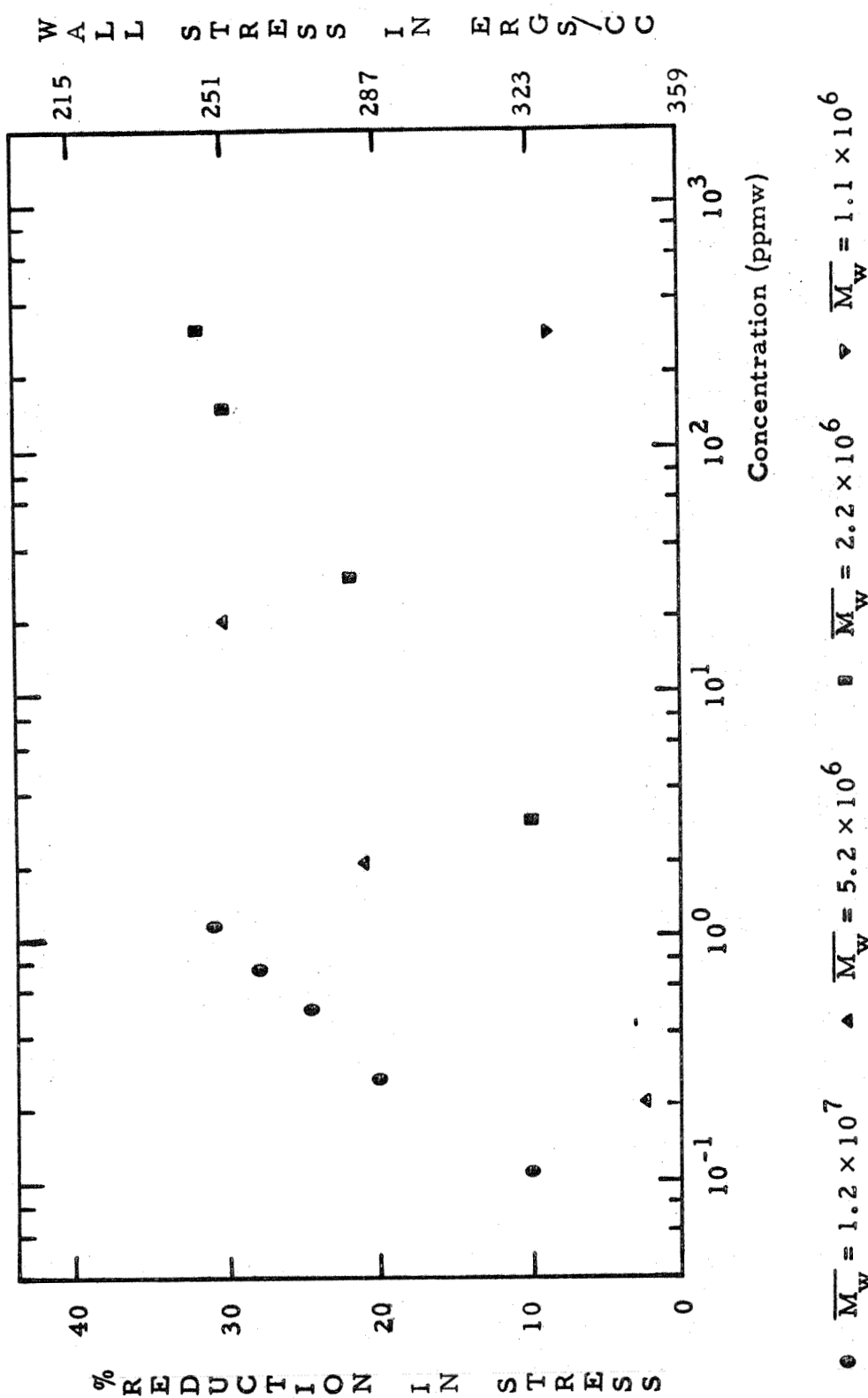
Shin (1965) was thus able to accurately characterize his solutions. His data represent a very significant contribution towards an understanding of the Toms Effect. His data are presented in Figures 3 and 4.

Figure 3 is a graph of the percent change in turbulent wall stress for four samples of undegraded, linear, unblended Polyox. The wall stress for the solution which would have been obtained had the flow remained laminar is 219 dynes/cm^2 .



Shin's Data for Four Polyox Samples in Water at 25°C

Figure 3



Shin's Data for Four PIB Samples in Cyclohexane at 25°C

Figure 4

Figure 4 shows Shin's data for percent reduction in wall stress plotted versus concentration for PIB of four different molecular weights dissolved in cyclohexane. The laminar wall stress is 222 dynes/cm².

Until May 1965 all published measurements of the Toms Effect had been made with wall turbulence. These experiments covered turbulent pipe flow, bodies moving through water, rotating disks and circular Couette flow.

Gadd (1965) appears to be the first to publish results for a free turbulent flow. Unfortunately he reported only the results of one experiment. He squirted a round jet of dyed solution out of a capillary tube into a tank of clear solution of the same strength. The solution used was a concentrated aqueous Polyox solution.

The resulting flow was photographed and compared with a similar jet of water into water. The Reynolds number based on the diameter of the capillary tube was 900. Gadd's photograph shows clearly that the stability of the jet is seriously altered by the molecules. However, it does not say anything about the turbulence.

Gadd's work was followed by that of Jackley (1966). Jackley studied the mean velocity profile of a free turbulent round jet growing in a large tank in order to determine whether the Toms Effect results from polymer molecules directly "damping the turbulence". Jackley found that when dilute aqueous polymer solution was pumped into similar stagnant solution, a mean velocity profile resulted which beyond ten diameters of the nozzle's mouth could not be distinguished from that of distilled water. Thus Jackley concluded that the Toms

Effect is "a phenomenon of the wall".

Fabula (1966) after an extensive and detailed investigation concluded from his measurements that for dilute solutions no measurable changes take place in the grid turbulence energy spectrum. For concentrated solutions ($c[\eta] = .27$), Fabula observed a depression in the spectral energy level at higher frequencies due to polymer addition. However, when the increase in viscosity due to addition is taken into account, Fabula found no evidence of non-Newtonian effects.

White (1966) has performed some unpublished experiments on the effect of high strain rate on the Toms Effect. These experiments are reported in some detail in Chapter VI.

II-4 Previous Theoretical Investigations of the Turbulent Flow of Dilute Solutions

Numerous attempts have been made to qualitatively explain the Toms Effect. However, all of these attempts with the possible exception of Tulin's work (1966) have been unsuccessful.

It is very easy with eighteen years of experimental evidence to find fault with explanations based on wall slip (Oldroyd, 1948), shear-thinning (Shaver and Merrill, 1959), a two-dimensional boundary-layer stability argument (Boggs and Tompisen, 1966), anisotropic viscosity (Merrill, 1965) or "the solvent-sequestering ball theory" (Shin, 1965). These must be looked on as theories which are not supported by the experimental evidence.

Unfortunately Tulin's work (1966) is available only in the

form of an abstract. It seems, however, that Tulin's approach is very similar to that taken in this thesis. He begins, as do we, by considering the mechanics of long, flexible, macromolecular chains in dilute solution. He calculates, as do we, the entropy and dissipation associated with the motions of the molecules. However, Tulin seems from his abstract to believe that it is necessary to go beyond small strains to produce changes in internal energy large enough to ultimately produce the Toms Effect. Apparently he was not aware of Shin's work. Further he appears to have used the Rouse theory in the high strain régime in order to calculate what he calls the "radiation damping". There is some reason to believe that the Rouse theory does not apply at high strain rate. Further, Tulin concludes that the Toms Effect varies quantitatively with the product, (concentration $\times \sqrt{\text{molecular weight}}$).

As Gadd (1966) points out, the explanation of the Toms Effect must be sought, not so much in the dissipation of turbulence, but rather in its generation. This realization is the only real theoretical progress that has been made since 1948.

II-5 The Object of this Thesis

The object of this thesis is threefold. First, the object is to develop a theory which will quantitatively predict the Toms Effect. This theory must in addition:

- i) Explain why an onset wall stress exists and predict its value for a given situation.
- ii) Explain why free turbulent flows are unaffected by polymer

addition.

iii) Develop parameters suitable for characterizing the Toms Effect.

Secondly, the object of this thesis is to explain why shear degradation takes place in turbulent, while it is customarily not observed in laminar flow.

It is the third and final object of this thesis to present data covering:

i) The turbulent pipe flow of dilute aqueous solutions of poly(methacrylic) acid at a variety of pHs, concentrations and two molecular weights.

ii) The effect of high strain rates on the Toms Effect.
(White, 1966).

III. THEORY OF ENERGY STORAGE AND DISSIPATION

III-1 Introduction - Some Definitions

In a dilute solution the polymer molecules may be considered to exist as long chains separated extensively from each other by pure solvent. Implied in the notion of a dilute solution is the assumption that the forces of attraction between the polymer and solvent are greater than those between polymer and polymer. Otherwise precipitation would occur.

A good solvent is one in which each polymer molecule tends to exclude all others from the volume which it occupies. If the solvent chosen for a given polymer becomes progressively poorer as the temperature is lowered, eventually a temperature may be reached where the polymer molecules distribute themselves over the volume like hypothetical point molecules which exert no forces on one another. This temperature is called the theta temperature. If the temperature is much below the theta temperature, precipitation occurs. It is customary to call solvents near the theta temperature, poor solvents.

A linear polymer chain consists of a series of monomer units connected together by valence bonds. The motion of one segment of the chain will ultimately affect the motions of the other segments. Any attempt to describe the allowable motions of the polymer chain in a dilute solution should take into account both intramolecular and intermolecular effects.

In order to take into account intermolecular effects, one

would need to know something about the forces of attraction between polymer and polymer and between polymer and solvent. Although much is known about this sort of thing, it is not convenient to analyze the situation in which the environment of a polymer chain comprises only solvent molecules. It is customary to assume that direct contacts of a segment of one molecule with segments of other molecules and with remotely connected segments of the same molecule merely contribute to the viscous force which opposes the thermal motions of the segment.

In order to exactly take into account the intramolecular forces influencing the motions of the chain, one would require knowledge about the exact nature of the bonding along the chain, the variation in the potential energy due to rotation about bonds, the effects of excluded volume and so forth. At the present time this exact problem is unsolved.

III-2 Rouse's Theory for a Dilute Polymer Solution

In 1953 Rouse (1953) proposed a theory of the linear visco-elastic properties of dilute polymer solutions. In Rouse's model of a polymer molecule short-range effects due to excluded volume, fixed bond angles, hindered rotation about bonds and so forth are not treated explicitly. Instead it is assumed that an analysis of these short-range effects has yielded the result that the fluctuations of the end-to-end length of a polymer molecule dissolved in a stagnant solvent are very nearly Gaussian.

This assumption results from very simple qualitative considerations. High-molecular-weight linear polymer molecules are

assumed to be many thousand times longer than they are thick and to be extremely flexible. Since in a stagnant solution no direction in space is preferred, the distribution function of the end-to-end distance, r , must be independent of any rotation of coordinate axes.

Thus the equilibrium distribution function, Ψ_0 , must be a function of r^2 . Let an orthogonal coordinate system be located at one end of the molecule and let r be specified in terms of the x -, y - and z -components of the other end of the molecule. Then $r^2 = x^2 + y^2 + z^2$.

The simplest assumption that can be made is that x , y and z are statistically independent. This, of course, is plausible only if r does not approach the full extended length of the chain. Since the molecule is extremely flexible, it is expected that full extension would be extremely unlikely and that, therefore, the assumption of statistical independence is a good one. The assumption of statistical independence and the realization that Ψ_0 is a function of r^2 together imply that Ψ_0 is a Gaussian distribution.

Rouse's contribution does not lie in his assumption that the end-to-end length of a polymer molecule in a stagnant solvent is very nearly Gaussian. This has been known for years. His contribution lies rather in his assumption that a polymer molecule may be divided into N equal submolecules. Each submolecule is a portion of the polymer chain just long enough so that, at equilibrium, the separation of its ends obeys, to a first approximation, a Gaussian probability function. This second assumption should be looked on as an assumption designed to replace the exact description of the polymer molecule by an approximate one which is readily amenable

to quantitative treatment. The validity of this assumption relies on the effective flexibility of the molecule. Since this cannot be directly determined, we can only measure the worth of this assumption by the agreement of what it predicts with experience.

Consider an ensemble of a very large number of isolated, independent systems, each consisting of one polymer molecule immersed in a volume V of solvent. It is understood that these systems represent molecules in different dynamical states. Each of these polymer molecules is considered to be made up of N equal, statistically identical submolecules joined in linear sequence, the ends of the submolecules being labeled 0, 1, 2, . . . , N .

We chose a fixed inertial system of Cartesian coordinates. The location of the j^{th} end in this system is denoted by the point (x_j, y_j, z_j) , where j equals 0, 1, 2, . . . , N .

The configuration of a polymer chain in any one dynamical state can now be represented by a single point in a $3N+3$ dimensional configuration space. By taking the number of systems in the ensemble large enough, the probability density or distribution function Ψ can be introduced so that, if a system is chosen at random from the ensemble, the probability that the configuration point representative of its dynamical state is in $dx_0 dy_0 dz_0 dx_1 \dots dz_N$ is $\Psi(x_0, \dots, z_N)$
 $dx_0 dy_0 dz_0 dx_1 \dots dz_N$.

Rouse's assumption that the separation of the ends of the submolecules at equilibrium obeys a Gaussian probability function implies that the equilibrium configuration distribution function Ψ_0 is:

$$(2\pi b^2)^{-3N/2} \exp \sum_{j=1}^N -\frac{(x_j - x_{j-1})^2 + (y_j - y_{j-1})^2 + (z_j - z_{j-1})^2}{2 b^2} \quad (7)$$

Here, the parameter b^2 is the mean square projected length of the submolecule.

This equilibrium distribution function represents the situation when the solution is not being deformed. The physical concept which is the basis of Rouse's theory is that a velocity gradient in the solution reduces the number of configurations available to the polymer molecule. The primary effect of the velocity gradient is to carry each segment of each molecule along with the liquid. This alters Ψ_0 to some new distribution Ψ . The molecules are not simply stretched out parallel to local streamlines because the coordinated Brownian motion of the submolecules tends to destroy this ordered state and return Ψ back to Ψ_0 , the distribution which maximizes the configurational entropy of the polymer chains.

In Rouse's theory the velocity gradient is thought of as an ordering process which is opposed by the Brownian motion of the submolecules, or a disordering process. The result of these two effects is a new distribution function Ψ . It is the purpose of Rouse's theory to calculate Ψ as a function of the local velocity field.

It has been assumed that all configurations have the same internal energy. Thus the increase in Helmholtz free energy due to the velocity gradient results only from changes in the configurational entropy. If the perturbed Helmholtz free energy is designated by F , then the increase is given by:

$$\begin{aligned}\Delta F &= F - F_o = +U - TS - U_o + TS_o \\ &= -TS + TS_o = -kT \ln(\Psi/\Psi_o)\end{aligned}\quad (8)$$

where $S = k \ln \Psi$.

The negative spatial gradient of ΔF represents the driving force tending to restore the system to equilibrium. This must be equal to the driving force which tends to throw the system out of equilibrium. The latter force is produced by the flow of solvent through the molecule.

Rouse assumed for simplicity that the viscous force on the whole length of the submolecule could be assumed to act only at the ends of the submolecule. He further assumed that, to a first approximation, the velocity field is not locally disturbed by the presence of the molecule. Let (u_j, v_j, w_j) be the velocity components of the solvent at (x_j, y_j, z_j) where both are referred to a fixed inertial system of Cartesian coordinates. $(\dot{x}_j, \dot{y}_j, \dot{z}_j)$ are the velocity components of the j^{th} end. $(u_j - \dot{x}_j, v_j - \dot{y}_j, w_j - \dot{z}_j)$ are the slip-velocity components. The viscous force driving the j^{th} end out of equilibrium is assumed to be linearly proportional to the local slip velocity.

Equating the viscous force to the force tending to restore the system to equilibrium produces in three directions:

$$f(u_j - \dot{x}_j) = -\frac{\partial \Delta F}{\partial x_j} = kT \frac{\partial}{\partial x_j} \ln\left(\frac{\Psi}{\Psi_o}\right) \quad (9)$$

$$f(v_j - \dot{y}_j) = -\frac{\partial \Delta F}{\partial y_j} = kT \frac{\partial}{\partial y_j} \ln\left(\frac{\Psi}{\Psi_o}\right) \quad (10)$$

$$f(w_j - \dot{z}_j) = -\frac{\partial \Delta F}{\partial z_j} = kT \frac{\partial}{\partial z_j} \ln\left(\frac{\Psi}{\Psi_o}\right) \quad (11)$$

Here f is an arbitrary constant, k is Boltzmann's constant, T is the temperature of the solution and $j = 0, 1, 2, \dots, N$. It is convenient to define a time τ such that:

$$\tau = fb^2/kT \quad (12)$$

Then (9), (10), and (11) may be rewritten:

$$\dot{x}_j = u_j - b^2/\tau \frac{\partial}{\partial x_j} \ln \left(\frac{\Psi}{\Psi_0} \right) \quad (13)$$

$$\dot{y}_j = v_j - b^2/\tau \frac{\partial}{\partial y_j} \ln \left(\frac{\Psi}{\Psi_0} \right) \quad (14)$$

$$\dot{z}_j = w_j - b^2/\tau \frac{\partial}{\partial z_j} \ln \left(\frac{\Psi}{\Psi_0} \right) \quad (15)$$

Polymer molecules are neither made nor destroyed. Thus continuity in configuration space requires that:

$$\frac{\partial \Psi}{\partial t} = - \sum_{j=0}^N \frac{\partial}{\partial x_j} (\dot{x}_j \Psi) + \frac{\partial}{\partial y_j} (\dot{y}_j \Psi) + \frac{\partial}{\partial z_j} (\dot{z}_j \Psi) \quad (16)$$

The problem of solving (16) for Ψ as a function of a given impressed velocity field (u_j, v_j, w_j) is, in general, very difficult. The rest of this section is devoted to developing a coordinate transformation which, for a special type of velocity field, transforms (16) to an equation which may be solved exactly. Rouse was never able to do this. The method used is essentially that of Blatz (1966).

The first transformation transforms the physical coordinates, (x_j, y_j, z_j) , to what are called the stretch coordinates, $(\lambda_j, \mu_j, \nu_j)$. We define:

$$\left. \begin{array}{l} \lambda_j = \frac{x_j - x_{j-1}}{b} \\ \mu_j = \frac{y_j - y_{j-1}}{b} \\ \nu_j = \frac{z_j - z_{j-1}}{b} \end{array} \right\} \quad 1 \leq j \leq N \quad (17)$$

and

$$\left. \begin{array}{l} \lambda_o = \sum_{j=0}^N \frac{x_i}{N+1} \\ \mu_o = \sum_{j=0}^N \frac{y_i}{N+1} \\ \nu_o = \sum_{j=0}^N \frac{z_i}{N+1} \end{array} \right\} \quad (18)$$

The vector $(\lambda_o, \mu_o, \nu_o)$ is proportional to the vector locating the center of mass of the molecule with respect to origin of the inertial frame. On the scale of the molecule (about 1000 Å) we assume that the velocity field may be approximated by

$$\begin{aligned} u_i &= \gamma_{11} x_i + \gamma_{12} y_i + \gamma_{13} z_i \\ v_i &= \gamma_{21} x_i + \gamma_{22} y_i + \gamma_{23} z_i \quad 0 \leq i \leq N \\ w_i &= \gamma_{31} x_i + \gamma_{32} y_i + \gamma_{33} z_i \end{aligned} \quad (19)$$

Here γ_{ij} is independent of the spatial coordinates but may depend on time. Since the impressed velocity field is assumed incompressible,

$$\gamma_{11} + \gamma_{22} + \gamma_{33} = 0 \quad (20)$$

On the scale of the molecule it is assumed that all velocity fields, be they laminar or turbulent, may be approximated by (19).

It is convenient at this point to define the Rouse matrix R as a $(N \times N)$ matrix such that

$$[R_{jk}] = \begin{bmatrix} 2 & -1 & 0 & \cdot & \cdot & \cdot & 0 & 0 \\ -1 & 2 & -1 & & & & 0 & 0 \\ 0 & -1 & 2 & & & & \cdot & \cdot \\ \cdot & \cdot & & & & & & \\ \cdot & \cdot & & & & & & \\ \cdot & \cdot & & & & & & \\ 0 & 0 & \cdot & \cdot & \cdot & \cdot & 2 & -1 \\ 0 & 0 & \cdot & \cdot & \cdot & \cdot & -1 & 2 \end{bmatrix} \quad (21)$$

Rouse originally pointed out that a coordinate transformation was at the heart of the problem of solving (16) and was the first to recognize the value of R . In order to see the relevance of R consider the equations of motion of the molecule in the x -direction, namely,

$$\dot{x}_j = u_j - \frac{b^2}{\tau} \frac{\partial}{\partial x_j} \ln \frac{\Psi}{\Psi_0} \quad (13)$$

First, the velocity components u_j are substituted into (13). From (19) this implies that

$$\dot{x}_j = \gamma_{11}x_j + \gamma_{12}y_j + \gamma_{13}z_j - \frac{b^2}{\tau} \frac{\partial}{\partial x_j} \ln \frac{\Psi}{\Psi_0}$$

$j = 0, 1, \dots, N$

Thus

$$\dot{x}_{j-1} = \gamma_{11}x_{j-1} + \gamma_{12}y_{j-1} + \gamma_{13}z_{j-1} - \frac{b^2}{\tau} \frac{\partial}{\partial x_{j-1}} \ln \frac{\Psi}{\Psi_0}$$

$$j = 1, 2, \dots, N$$

Subtracting the second equation from the first, dividing the result through by b and then substituting in the definitions of the stretch coordinates implies that (13) becomes

$$\dot{\lambda}_j = \gamma_{11}\lambda_j + \gamma_{12}\mu_j + \gamma_{13}\nu_j - \frac{b}{\tau} \left(\frac{\partial}{\partial x_j} - \frac{\partial}{\partial x_{j-1}} \right) \ln \frac{\Psi}{\Psi_0} \quad (22)$$

$$j = 1, 2, \dots, N$$

However, (17) and (18) imply that

$$b \frac{\partial}{\partial x_j} = \frac{1}{N+1} \frac{\partial}{\partial \lambda_0} + \frac{\partial}{\partial \lambda_j} - \frac{\partial}{\partial \lambda_{j+1}} \quad (23)$$

$$j = 1, 2, \dots, N-1$$

and

$$b \frac{\partial}{\partial x_0} = \frac{1}{N+1} \frac{\partial}{\partial \lambda_0} - \frac{\partial}{\partial \lambda_1} \quad (24)$$

$$b \frac{\partial}{\partial x_N} = \frac{1}{N+1} \frac{\partial}{\partial \lambda_0} + \frac{\partial}{\partial \lambda_N} \quad (25)$$

Thus

$$b \left(\frac{\partial}{\partial x_j} - \frac{\partial}{\partial x_{j-1}} \right) = R_{jk} \frac{\partial}{\partial \lambda_k} \quad (26)$$

Here R_{jk} are the coefficients of the Rouse matrix.

From this point forward we will assume that the usual summation convention holds. Thus the repeated subscripts in (26) are

to be summed from one to N. From now on, unless otherwise stated, the subscripts will always range from one to N.

The substitution of (26) into (22) implies that (in the stretch coordinates) (13) becomes

$$\left. \begin{aligned} \tau \dot{\lambda}_j &= \theta_{11} \lambda_j + \theta_{12} \mu_j + \theta_{13} \nu_j - R_{jk} \frac{\partial}{\partial \lambda_k} \ln \frac{\Psi}{\Psi_0} \\ \tau \dot{\lambda}_0 &= \theta_{11} \lambda_0 + \theta_{12} \mu_0 + \theta_{13} \nu_0 - \frac{\partial}{\partial \lambda_0} \ln \frac{\Psi}{\Psi_0} \end{aligned} \right\} \quad (27)$$

where

$$\theta_{ij} = \tau \gamma_{ij} \quad (28)$$

(i = 1, 2, 3 and j = 1, 2, 3)

(27) may be somewhat simplified by noting that from (7) and (17)

$$\ln \Psi_0 = -\frac{3N}{2} \ln 2\pi - \frac{1}{2} (\lambda_j^2 + \mu_j^2 + \nu_j^2) \quad (29)$$

Thus

$$\frac{\partial}{\partial \lambda_k} \ln \Psi_0 = -\lambda_k \quad (30)$$

Further,

$$\frac{\partial}{\partial \lambda_0} \ln \Psi_0 = \frac{\partial}{\partial \lambda_0} \ln \Psi = 0 \quad (31)$$

By virtue of our choice of velocity field the distribution function must be independent of the arbitrary origin of the inertial frame.

Thus Ψ cannot depend on λ_0 , μ_0 or ν_0 .

Thus (27) may be rewritten

$$\tau \dot{\lambda}_j = \theta_{11} \lambda_j + R_{jk} \lambda_k + \theta_{12} \mu_j + \theta_{13} \nu_j - R_{jk} \frac{\partial}{\partial \lambda_k} \ln \Psi \quad (32)$$

$$\tau \dot{\lambda}_o = \theta_{11} \lambda_o + \theta_{12} \mu_o + \theta_{13} \nu_o$$

Similar arguments may be applied to (14) and (15), the equations of motion for the molecule in the y- and z-directions. In terms of the stretch variables, (14) and (15) become:

$$\tau \dot{\mu}_j = \theta_{21} \lambda_j + \theta_{22} \mu_j + R_{jk} \mu_k + \theta_{23} \nu_j - R_{jk} \frac{\partial}{\partial \mu_k} \ln \Psi \quad (33)$$

$$\tau \dot{\mu}_o = \theta_{21} \lambda_o + \theta_{22} \mu_o + \theta_{23} \nu_o$$

and

$$\tau \dot{\nu}_j = \theta_{31} \lambda_j + \theta_{32} \mu_j + \theta_{33} \nu_j + R_{jk} \nu_k - R_{jk} \frac{\partial \ln \Psi}{\partial \nu_k} \quad (34)$$

$$\tau \dot{\nu}_o = \theta_{31} \lambda_o + \theta_{32} \mu_o + \theta_{33} \nu_o$$

Using (23), (24) and (25), (16) becomes in the stretch variables:

$$\begin{aligned} -\frac{\partial \Psi}{\partial t} = & \frac{\partial}{\partial \lambda_o} (\dot{\lambda}_o \Psi) + \frac{\partial}{\partial \mu_o} (\dot{\mu}_o \Psi) + \frac{\partial}{\partial \nu_o} (\dot{\nu}_o \Psi) \\ & + \frac{\partial}{\partial x_j} (\dot{\lambda}_j \Psi) + \frac{\partial}{\partial \mu_j} (\dot{\mu}_j \Psi) + \frac{\partial}{\partial \nu_j} (\dot{\nu}_j \Psi) \end{aligned} \quad (35)$$

The first three terms on the right hand side of (35) are associated with the position of the center of mass of the molecule in the inertial reference frame. Their sum is identically zero because of

the choice of velocity field.

Thus Ψ becomes a function of $3N$ stretch variables and time. The equation which must now be solved is (36), where (36) is formed by substituting (32), (33) and (34) into (35). (36) is shown on the next page. This equation is identical with Blatz's (1966) Equation 26.

A glance at (36) is sufficient to determine that a second transformation is necessary. The $3N$ stretch variables $(\lambda_j, \mu_j, \nu_j)$ must be transformed to the $3N$ set of variables $(\delta_j, \epsilon_j, \eta_j)$. These must be chosen such that R is diagonalized. δ_j, ϵ_j and η_j are called the diagonalizing variables. In order to choose them correctly, we examine the Rouse matrix in Appendix A.

In Appendix A we find that R has N distinct eigenvalues, e_k , where:

$$e_k = 4 \sin^2 \left(\frac{\pi k}{2(N+1)} \right) \quad (37)$$

Then we find the matrix A such that A is orthogonal and such that the coefficients of A , A_{jk} , satisfy the equation:

$$R_{ij} A_{jk} = e_k A_{ik}, \quad k \text{ not summed} \quad (38)$$

We find that:

$$A_{jk} = \sqrt{\frac{2}{N+1}} \sin \left(\frac{jk\pi}{N+1} \right) \quad (39)$$

We can now define the diagonalizing variables as

$$\left. \begin{aligned} \delta_j &= A_{jk}^T \lambda_k \\ \epsilon_j &= A_{jk}^T \mu_k \\ \eta_j &= A_{jk}^T \nu_k \end{aligned} \right\} \quad (40)$$

$$\begin{aligned}
 0 = \tau \frac{\partial \Psi}{\partial t} + \theta_{11} \frac{\partial \Psi}{\partial \lambda_j} \lambda_j + \theta_{12} \frac{\partial \Psi}{\partial \lambda_j} \mu_j + \theta_{13} \frac{\partial \Psi}{\partial \lambda_j} \nu_j - R_{jk} \frac{\partial^2 \Psi}{\partial \lambda_j \partial \lambda_k} - R_{jk} \frac{\partial \Psi}{\partial \lambda_j} \lambda_k - 6N\Psi \\
 + \theta_{21} \frac{\partial \Psi}{\partial \mu_j} \lambda_j + \theta_{22} \frac{\partial \Psi}{\partial \mu_j} \mu_j + \theta_{23} \frac{\partial \Psi}{\partial \mu_j} \nu_j - R_{jk} \frac{\partial^2 \Psi}{\partial \mu_j \partial \mu_k} - R_{jk} \frac{\partial \Psi}{\partial \mu_j} \lambda_k \\
 + \theta_{31} \frac{\partial \Psi}{\partial \nu_j} \lambda_j + \theta_{32} \frac{\partial \Psi}{\partial \nu_j} \mu_j + \theta_{33} \frac{\partial \Psi}{\partial \nu_j} \nu_j - R_{jk} \frac{\partial^2 \Psi}{\partial \nu_j \partial \nu_k} - R_{jk} \frac{\partial \Psi}{\partial \nu_j} \lambda_k
 \end{aligned} \tag{36}$$

$$\begin{aligned}
 0 = \tau \frac{\partial \Psi}{\partial t} + \theta_{11} \frac{\partial \Psi}{\partial \delta_j} \delta_j + \theta_{12} \frac{\partial \Psi}{\partial \delta_j} \epsilon_j + \theta_{13} \frac{\partial \Psi}{\partial \delta_j} \eta_j - \Sigma_j e_j \frac{\partial^2 \Psi}{\partial \delta_j \partial \delta_j} - \Sigma_j e_j \frac{\partial \Psi}{\partial \delta_j} \delta_j - 6N\Psi \\
 + \theta_{21} \frac{\partial \Psi}{\partial \epsilon_j} \delta_j + \theta_{22} \frac{\partial \Psi}{\partial \epsilon_j} \epsilon_j + \theta_{23} \frac{\partial \Psi}{\partial \epsilon_j} \eta_j - \Sigma_j e_j \frac{\partial^2 \Psi}{\partial \epsilon_j \partial \epsilon_j} - \Sigma_j e_j \frac{\partial \Psi}{\partial \epsilon_j} \epsilon_j \\
 + \theta_{31} \frac{\partial \Psi}{\partial \eta_j} \delta_j + \theta_{32} \frac{\partial \Psi}{\partial \eta_j} \epsilon_j + \theta_{33} \frac{\partial \Psi}{\partial \eta_j} \eta_j - \Sigma_j e_j \frac{\partial^2 \Psi}{\partial \eta_j \partial \eta_j} - \Sigma_j e_j \frac{\partial \Psi}{\partial \eta_j} \eta_j
 \end{aligned} \tag{42}$$

Here A_{jk}^T are the coefficients of the transpose of A , or, in this special case, of A .

Thus

$$\begin{aligned}\frac{\partial}{\partial \lambda_j} &= A_{jk} \frac{\partial}{\partial \delta_k} \\ \frac{\partial}{\partial \mu_j} &= A_{jk} \frac{\partial}{\partial \epsilon_k} \\ \frac{\partial}{\partial \nu_j} &= A_{jk} \frac{\partial}{\partial \eta_k}\end{aligned}\tag{41}$$

(40) and (41) may now be used to transform (36) from the stretch variables to the diagonalizing variables. Then noting that A is orthogonal and satisfies (38), (36) becomes in the new coordinate system (42).

This equation was solved approximately by Rouse by setting all but θ_{12} equal to zero and by assuming that Ψ could be expanded in a power series of θ_{12} times Ψ_0 . θ_{12} was assumed small. Rouse used his result to calculate the added dissipation resulting from polymer addition.

Pao (1962) and Zimm (1955) have attempted to somewhat modify Rouse's theory and have then solved equations similar to (42) using power series techniques. Neither mentions the energy storage in the polymer molecules due to the deformation of the solution.

Blatz (1966) appears to have been the first to solve (42) exactly for the special case of simple shear in which θ_{12} is the only non-zero component of θ_{ij} .

Using Blatz's method, the solutions of (42) are straightforward

but tedious. In an effort to emphasize the physics as distinguished from the mathematics of this problem, the two exact solutions used in the next two sections will merely be written down as trial solutions. These trial solutions can be then substituted into (42) and thus it can be proved that they satisfy (42) for the two velocity fields chosen.

Appendix B is recommended for readers interested in synthesizing their own solutions.

III-3 Extension of Rouse's Theory to Include Energy Storage

In order to verify that (42) produces the same results Rouse (1953) originally derived for small strain rate and to extend Rouse's results to large strain rate, we choose the flow field:

$$\gamma_{12} = \alpha_0 \cos \omega t \quad (43)$$

All of the other γ_{ij} are set equal to zero.

Rouse argued that physically this choice of flow field is equivalent to assuming that the molecules are being subjected to a sinusoidally oscillating linear plane strain field. Presumably this could be approximately created by applying a shearing stress to the solution with a plane surface lying in the plane $y = 0$ of a right-handed system of Cartesian coordinates. The surface executes simple harmonic motions in the x -direction with an angular frequency ω . The velocity gradient varies rapidly with y , the distance from the oscillating surface.

Despite this rapid variation, the molecules are small enough

(1000 Å across) so that for frequencies below 60 kc, the velocity gradient varies by less than five percent over the entire volume pervaded by the molecule. Thus (43) would appear to be a good local approximation for this experiment.

Substitution of (43) into (42) produces, with a bit of rearranging, (44). The trial solution for this equation will be (45). (44) and (45) are shown on the next page. Substitution of the trial solution (45) into (44) proves that this solution is, in fact, the correct one.

The viscoelastic properties of the solution may now be calculated.

The shearing stress which will produce a velocity gradient $v_{12} = \alpha_o \cos \omega t$ in a liquid with a complex viscosity $\eta^* = \eta_1 - \sqrt{-1} \eta_2$ is t^{12} , where

$$t^{12} = \alpha_o (\eta_1 \cos \omega t + \eta_2 \sin \omega t) \quad (49)$$

The rate at which work is done by the application of this shearing stress to a unit volume of solution is P where:

$$P = t^{12} \alpha_o \cos \omega t \quad (50)$$

$$= \alpha_o (\eta_1 \cos^2 \omega t + \eta_2 \sin \omega t \cos \omega t) \quad (51)$$

The rate at which work is done on a given molecule in the ensemble is the scalar product of the velocity of the solvent with respect to the center of mass of the molecule times the forces tending to restore each of the ends of the submolecules back to equilibrium. This rate of work, D , equals:

$$0 = \tau \frac{\partial \Psi}{\partial t} - \sum_{i=1}^N e_i \left(\frac{\partial \Psi}{\partial \delta_i} \delta_i + \frac{\partial \Psi}{\partial \epsilon_i} \epsilon_i + \frac{\partial \Psi}{\partial \eta_i} \eta_i + \frac{\partial^2 \Psi}{\partial \delta_i^2} + \frac{\partial^2 \Psi}{\partial \epsilon_i^2} + \frac{\partial^2 \Psi}{\partial \eta_i^2} \right) - 6N\Psi + \sum_{i=1}^N \tau \alpha_o \cos \omega t \frac{\partial \Psi}{\partial \delta_i} \epsilon_i \quad (44)$$

$$\Psi = \frac{-3N}{2} \prod_{i=1}^N \kappa_i \exp - \frac{1}{2} (\kappa_i^2 [\delta_i - \nu_i \epsilon_i]^2 + \epsilon_i^2 + \eta_i^2) \quad (45)$$

where

$$\frac{1}{\kappa_i^2} = 1 + \frac{(\tau_i \alpha_o)^2 [\cos^2 \omega t + 2(\omega \tau_i) \sin 2\omega t + (\omega \tau_i)^2 [\frac{1}{2} + 5 \sin^2 \omega t - \sin \omega t \cos \omega t]]}{(1 + 4(\omega \tau_i)^2 (1 + (\omega \tau_i)^2)^2} \quad (46)$$

$$\nu_i = \frac{(\tau_i \alpha_o) [(\omega \tau_i) \sin \omega t + \cos \omega t]}{1 + (\omega \tau_i)^2} \quad (i \text{ not summed}) \quad (47)$$

$$\tau_i = \tau / 2e_i = \text{retardation times of the molecule} \quad (48)$$

$$D = \alpha_o \cos \omega t kT \mu_i \frac{\partial}{\partial \lambda_i} \ln \frac{\psi}{\psi_o} \quad (52)$$

or using (40) and (41):

$$D = \alpha_o kT \cos \omega t \epsilon_i \frac{\partial}{\partial \delta_i} \ln \frac{\psi}{\psi_o} \quad (53)$$

The ensemble average of D times the number of molecules per unit volume, n , is what Rouse calls P_m , or the average power absorbed by the molecules per unit volume of solution. Thus

$$P_m = n \bar{D} = nkT \alpha_o \cos \omega t \prod_{j=1}^N \int_{-\infty}^{\infty} \int_{-\infty}^{\infty} \int_{-\infty}^{\infty} \psi \epsilon_i \frac{\partial}{\partial \delta_i} \ln \frac{\psi}{\psi_o} d\delta_j d\epsilon_j d\eta_j \quad (54)$$

With the use of (45) and (29) this integral may be exactly evaluated.

This is done in Appendix C. The result is that:

$$P_m = \alpha_o^2 nkT \sum_{i=1}^N \frac{\tau_i (\cos^2 \omega t + \tau_i \omega \sin \omega t \cos \omega t)}{1 + (\omega \tau_i)^2} \quad (55)$$

This result is exactly equal to Rouse's (1953) equation for P_m . Because of the method Rouse uses to calculate ψ , he assumes that (55) is limited to small values of $\tau \alpha_o \cos \omega t$. In fact, he specifically qualifies his result by stating that "terms containing powers of α higher than the second have been disregarded". Since (55), as derived here, does not depend on any restrictions on the magnitude of $\alpha_o \cos \omega t$, Rouse's qualification is unnecessary. (55) may be regarded as a general result of the Rouse model, valid at large values of $\alpha_o \cos \omega t$. The validity of the Rouse model at high strain rate may be debated. However, our result shows that if weaknesses are present, they arise from the model rather than from the mathematics.

Adding (55) to the energy input into the solvent,

$$P_s = \eta_o \alpha_o^2 \cos^2 \omega t$$

and comparing the result with (51) shows that:

$$\eta_1 = \eta_o + nkT \sum_{i=1}^N \tau_i / 1 + \omega^2 \tau_i^2 \quad (56)$$

$$\eta_2 = nkT \sum_{i=1}^N \omega \tau_i^2 / 1 + \omega^2 \tau_i^2 \quad (57)$$

where η_o is the viscosity of the solvent. (56) and (57) are identical to Rouse's (1953) (29b) and (29d).

Consider now the case for which $\omega = 0$. This is the case for steady flow. (57) indicates that η_2 equals zero. The addition of polymer molecules to a solvent increases the viscosity of the solvent by an amount $\Delta\eta$ where:

$$\Delta\eta = nkT \sum_{i=1}^N \tau_i \quad (58)$$

With the use of (48) and (37) this becomes:

$$\Delta\eta = \frac{cRT}{M} \sum_{i=1}^N \tau / 8 \sin^2(\pi i / 2N + 2) \quad (59)$$

Here c is the weight concentration of the solution and M is the molecular weight of the polymer sample.

N is typically larger than one hundred. Thus for small values of i , the sine is excellently approximated by its argument. For larger values of i the terms in the sum are negligible anyway. Thus to a good approximation,

$$\Delta\eta = \frac{cRT\tau(N+1)^2}{2\pi^2} \sum_{i=1}^N i^{-2} \quad (60)$$

or summing,

$$\Delta\eta = \frac{cRT(N+1)^2\tau}{12M} \quad (61)$$

The intrinsic viscosity is directly accessible from experimental data. It is defined as

$$[\eta] = \lim_{c \rightarrow 0} \frac{\Delta\eta}{c\eta_0}$$

which using (61) becomes

$$[\eta] = \frac{RT(N+1)^2\tau}{12M\eta_0} \quad (62)$$

Thus

$$\tau(N+1)^2 = 12\eta_0 M[\eta]/RT \quad (63)$$

(63) is the simplest way in which the parameters in the Rouse model, τ and N , may be related to the readily measurable quantities, M , T and $[\eta]$. It is a well-known and very useful result.

The energy stored by the polymer molecules can finally be calculated. The Helmholtz free energy for a given molecule in the ensemble is assuming the internal energy is constant

$$F = -kT \ln \psi + U_0 \quad (64)$$

The average molecule in the ensemble thus has an average energy corresponding to

$$F = -kT \int_V \psi \ln \psi dV + U_0 \quad (65)$$

where V is the configuration volume. With the use of (45) this integral may be exactly evaluated. This is done in Appendix D. The energy stored by altering the average configurational entropy of the average molecule is thus

$$\overline{\Delta F} = \overline{F} - \overline{F}_0 \quad (66)$$

$$= \frac{kT}{2} \sum_{i=1}^N \ln \kappa_i^{-2} \quad (67)$$

κ_i^{-2} is defined in (46). The energy stored per unit volume by the polymer molecules is thus W where

$$W = \frac{cRT}{2M} \sum_{i=1}^N \ln \kappa_i^{-2} \quad (68)$$

(68) is a new result. Rouse and his followers were primarily interested in the dissipation produced by polymer addition. Thus Rouse, Bueche, Zimm and Pao do not calculate the energy storage arising from the configurational entropy reduction in the flow of dilute solutions. (68) is fundamental for an understanding of the Toms Effect. This will be discussed at some length in the next chapter.

The energy stored by the polymer molecules has been calculated by assuming that the internal energy of a polymer molecule is independent of the particular configuration the molecule happens to adopt. This assumption is based on the results of numerous experiments performed over the last 162 years. Treloar (1958)

gives a full account of the evidence supporting this assumption and shows that for high-polymers subjected to extensions not exceeding 230 per cent of the undeformed length, this assumption is an excellent one.

This assumption combines with the first and second laws of thermodynamics to imply that the infinitesimal and reversible deformation of high polymers involves a reversible transformation of work into heat.

The work done by the fluid in stretching the polymer molecules out along streamlines is stored as heat in the solvent. If the velocity gradient decreases, the thermal agitations of the solvent surrounding the polymer molecules cause the polymer molecules to return to the more coiled, thus shortened, form. As the molecules contract they do work on the fluid. For infinitesimal, reversible changes, the change in heat content of the solvent must exactly equal the work done by the molecules.

In a real sense, the energy stored due to the rate of deformation of the polymer solution is stored not in the polymer molecules, but rather in the solvent as heat.

III-4 Possible Mechanism for Degradation

On the scale of the molecule (1000 Å) it seems unlikely that there is any inherent difference between unsteady laminar flows and turbulent flows. The current laminar flow data (Merrill et al. 1962)

indicates that changes in the molecular weight of the polymer are relatively slight and do not seem to follow a pattern that would be expected if scission were occurring. On the other hand, when these same solutions are placed in bottles and shaken, i.e., placed in a turbulent flow, the molecular weight as estimated by intrinsic viscosity measurements appears to drop with time to a given plateau value for a given level of agitation. This plateau value does not appear to depend on the initial molecular weight of the sample used.

This apparent degradation appears to take place to some extent in all turbulent flows of dilute solutions. The explanation of this effect may lie in the fact that most conventional laminar flow experiments do not contain velocity fields of the form shown in (69).

$$\left. \begin{array}{l} u = \gamma_n x/2 \\ v = -\gamma_n y \\ w = \gamma_n z/2 \end{array} \right\} \quad (69)$$

Here γ_n is a constant.

The flow field defined by (69) will exist locally in turbulent flows for times much longer than τ over lengths large compared with the size of the molecule. Physically local regimes of the type shown in (69) exist due to the relative motion of one element of fluid towards another or the motion of an element of fluid towards a wall.

For this simple flow field (42) becomes (70). The trial solution for (70) will be (71). (70) and (71) are shown on the next page. Substitution of the trial solution (71) into (70) proves that this solution is, in fact, the correct one.

$$0 = \sum_{i=1}^N e_i \left[(1-\theta_i) \frac{\partial \Psi}{\partial \delta_i} \delta_i + (1+2\theta_i) \frac{\partial \Psi}{\partial \epsilon_i} \epsilon_i + (1-\theta_i) \frac{\partial \Psi}{\partial \eta_i} \eta_i + \frac{\partial^2 \Psi}{\partial \delta_i^2} + \frac{\partial^2 \Psi}{\partial \epsilon_i^2} + \frac{\partial^2 \Psi}{\partial \eta_i^2} \right] + 6N\Psi \quad (70)$$

$$\Psi = (2\pi)^{-\frac{3N}{2}} \prod_{i=1}^N (1-\theta_i)^{\frac{1}{2}} (1+2\theta_i)^{\frac{1}{2}} \exp^{-\frac{1}{2}[(1-\theta_i)\delta_i^2 + (1+2\theta_i)\epsilon_i^2 + (1-\theta_i)\eta_i^2]} \quad (71)$$

where

$$\theta_i = \frac{\tau_i \gamma_n}{2e_i} = \tau_i \gamma_n \quad (72)$$

The mean internal energy stored by a polymer molecule subjected to this flow field may be directly calculated using (65). Integration produces the result that

$$\bar{F}/kT = 3N/2 (1 + \ln 2\pi) + 1/2 \sum_{i=1}^N \ln\left(\frac{1}{1-\theta_i}\right)^2 \left(\frac{1}{1+2\theta_i}\right) \quad (73)$$

Obviously as the largest θ_i , θ_1 , approaches one, \bar{F} grows without bound.

Physically the flow field chosen corresponds to the case of two steady "jets" of solution flowing in from plus and minus y-infinity. The jets meet at the origin and flow out along the x- and z-axes. In this type of flow field, it is expected that the polymer molecules would be stretched in planes perpendicular to the y-axis. This stretching will produce a tension along the length of the molecule. This tension will be applied for long times and as the molecules extended length increases, this tension will increase. If this tension is large enough and acts long enough, the probability of breaking bonds in the central part of the chain will become close to one. In the Rouse model there is no way of estimating the force necessary to break the molecular chain. However, if the chain is going to break, it should take place when the molecule begins to become fully extended, or when the energy \bar{F} starts to become infinite. (73) suggests that this takes place when

$$\theta_1 = \frac{\tau \gamma_n}{2e_1} = \frac{\tau \gamma_n}{8 \sin^2(\pi/2N+2)} = \frac{\gamma_n \tau (N+1)^2}{2\pi^2} \rightarrow 1 \quad (74)$$

With the use of (63), (74) implies that the critical strain rate required

to break the molecules up should be γ_n^* where:

$$\gamma_n^* = \frac{\pi^2 R T}{6[\eta] \eta_0 M} \quad (75)$$

Merrill et al. (1962) have suggested that the "rate of change of shear stress" is the more important variable in determining whether molecular scission will occur rather than steady shear stress. The preceding analysis suggests that Merrill et al. (1962) may not be quite correct. The degradation appears to result from a steady flow field of a certain type not customarily found in laminar flows.

A check on this theory could be accomplished by setting up two opposing jets of dilute polymer solution. This would partially simulate the flow field under consideration. The intrinsic viscosity of the solution leaving the impact point could be plotted versus γ_n and γ_n steadily increased. It would be expected that the intrinsic viscosity of the solution would begin to drop when γ_n reached the critical value shown in (75).

III-5 Qualitative Approach Using Dimensional Analysis

The preceding discussion of energy storage by polymer molecules has concentrated on applying a rather formidable mathematical theory to a rather idealized model. There is a tendency in this discussion to lose sight of the physics of the situation. Therefore, it is physically instructive to note that the basic assumptions involved in this theory may be used to derive a linearized version of (68) using nothing more sophisticated than dimensional analysis.

For the case of a locally steady shear flow $\omega = 0$ and κ_i^{-2} becomes, using (46):

$$\kappa_i^{-2} = 1 + (\tau_i \alpha_o)^2 \quad (i \text{ not summed}) \quad (76)$$

Thus the energy per unit volume stored by the molecules is using (68):

$$W = \frac{cRT}{2M} \sum_{i=1}^N \ln (1 + (\tau_i \alpha_o)^2) \quad (77)$$

For the case where $\tau_i \alpha_o$ is less than one, (77) may be approximated by (78) where:

$$W = \frac{cRT}{8M} \sum_{i=1}^N \left(\frac{\tau \alpha_o}{e_i} \right)^2 \quad (78)$$

Recalling that the eigenvalues of the Rouse matrix are e_i where:

$$e_i = 4 \sin^2 \left(\frac{\pi i}{2N+2} \right) \quad (37)$$

we note that most of the energy stored will come from the contributions of the first few eigenvalues. Thus approximating e_i by:

$$e_i = \frac{\pi^2 i^2}{(N+1)^2} \quad (79)$$

substituting this into (78) and summing, assuming N is large, produces:

$$W = \frac{cRT(\tau \alpha_o)^2 (N+1)^4}{720M} \quad (80)$$

which using (63) becomes:

$$W = \left(\frac{c M[\eta]^2 \eta_o^2}{5RT} \right) \alpha_o^2 \quad (81)$$

Now examine the problem of energy storage from a physical

point of view. Assume that a small number of molecules are added to a solvent and that they dissolve so that they are homogeneously distributed in the solvent. If the solvent is at rest the energy of these molecules per unit volume will be a function of nkT , where n is the number of molecules per unit volume, k is Boltzmann's constant and T is the temperature of the solution.

Now subject a small volume of this fluid to a strain rate α_0 . The forces produced by the interaction of the molecular coils with the solvent do work on the solvent and provide an additional mechanism for energy dissipation. This will on a macroscopic scale be measured as an increase in the viscosity of the solvent. Call this change in viscosity $\Delta\eta$.

The interaction forces also do work on the molecular coils by tending to stretch the molecules out along streamlines. This work is the energy stored in the molecules due to α_0 . The energy stored in the molecules is a function of the strain in the molecules. The strain in the molecules is a function of the forces applied to the molecules. The forces are a function only of α_0 , $\Delta\eta$ and nkT . Thus the energy stored in the molecules per unit volume, W , is only a function of α_0 , $\Delta\eta$ and nkT . By dimensional analysis,

$$\frac{W}{nkT} = f \left(\frac{\alpha_0 \Delta\eta}{nkT} \right) \quad (82)$$

This function f is, in general, unknown. However, for the special case of small α_0 , it is customary to assume that high-molecular-weight polymers deform as Hookean springs. In Rouse's model this assumption is equivalent to assuming that the separation

of the ends of the submolecule obeys a Gaussian probability function.

It is also customary to assume that the local viscous forces on the molecule are directly proportional to the relative motions of sections of the molecule and the solvent. In the Rouse model this justifies the force balance in the three directions as represented by (9), (10) and (11).

Since Hookean springs store energy as their strain squared, these molecules store energy as their strain squared, or as the local forces squared or as the local fluid strain rate squared. This result combines with (82) to produce

$$W \propto \frac{\alpha_o^2 \Delta\eta^2}{nkT} \quad (83)$$

which is, rearranging terms,

$$W \propto \left(\frac{\Delta\eta}{c\eta_o} \right)^2 \left(\frac{c^2 \eta_o^2 M}{cRT} \right) \alpha_o^2 \quad (84)$$

which for dilute solutions becomes:

$$W \propto \frac{c M[\eta]^2 \eta_o^2}{RT} \alpha_o^2 \quad (85)$$

This result is exactly the same as (81), the result from Rouse's theory derived under the same assumptions. The proportionality constant is, of course, not determined by this qualitative approach.

III-6 Discussion of the Validity of the Results

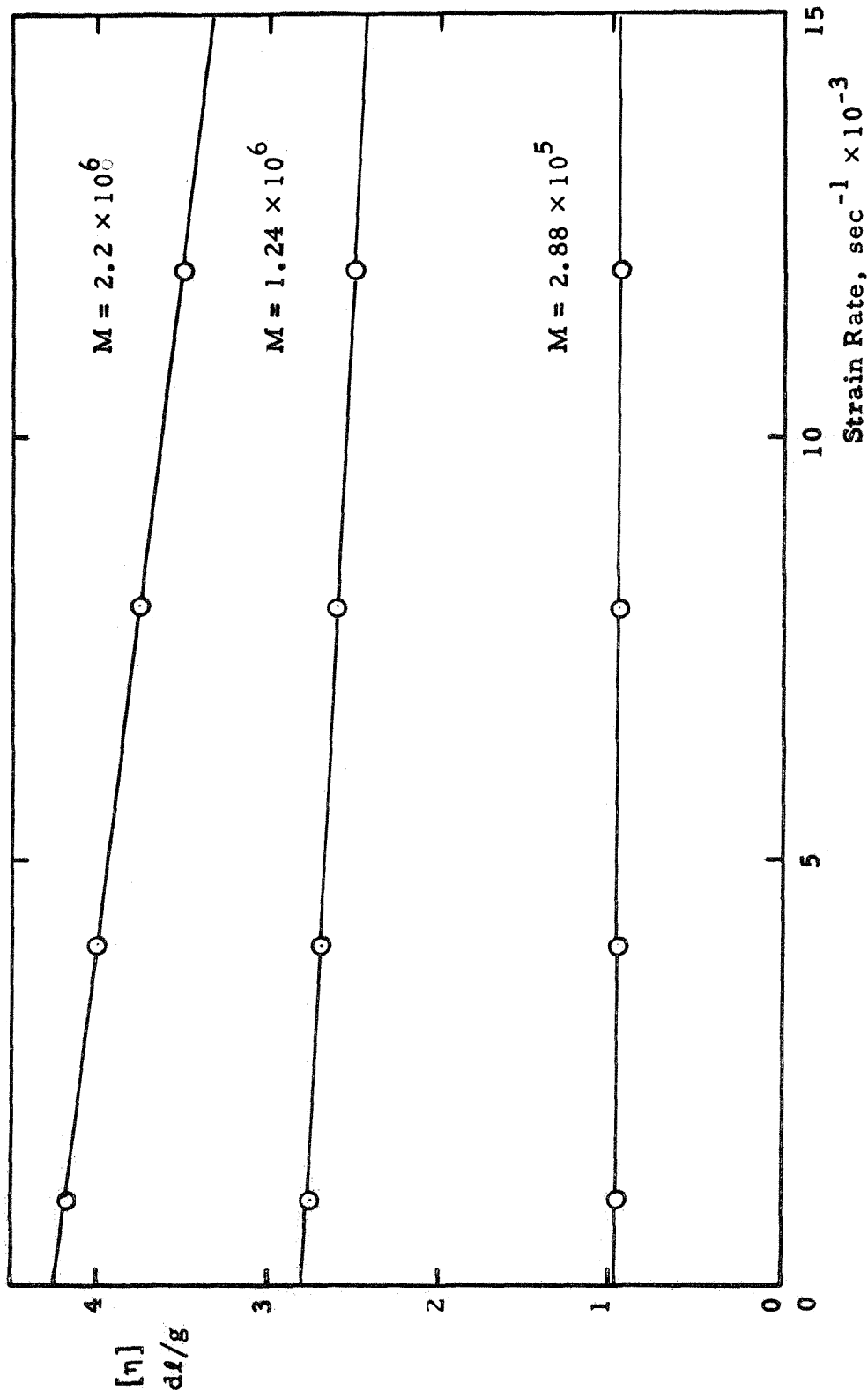
Rouse's theory for the energy dissipated by a dilute polymer solution was quickly followed by measurements (Rouse and Sittel,

1953) of the viscoelastic properties of dilute solutions of polystyrene in toluene and of polyisobutylene in various solvents. The measurements were made at frequencies ranging from 220 cycles up to 60 kc. Excellent agreement was obtained between theory and experiment. Since Rouse's theoretical results as represented by (56), (57) and (63) contain no adjustable constants, this theory provides a good first approximation to the viscoelastic properties of dilute solutions of polymers in good solvents.

We have shown that the Rouse model predicts that the intrinsic viscosity should be independent of α_0 regardless of α_0 . Figure 5 presents typical data for polystyrene fractions in toluene. It is clear from Figure 5 that for low molecular weight material the Rouse model is adequate. For high molecular weights, however, there seems to be a problem. The theory does not predict the observed dependence of intrinsic viscosity on strain rate.

Zimm (1956) attempted to modify Rouse's model to include the effects of hydrodynamic interactions. However, his calculated intrinsic viscosity also does not depend on α_0 . He attributed this discrepancy to a defect in the Rouse model.

Others have attempted to clarify this problem. Considerable controversy has centered on determining the exact defect in the Rouse model. The reader is referred to the work of Takamura (1958), Peterlin and Copic (1956), Cerf (1959) and Pao (1962). In order to get some physical insight into this problem, we consider the simplest possible non-trivial flow field, namely, the case in the first exact solution where $\omega = 0$.



Intrinsic Viscosity vs Strain Rate for 3 Different Polystyrene Fractions in Toluene at 25°C

Sharman, Sones and Cragg (1953), p. 708

Figure 5

In the diagonalizing coordinates, (13), (14) and (15) become with this choice of flow field (86), (87) and (88) where:

$$\tau \dot{\delta}_i = \tau \alpha_o \epsilon_i - e_i \frac{\partial}{\partial \delta_i} \ln \left(\frac{\psi}{\psi_o} \right) \quad (86)$$

$$\tau \dot{\epsilon}_i = -e_i \frac{\partial}{\partial \epsilon_i} \ln \left(\frac{\psi}{\psi_o} \right) \quad (87)$$

$$\tau \dot{\eta}_i = -e_i \frac{\partial}{\partial \eta_i} \ln \left(\frac{\psi}{\psi_o} \right) \quad (88)$$

In this coordinate system with this flow field (45) implies that:

$$\ln \left(\frac{\psi}{\psi_o} \right) = -1/2 \sum_{i=1}^N \left[\ln \left(1 + (\tau_i \alpha_o)^2 \right) + \frac{(\delta_i - \tau_i \alpha_o \epsilon_i)^2}{1 + (\tau_i \alpha_o)^2} - \delta_i^2 \right] \quad (89)$$

Differentiating (89) with respect to η_i implies that:

$$\frac{\partial}{\partial \eta_i} \ln \left(\frac{\psi}{\psi_o} \right) = 0 \quad (90)$$

Thus the Rouse model does not allow for coupling between the forced motions in the x-y plane and the random fluctuations in the z-direction. This follows physically from the assumption of the statistical independence of the three projections of the separation of the ends of a submolecule.

In the x-y plane there is a coupling of the motions of the ends as represented by (86) and (87). Solution of these for the motions of the ends can best be accomplished by introducing the transformation:

$$\delta'_i = \frac{\delta_i - \tau_i \alpha_o \epsilon_i}{\sqrt{1 + (\tau_i \alpha_o)^2}} \quad (\text{i not summed}) \quad (91)$$

$$\epsilon'_i = \epsilon_i \quad (92)$$

In the (δ'_i, ϵ_i) coordinate system the equations of motion for the N ends become after some algebra:

$$\dot{\delta}'_i = \omega_i \epsilon_i \quad (i \text{ not summed}) \quad (93)$$

$$\dot{\epsilon}_i = -\omega_i \delta'_i \quad (i \text{ not summed}) \quad (94)$$

where

$$\omega_i = \frac{\alpha_o}{\sqrt{4 + \left(\frac{\tau \alpha_o}{e_i}\right)^2}} \quad (i \text{ not summed}) \quad (95)$$

Suppose that we pick a molecule out of the ensemble. Suppose we are given the fact that the i^{th} end at $t = 0$ is located at $(\delta'_{oi}, \epsilon_{oi}, \eta_{oi})$ in $(\delta'_i, \epsilon_i, \eta_i)$ space. We ask what is the subsequent motion of this end in this space.

(88) and (90) imply that the end remains for all subsequent time in the plane $\eta_i = \eta_{oi}$. In this plane the i^{th} end's motion is described by (93) and (94). These equations may be rewritten:

$$\ddot{\delta}'_i + \omega_i^2 \delta'_i = 0 \quad (96)$$

$$\ddot{\epsilon}_i + \omega_i^2 \epsilon_i = 0 \quad (97)$$

where the dots represent derivatives with respect to time. The initial conditions and these differential equations require that the i^{th} end move according to the relations:

$$\delta'_i = -\epsilon_{oi} \sin \omega_i t + \delta'_{oi} \cos \omega_i t \quad (98)$$

$$\epsilon_i = \delta'_{oi} \sin \omega_i t + \epsilon_{oi} \cos \omega_i t \quad (99)$$

Thus in this coordinate system the ends move in elliptical orbits.

These equations may be rewritten in the diagonalizing coordinates:

$$\delta_i = \left(\frac{-\epsilon_{oi} - 2(\tau_i \alpha_o)^2 \epsilon_{oi} + (\tau_i \alpha_o) \delta_{oi}}{\sqrt{1 + (\tau_i \alpha_o)^2}} \right) \sin \omega_i t + \delta_{oi} \cos \omega_i t \quad (100)$$

$$\epsilon_i = \left(\frac{\delta_{oi} - (\tau_i \alpha_o) \epsilon_{oi}}{\sqrt{1 + (\tau_i \alpha_o)^2}} \right) \sin \omega_i t + \epsilon_{oi} \cos \omega_i t \quad (101)$$

For large α_o these become

$$\delta_i = \left(-\frac{\tau \alpha_o}{e_i} \epsilon_{oi} + \delta_{oi} \right) \sin \left(\frac{e_i t}{\tau} \right) + \delta_{oi} \cos \left(\frac{e_i t}{\tau} \right) \quad (102)$$

$$\epsilon_i = \left(\frac{2e_i}{\tau \alpha_o} \delta_{oi} - \epsilon_{oi} \right) \sin \left(\frac{e_i t}{\tau} \right) + \epsilon_{oi} \cos \left(\frac{e_i t}{\tau} \right) \quad (103)$$

For the ensemble average molecule for large α_o :

$$\overline{\delta_i^2} = 1/2 (\tau \alpha_o / e_i)^2 \quad (104)$$

$$\overline{\epsilon_i^2} = 1 \quad (105)$$

Here i is not summed.

We originally chose ϵ_{oi} and δ_{oi} (or equivalently δ'_{oi}) by first picking a molecule at random from the ensemble and then by simply noting the location of the i^{th} end at $t=0$. In order to investigate the behavior of the average molecule we now equate the ensemble average values of $\overline{\delta_i^2}$ and $\overline{\epsilon_i^2}$ with their respective time average values. The two resulting equations are then solved for $\overline{\delta_{oi}}$ and $\overline{\epsilon_{oi}}$, the initial conditions of the average molecule. The result is that:

$$\overline{\delta_{oi}} = \left(\frac{\tau \alpha_o}{e_i} \right) \gg 1 \quad (106)$$

$$\bar{\epsilon}_{oi} = 1 \quad (107)$$

Thus the average molecule moves such that its i^{th} end moves for large α_o according to the relations:

$$\delta_i = \left(\frac{\tau \alpha_o}{e_i} \right) \cos(e_i t / \tau) \quad (108)$$

$$\epsilon_i = \sin(e_i t / \tau) + \cos(e_i t / \tau) \quad (109)$$

$$\eta_i = 1 \quad (110)$$

Here i is not summed.

(109) implies that for large α_o the average stretch in the y -direction becomes independent of α_o . Thus built into the Rouse model is the notion that no matter how much the molecules are stretched out in the x -direction due to the flow field, there is no change in the average magnitude of the stretches in the y - and z -directions. Real molecules have a finite length. Thus as the stretch in the x -direction starts to approach the full extended length of the molecule, the stretches in the y - and z -directions should go to zero. Thus it is not expected that this model will predict the correct high strain behavior of the solution.

III-7. Qualitative Extension to Large Strain Rate

A guess at the correct high strain rate dependence of energy storage and dissipation may be made from a heuristic argument. For strain rates less than e_1 / τ we have shown that the energy stored locally per unit volume is

$$W = \frac{c M [\eta]^2 \eta_o^2 \alpha_o^2}{5 R T} \quad (81)$$

and

$$[\eta] = \frac{\tau(N+1)^2 R T}{12 \eta_o M} \quad (62)$$

As the strain rate becomes large compared to ϵ_1/τ we expect the Rouse model will no longer represent the physical situation and we expect the intrinsic viscosity to vary with α_o . Since the molecules are becoming stretched out along streamlines it might be expected that the limiting value approached by the intrinsic viscosity would by analogy with the Einstein viscosity relation be:

$$[\eta] \propto \frac{A V_e}{M} \quad (111)$$

where V_e is the effective volume occupied by a molecule, M is the molecular weight of the molecule and A is Avogadro's number. The effective volume occupied by a molecule should be directly proportional to the molecular weight of the molecule if the molecule is almost completely stretched out. Thus (111) suggests that:

$$\lim_{\frac{\alpha_o \tau}{\epsilon_1} \rightarrow \infty} [\eta] \rightarrow \text{constant} \quad (112)$$

Data in this region are difficult to obtain primarily because in most conventional instruments for measuring intrinsic viscosity either the strain rates are too low or there is some question whether the polymer solution is in laminar flow. By way of a numerical example, polystyrene with a molecular weight of one million dissolved in

toluene requires a strain rate large compared with $20,000 \text{ sec}^{-1}$ before the molecules begin to become stretched out along streamlines.

Energy storage is even a more difficult subject on which to speculate. The behavior of the Rouse model at high strain rate has been shown not to resemble the behavior of actual molecules. Thus we are left with an expression similar to (82) which was derived from dimensional considerations.

$$\frac{W}{nkT} = f \left(\frac{\alpha_o \Delta\eta}{nkT} \right) \quad (82)$$

This function may be expanded in even powers of the strain rate.

In view of (112) this becomes:

$$W = \frac{cRT}{M} \left(a_o + a_1 \left(\frac{\alpha_o \eta_o M}{RT} \right)^2 \left(\frac{\Delta\eta}{\eta_o c} \right)^2 + a_2 \left(\frac{\alpha_o \eta_o M}{RT} \right)^4 \left(\frac{\Delta\eta}{\eta_o c} \right)^4 + \dots \right) \quad (113)$$

The a_i are a series of constants and it is impossible to say anything about their relative size without resorting to experiments. The interesting thing about (113) is that the energy stored by the polymer molecules depends on odd powers of the molecular weight.

IV. EFFECT OF POLYMERS ON THE TURBULENT ENERGY BALANCE

IV-1 Introduction

In the previous chapter a dilute polymer solution was considered from a molecular point of view. Rouse's model was used in a systematic fashion to approximate the behavior of a single molecule subjected to both Brownian motion and a velocity field composed of spatially constant velocity gradients. It was shown in Appendix B that the equation implied by the model may be solved exactly.

That polymer molecules store energy has long been known from experiment. However, it is not generally realized that the simple Rouse model quantitatively predicts the amount of energy locally stored as a function of the local strain rate, the concentration, and readily measurable molecular parameters. For low strain rates excellent agreement is obtained between the theory for energy dissipation and measurements of energy dissipation. The Rouse results contain no adjustable constants so this theory must be considered a good first approximation to the viscoelastic properties of dilute solutions of polymers in good solvents. Thus it is expected that the predicted energy storage will also agree with experiments.

In this chapter, the effect of the polymer molecules on the behavior of the solvent will be considered from a macroscopic point of view. In the final section of this chapter these views will be equated by assuming that the energy stored per unit volume of solution is proportional to the number of molecules per unit volume times the energy stored in each molecule. The union of these two views

produces a theory which predicts the Toms Effect.

IV-2 A Constitutive Law - Two Assumptions

Our first assumption is that a dilute polymer solution is incompressible. Experiments performed by Ellis (1966) indicate that for 10 ppmw polyethylene oxide ($M_w = 3 \times 10^6$) in water at room temperature the speed of sound does not differ from that of water with a similar air content to at least one part in one hundred. Similar results have been reported by Hoyt and Tulin. Thus for a dilute solution we assume a constitutive law of the form:

$$t_{ik} = -p\delta_{ik} + 2\eta_o e_{ik} + \rho_o \Phi_{ik} \quad (114)$$

where t_{ik} is a Cartesian stress tensor, p is the hydrostatic pressure, δ_{ik} is the Kronecker delta, η_o is the Newtonian viscosity of the solvent, e_{ik} is the rate of deformation tensor, ρ_o is the density of the solvent and Φ_{ik} is a Cartesian tensor expressing the contribution of the polymer molecules to the behavior of the solution.

In principle, Φ_{ik} might be determined at some point in a flow field by measuring at that position t_{ik} , p and e_{ik} . η_o and ρ_o are assumed to be known. Knowing t_{ik} , p and e_{ik} , Φ_{ik} could be determined from (114). In practice, however, Φ_{ik} is unknown.

There exist in the literature many speculations as to what Φ_{ik} might look like for different situations. Thus one comes across terms such as "Stokesian fluid", "power-law fluid" (which includes pseudoplastic and dilatant fluids), Bingham fluid, Reiner-Rivlin fluid, Rivlin-Ericksen fluid, "simple fluid", "second-order fluid",

etc.. The particular choice of Φ_{ik} depends on the experimental evidence. If a model appears to work, it is adopted.

For dilute solutions the problem of choosing a model is complicated by the experimental fact that in every known laminar flow experiment the stress contribution of the solvent far exceeds the stress contribution of the polymer molecules. In fact, steady laminar flow experiments indicate that for dilute solutions the ratio of the stress contribution of the polymer molecules to the viscous stress is less than or equal to $c[\eta]$ where c is the weight concentration and $[\eta]$ is the intrinsic viscosity of the solution at low strain rate. Thus experimentally it appears that:

$$\rho_o \Phi_{ik} / 2\eta_o e_{ik} \leq c[\eta] \quad (i \text{ and } k \text{ not summed}) \quad (115)$$

For dilute solutions $c[\eta]$ is typically less than one hundredth. Thus stress measurements accurate to at least one part in one thousand are necessary before the true nature of Φ_{ik} may be measured.

In the absence of accurate stress measurements investigators have adopted numerous constitutive relations for dilute solutions. For example, Boggs and Tompisen (1966) set Φ_{jl} equal to the expression shown in (116):

$$\begin{aligned} \Phi_{jl} = & \nu_2 (a_{j,l} + a_{l,j} + 2u_{k,j} u_{k,l}) \\ & + \nu_3 (u_{j,k} + u_{k,j})(u_{k,l} + u_{l,k}) \end{aligned} \quad (116)$$

where the acceleration, a_j , is given by:

$$a_j = \frac{\partial u_j}{\partial t} + u_k u_{j,k} \quad (117)$$

Here the comma indicates differentiation in a Cartesian coordinate system. v_2 and v_3 are constants, u_j are the components of the velocity field in the three directions, and the usual summation convention is assumed.

Shaver and Merrill (1959), Metzner and Reed (1955), and Dodge and Metzner (1959) have had some success using a power law model of the form

$$\text{stress} = b (\text{strain rate})^s \quad (118)$$

to express the rheology of the laminar and turbulent pipe flow of concentrated polymer solutions. b and s are parameters which remain constant over extended ranges of strain rate for a given solution.

Spriggs, Huppler and Bird (1966) tabulate no less than twenty different rheological models for viscoelastic fluids. They present experimental data which tend to support some of these models. However, in general, the specific choice of constitutive law which describes the behavior of dilute solutions is open to extended debate.

Rather than enter into this debate our assumption will be that Φ_{ij} is unknown, but that in principle it could be measured. If it were measured we assume that in general one would find that:

$$\rho_o \Phi_{ij} / 2\eta_o e_{ij} \leq c[\eta] \quad (i \text{ and } j \text{ not summed}) \quad (119)$$

This assumption is consistent with current experimental results. There may exist a flow field in which (119) does not hold. However,

to date it appears not to have been discovered.

IV-3 The Toms Effect: A Wall Phenomenon

In Chapter II we discussed the measurements which indicate that turbulent momentum transport can be markedly altered even in very dilute solutions. Momentum transport is determined in turbulent flows by the Reynolds stresses. These Reynolds stresses are produced primarily by disturbances which, once formed, are insensitive to the viscous stresses. Since we have assumed in (119) that the stresses produced by the addition of polymers are very much smaller than these viscous stresses, a small quantity, we conclude that the polymer molecules cannot alter the turbulence once it has been formed.

This conclusion is very important. Previous investigators have suggested that the polymer molecules directly "damp the turbulence". The assumption stated in (119) makes this mechanism for the Toms Effect impossible.

In free turbulent flows the effects of viscosity are removed from those turbulent motions which control the mean motion. The effects of viscosity are rather relegated to the small scale eddies which take part in the final decay and the production of heat. Polymer molecule addition should slightly influence this final decay but should not influence the turbulent motions which control the mean motion. Thus we expect that the structure in grid and free-jet turbulence should in no measurable way differ from the structure found in the flow of the solvent under similar conditions. Thus

measurements of grid and free jet turbulence should provide an excellent indirect check for (119).

Fabula (1966) has published a detailed experimental study of grid turbulence in dilute high-polymer solutions. The major purpose of this investigation was to determine the effects of the non-Newtonian properties of polymer solutions upon the grid-turbulence energy spectrum.

The turbulence was generated by towing a grid of regularly spaced bars through a tank of stagnant fluid. At a sufficient distance from the grid to insure spreading and mixing of the turbulent wakes of the bars, hot-film sensors were used to measure the instantaneous longitudinal velocity. From this signal the longitudinal, one-dimensional wavenumber spectrum was determined for water at various temperatures for a wide variety of aqueous polymer solutions.

Fabula concluded from his measurements that for dilute solutions no measurable changes took place in the grid-turbulence energy spectrum. For concentrated solutions ($c[\eta] = .27$), Fabula observed a depression in the spectral level at higher frequencies due to polymer addition. However, when the increase in viscosity due to polymer addition was taken into account, Fabula found no evidence of non-Newtonian effects.

Jackley (1966) studied the mean velocity profile of a free turbulent round jet growing in a large tank in order to determine whether the Toms Effect is the result of polymer molecules "directly damping the turbulence". Jackley found that when dilute aqueous solution was pumped into similar stagnant solution, a mean velocity

profile resulted which, beyond ten diameters of the nozzle mouth, could not be distinguished from that of distilled water. Jackley concluded that the Toms Effect is "a phenomenon of the wall".

Thus the best experimental evidence to date appears to support (119).

IV-4 A Qualitative Explanation

In wall turbulence the effects of initial conditions never completely disappear from the structure of the turbulence.

Immediately adjoining the wall there is a thin layer of fluid in which the mean velocity, $U_1(x_2)$, varies linearly with the distance from the wall, x_2 . This velocity is small throughout the layer, varying from zero at the wall itself to values of the order of ten times the friction velocity, U_τ , at the outer edge of the layer. Here,

$$U_\tau = \sqrt{\tau_w / \rho} \quad (120)$$

τ_w is the turbulent wall stress and ρ is the density of the fluid.

We call this thin layer the viscous sublayer.

The viscous sublayer is characterized by small but high frequency velocity fluctuations. In fact, the local turbulence level, $\sqrt{u_1^2} / U_1(x_2)$, where $\sqrt{u_1^2}$ is the local root-mean-square value of the velocity fluctuations in the flow direction, rises to a maximum value at the wall. Thus the flow is highly disturbed all the way to the wall.

These disturbances in the velocity field are produced by the motions of volumes of fluid in the outer part of the boundary layer. This outer part of the boundary layer is a region where the viscous

stresses are everywhere small compared to the Reynolds stresses.

The velocity fluctuations are of a scale very much larger and of frequencies very much lower than those in the viscous sublayer. In fact, the characteristic time scales of the turbulence in this outer region are so long that a sample volume of turbulent fluid could be transported a considerable distance by a convective motion without undergoing a large change in its structure or identity. These large volumes of fluid eventually interact with the wall and with each other to form smaller, but higher frequency disturbances.

In the outer part of the boundary layer these small, violent disturbances decay into heat. Close to the wall, however, these small disturbances tend to grow because they can locally extract energy from the local velocity profile through their Reynolds stresses. Simultaneously these small disturbances tend to lose energy because their gradients locally dissipate energy into heat. In polymer solutions these small disturbances tend to store energy in the polymer molecules.

If a small disturbance extracts more energy locally than it loses, it will grow. The disturbances, or vortices, so generated move out from the wall as they are convected downstream. Thus small disturbances at the edge of the viscous sublayer ultimately become part of the structure of the turbulence in the outer part of the boundary layer and ultimately become responsible for the Reynolds stresses of the turbulent flow.

The idea fundamental to this theory is that the large scale disturbances which produce the Reynolds stresses some distance

downstream were, at an earlier time, small disturbances at the edge of the viscous sublayer some distance upstream.

Once the small disturbances start to grow the effect of the polymer molecules may be neglected. All the polymer molecules do is slightly alter the energy balance of the turbulent fluctuations close to the wall. By slightly altering this balance, the molecules allow viscous dissipation to destroy disturbances which would have had sufficient kinetic energy to grow had the polymer molecules not been present.

By decreasing the number of disturbances which grow per unit area and time and move out from the edge of the viscous sublayer, the addition of the polymer molecules ultimately changes the structure of the turbulence in the outer part of the boundary layer. This change results in lower Reynolds stresses and hence the Toms Effect.

IV-5 A Quantitative Explanation of the Toms Effect

The equations of motion for an incompressible fluid in the absence of body forces may be written

$$u_{i,t} + u_j u_{i,j} = \frac{1}{\rho} t_{ij,j} \quad (121)$$

Let U_i be a steady mean flow field and u_i' be the components of the turbulent velocity fluctuations. Let T_{ij} be a steady mean Cartesian stress tensor and t_{ij}' be the turbulent stress fluctuations. Let a bar over a quantity imply a time mean value, namely,

$$\bar{X} = \lim_{T \rightarrow \infty} \frac{1}{2T} \int_{-T}^T X dt \quad (122)$$

Thus the velocities and stresses can be rewritten

$$u_i = U_i + u'_i \quad (123)$$

$$t_{ij} = T_{ij} + t'_{ij} \quad (124)$$

where

$$\bar{u}_i = U_i \text{ and } \bar{t}_{ij} = T_{ij} \quad (125)$$

Substituting (123) and (124) into (121), multiplying the resulting equation through by u'_i , and then averaging the resulting equation produces

$$\overline{u'_i u'_j} U_{i,j} + \frac{1}{2} \left[\overline{U_j u'^2_i} + \overline{u'_j u'^2_i} \right]_{,j} = \frac{1}{\rho} \overline{t'_{ij,j} u'_i} \quad (126)$$

The qualitative argument in the preceding section suggests that we consider this equation in the neighborhood of a wall. For simplicity, consider a dilute solution moving with a steady mean velocity $U_1(x_2)$ along a flat plate in the x_1 -direction.

If we introduce length scales L_1 and L_2 representative of the x_1 - and x_2 -directions, respectively, the narrowness of the boundary-layer region leads to the conclusion that $L_2/L_1 \ll 1$.

By virtue of the continuity equation, the velocity scales Γ_1 and Γ_2 representative of the typical velocities parallel and normal to the plate should satisfy the requirement that

$$\frac{\Gamma_2}{\Gamma_1} \approx \frac{L_2}{L_1} \ll 1 \quad (127)$$

Despite the presence of the wall, it will be assumed that the

turbulent intensities in the various directions are still of the same order of magnitude. Accordingly, it will be assumed that it is permissible to consider one velocity scale, V , for $u_i^!$ where $i = 1, 2, 3$. V is assumed small compared with Γ_1 .

Now consider the constitutive law

$$t_{ij} = -p\delta_{ij} + 2\eta_o e_{ij} + \rho_o \Phi_{ij} \quad (114)$$

Let p' and $\phi_{ij}^!$ represent the turbulent fluctuations of p and Φ_{ij} . ν is the kinematic viscosity of the solvent. Then

$$\frac{\overline{u_i^! t_{ij}^!}}{\rho} = -\frac{1}{\rho_o} \overline{u_i^! p'_{,i}} + \nu \overline{u_i^! u_{i,j}^!} + \overline{u_i^! \phi_{ij}^!} \quad (128)$$

It is worthwhile to note that incompressibility requires that

$$\nu \overline{u_i^! u_{i,j}^!} = -\nu \overline{(u_{i,j}^!)^2} + \frac{\nu}{2} \overline{(u_i^!)^2}_{,jj} \quad (129)$$

p'/ρ is assumed, close to the wall, to be of the order V^2 .

Thus assuming the correlation coefficients are all of order 1, (126) may be rewritten (Townsend (1956))

$$\begin{aligned} \overline{u_1^! u_2^!} U_{1,2} - \nu \overline{(u_{i,j}^!)^2} &= \overline{+u_2^! (p'/\rho + u_i^!^2/2)}_{,2} \\ - \overline{u_i^! \phi_{i2}^!} + \text{terms of order } V^2 \Gamma_1 L_2^{-1} \end{aligned} \quad (130)$$

The first two terms in (130) are both of order $V^2 \Gamma_1 L_2^{-1}$ and represent the local rate of turbulent production and dissipation. Their difference produces a small positive term of order $V^3 L_2^{-1}$. This difference drives the right hand side of (130).

The third term is customarily called the "advection" or "energy diffusion" term. The latter is perhaps a more descriptive term for what is taking place. The third term represents the net rate at which energy is diffusing from the edge of the viscous sublayer towards the outer part of the boundary layer.

For turbulent flows of Newtonian solvents it has been observed (Townsend, 1956) that while changes in the energy diffusion term have no immediate effect on the turbulent intensity or stresses in the outer part of the boundary layer, they do have a cumulative effect which is felt some distance downstream. Thus by altering this third term one can alter the structure of the turbulence.

The fourth term represents the contribution of the polymer molecules to this energy balance. For very, very dilute solutions it is to be expected that this term will be of order $V^2 \Gamma_1 L_1^{-1}$ or smaller. Then (130) will be, to an excellent approximation, identical with the case for flow of a Newtonian solvent. Thus there should be no Toms Effect.

However we define the dimensionless parameter H such that

$$H = \left[\frac{u'_i \phi'_{i2,2}}{u'_2 (p'/\rho + u'^2_i/2)_{,2}} \right] \quad (131)$$

As H begins to approach one, presumably the rate energy is diffusing from the edge of the sublayer towards the outer part of the boundary layer will be changed. For H much greater than one, nothing can be said.

Measuring velocities in dilute polymer solutions is difficult enough. Measuring the fluctuating part of an unknown portion of a stress tensor is, at the present time, impossible. Thus the success of this analysis rests on our ability to estimate $\overline{u_i^! \phi_{12,2}^!}$ without having to perform direct measurements.

IV-6 An Estimate of H

In this chapter the effect of the polymer molecules on the behavior of the solvent has been considered from a macroscopic point of view. Rather than examine the behavior of the molecules individually, we have assumed that the effect of polymer addition might conceptually be measured as an additional term in a constitutive relation, namely, $\rho \Phi_{ij}$. (This assumes that the polymer molecules are homogeneously distributed throughout the solvent.)

Polymer molecules store energy. The average rate work is done, \dot{E} , by the stress contribution of the molecules, $\rho_o \Phi_{ij}$, during the deformation of the flowing fluid is

$$\dot{E} = (\rho_o \Phi_{ij} u_j^!),_i \quad (132)$$

This must equal the average local rate of change of internal energy of the molecules, \dot{W} . In Chapter III we have shown that each molecule stores energy as a function of the local strain rate. For dilute polymer solutions subjected to low strain rates we have shown that the energy stored per unit volume by the molecules due to a strain rate α_o is just

$$W = A \alpha_o^2 \quad (81)$$

where

$$A = \frac{c M [\eta]^2 \eta_0^2}{5 R T} \quad (133)$$

(81) was obtained by assuming that the energy stored per unit volume of solution is proportional to the number of molecules per unit volume times the energy stored in each molecule. (This assumes that the solution is dilute.)

For the purposes of this estimate we assume

$$W = 4A e_{ij}^2 \quad (134)$$

Since the following argument involves only an order of magnitude analysis, the shortcomings of this generalization are not significant. Thus the average local rate of change of internal energy of the molecules \dot{W} is

$$\dot{W} = \overline{4A [u_k e_{ij}^2]_{,k}} \quad (135)$$

$$= \overline{4A (U_k e'_{ij}^2)_{,k}} + \overline{4A (u'_i e'_{ij}^2)_{,k}} \quad (136)$$

$$+ 8A \overline{(u'_k e'_{ij} E_{ij})_{,k}} + \overline{4A (U_k E_{ij}^2)_{,k}}$$

Here E_{ij} and e'_{ij} are the mean and fluctuating parts of the rate of deformation tensor.

For flow past a flat plate in the x_1 -direction, close to the plate, most of these terms are small and

$$\dot{W} = \overline{4A (u'_2 e'_{ij}^2)_{,2}} + \text{negligible terms} \quad (137)$$

Similarly (132) becomes

$$\dot{E} = (\rho \Phi_{ij} U_j),_i + \overline{\rho(\phi'_{ji} u'_j)},_i$$

which for flow past a flat plate in the x_1 -direction, close to the plate, becomes

$$\dot{E} = \overline{\rho(\phi'_{j2} u'_j)},_2 + \text{negligible terms} \quad (138)$$

Equating (137) and (138) produces the result that to first order

$$\overline{\rho(\phi'_{j2} u'_j)},_2 = 4A \overline{(u'_2 e'_{ij})},_2 \quad (139)$$

Thus, assuming that it is permissible to consider one scale, ϕ , for ϕ'_{j2} , then the magnitude of this scale must be of the order of

$$\phi \approx \frac{4A}{\rho_0} \left(\frac{V^2}{\ell^2} \right) \quad (140)$$

where ℓ is a length scale characteristic of a disturbance. Thus H

may be estimated from (131) as (141) where

$$H \approx \frac{V \left(\frac{4A}{\rho_0} \frac{V^2}{\ell^2} \right) \left(\frac{1}{\ell} \right)}{V^3 L_2^{-1}} \\ \approx \left(\frac{4A}{\rho_0} \right) \left(\frac{L_2}{\ell^3} \right) \quad (141)$$

Implied in the notion that close to the wall energy production very nearly equals dissipation is the relation

$$\frac{V^2 \Gamma_1}{L_2} \approx \frac{\nu V^2}{\ell^2} \quad (142)$$

Thus

$$\left(\frac{1}{\ell^3} \right) \approx \left(\frac{\Gamma_1}{L_2 \nu} \right)^{3/2} \quad (143)$$

Thus from (141) and (143)

$$H \approx \left(\frac{4A}{\rho_o} \right) L_2 \left(\frac{\Gamma_1}{L_2 v} \right)^{3/2} \quad (144)$$

$$\begin{aligned} &\approx \left(\frac{4A}{\rho L_2^2} \right) \left(\frac{\Gamma_1 L_2}{v} \right)^{3/2} \\ &\approx \left(\frac{4AU_\tau^2}{\rho_o v^2} \right) \left(\frac{v^2}{L_2^2 U_\tau^2} \right) \left(\frac{\Gamma_1}{U_\tau} \right)^{3/2} \left(\frac{U_\tau L_2}{v} \right)^{3/2} \\ &\approx \left(\frac{4AU_\tau^2}{\rho_o v^2} \right) \left(\frac{\Gamma_1}{U_\tau} \right)^{3/2} \left(\frac{U_\tau L_2}{v} \right)^{-1/2} \end{aligned} \quad (145)$$

The latter three terms may be identified as follows:

$$\begin{aligned} \frac{4AU_\tau^2}{\rho_o v^2} &= \frac{4cM[\eta]^2 \eta_o^2 \tau_w}{5 \rho_o^2 v^2 R T} \\ &= \left(\frac{4cM[\eta]^2 \tau_w}{5 R T} \right) \end{aligned}$$

Thus the viscosity of the solvent drops out of the first term.

In the second and third terms Γ_1 and L_2 may, for the purpose of estimating H , be equated with $U_1(x_2)$ and x_2 . x_2 is the distance from the plate and $U_1(x_2)$ is the velocity along the plate.

The law of the wall

$$U_1/U_\tau = 5.75 \log \left(\frac{U_\tau x_2}{v} \right) + 5.10 \quad (146)$$

for a Newtonian solvent is (when Reynolds number is high and the pressure either constant or the adverse gradients are not excessive) remarkably insensitive to conditions in the outer part of the boundary layer. Thus it is quite relevant for estimating (U_1/U_τ) as a function

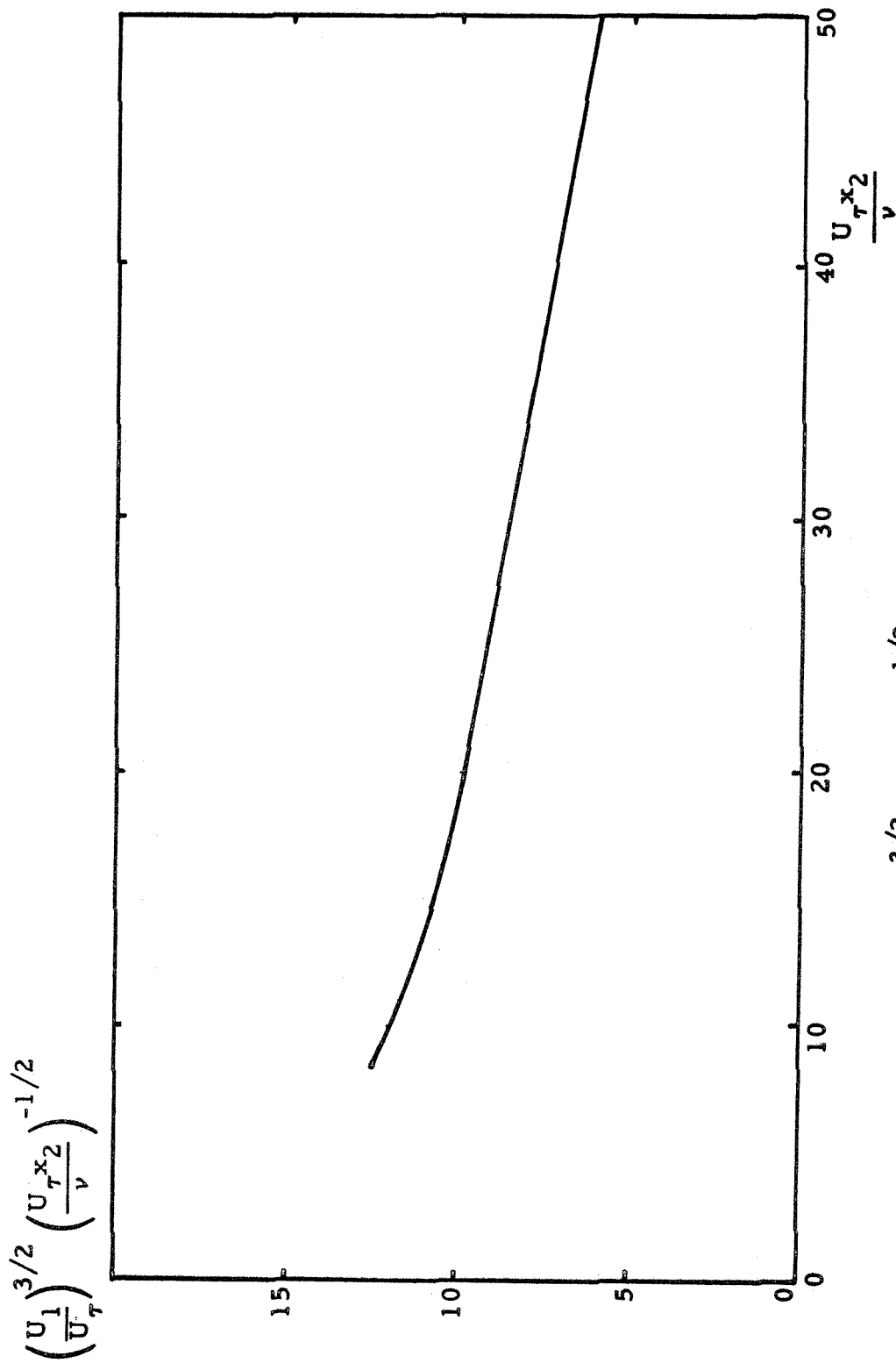
of $(U_\tau \frac{x_2}{\nu})$ for dilute solutions.

For very, very dilute solutions where no Toms Effect takes place, (146) will in general hold. As the concentration is raised to the point where the Toms Effect begins, (146) will start to change. However, for a first approximation of the relationship between (U_1/U_τ) and $(U_\tau \frac{x_2}{\nu})$, (146) will be used.

Figure 6 shows $(U_1/U_\tau)^{3/2} (U_\tau \frac{x_2}{\nu})^{-1/2}$ plotted versus $(U_\tau \frac{x_2}{\nu})$ using the law of the wall. From this graph it is clear that at the edge of the viscous sublayer, $(U_1/U_\tau)^{3/2} (U_\tau \frac{x_2}{\nu})^{-1/2} \approx 10$.

In conclusion, for dilute polymer solutions the Toms Effect should start taking place when H starts to approach one. H is estimated from (145) and Figure 6 as

$$H \approx \left(\frac{8c M[\eta]^2 \tau_w}{R T} \right) \quad (147)$$



Relationship Between $\left(\frac{U_\tau x_2}{v}\right)$ and $\left(\frac{U_1}{U_\tau}\right)^{3/2} \left(\frac{U_\tau x_2}{v}\right)^{-1/2}$ from the Law of the Wall

Figure 6

V. COMPARISON OF THEORY WITH EXPERIMENT

V-1 Discussion of Theory

As H approaches one, we expect that significant amounts of energy, which would ordinarily have been convected away from the wall in the form of turbulent disturbances, will be convected away stored in polymer molecules. H is a dimensionless measure of the effect of the molecules on the rate turbulent energy is diffusing from the wall.

In Chapter II we introduced the function L , the percent approach to laminar flow. L is a dimensionless measure of the structure of the turbulence responsible for the turbulent momentum transport of the flow.

H as defined by (131) is a dimensionless measure of the effect of the polymer molecules on the structure of this turbulence. Thus for a given Reynolds number flow and a given wall flow geometry, L must be a unique function of H .

Since the structure of wall turbulence does not depend strongly on Reynolds number above transition, we do not expect L to be strongly dependent on Reynolds number.

As H becomes greater than one, subject to the restriction that the solution remains dilute, it is not clear what will happen. Our estimate of H required use of the law of the wall. Presumably changes in the structure of the turbulence (due to changes in the energy balance at the edge of the viscous sublayer) will be reflected in changes in the law of the wall.

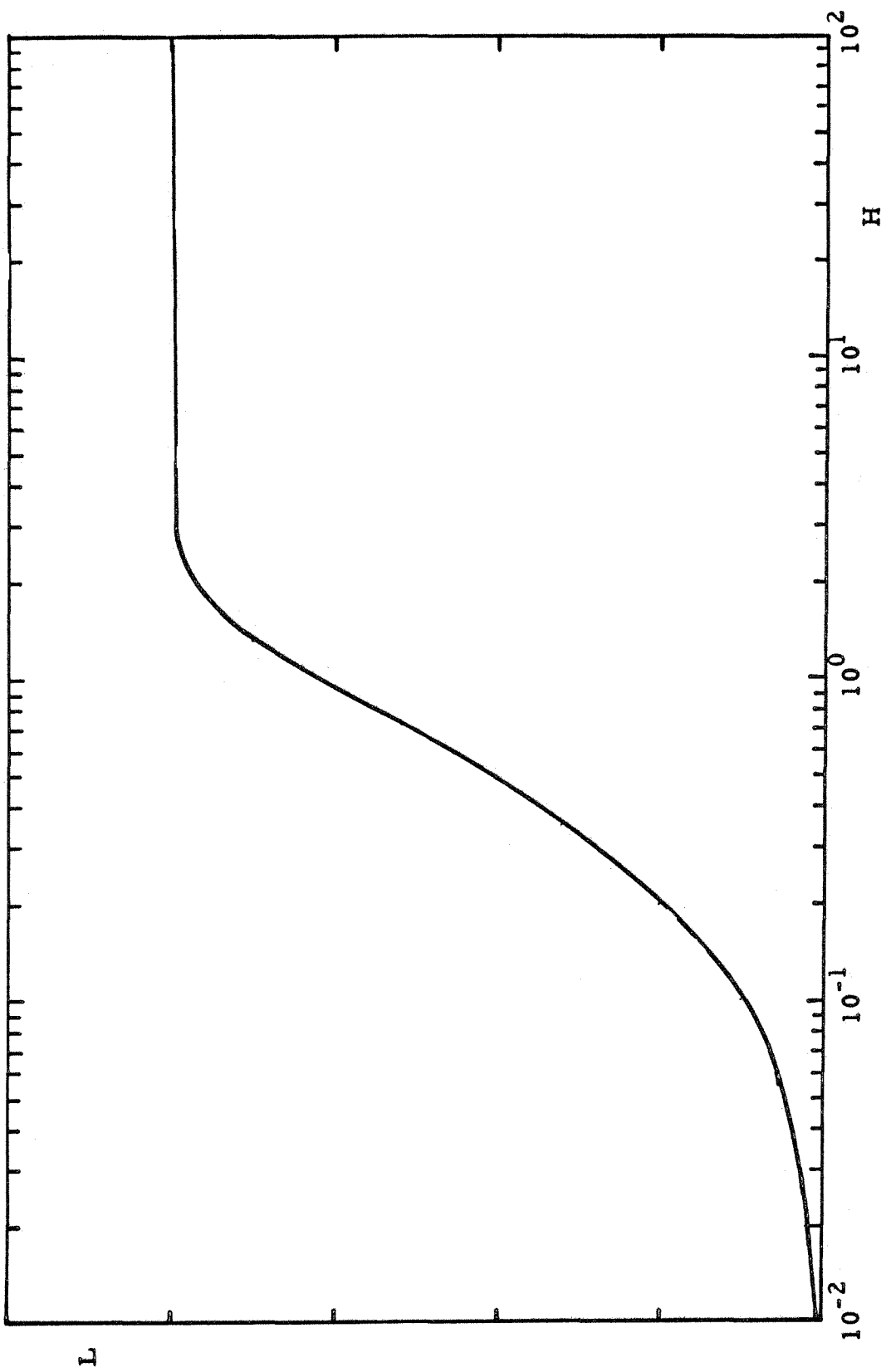
Physically, however, we expect that the elastic terms in the boundary layer will start to stabilize most of the disturbances. Thus the sublayer will become effectively thicker. There will be fewer disturbances, but each will have, on the average, larger Reynolds stresses. Some of these disturbances will still be able to extract energy from the mean velocity gradient and grow. Because of the latter effect, it seems unlikely that laminar flow will ever be reached.

Thus, theoretically we expect that if H were plotted against L , then one would find a functional relationship between these two parameters similar to that shown in Figure 7.

Here when H is small, L is zero. As H approaches one, L begins to rise. As H becomes large, L approaches a constant value of less than 100 percent. This theory does not predict the exact mathematical form of the relationship between L and H . To do this would require a detailed knowledge of the relationship between the structure of the turbulence at the edge of the viscous sublayer and in the outer part of the boundary layer. One would also need to know the relationship between this structure and L .

Perhaps this would be made possible by postulating a model which behaves in some approximation like real wall turbulence. A model of this kind might help provide insight into the whole problem of wall turbulence, much as the Rouse model helps provide insight into the behavior of dilute polymer solutions.

It should be reemphasized that our quantitative estimate of H as represented by (147) is limited to solutions subjected to low strain rates. By this it is meant that the local strain rate:



Predicted Relationship Between L and H

Figure 7

$$\alpha_o < e_1 / \tau \quad (148)$$

which from (63) and (79) means that:

$$\alpha_o < \frac{\pi^2 R T}{12[\eta] \eta_o M} \quad (149)$$

Roughly, this means that the turbulent wall stress must be less than, at a minimum, $10RT/[\eta]M$. For Polyox in water at 25°C, using (5),

$$\tau_w < 2.4 \times 10^{+13} M^{-1.78} \text{ dynes/cm}^2 \quad (150)$$

Figure 8 shows the region of validity of (148) for Polyox solutions. Shin (1966) and Pruitt and Crawford's (1965) data are indicated by triangles and circles. It is evident that except for the higher molecular weight material, these data are all in the low strain rate régime.

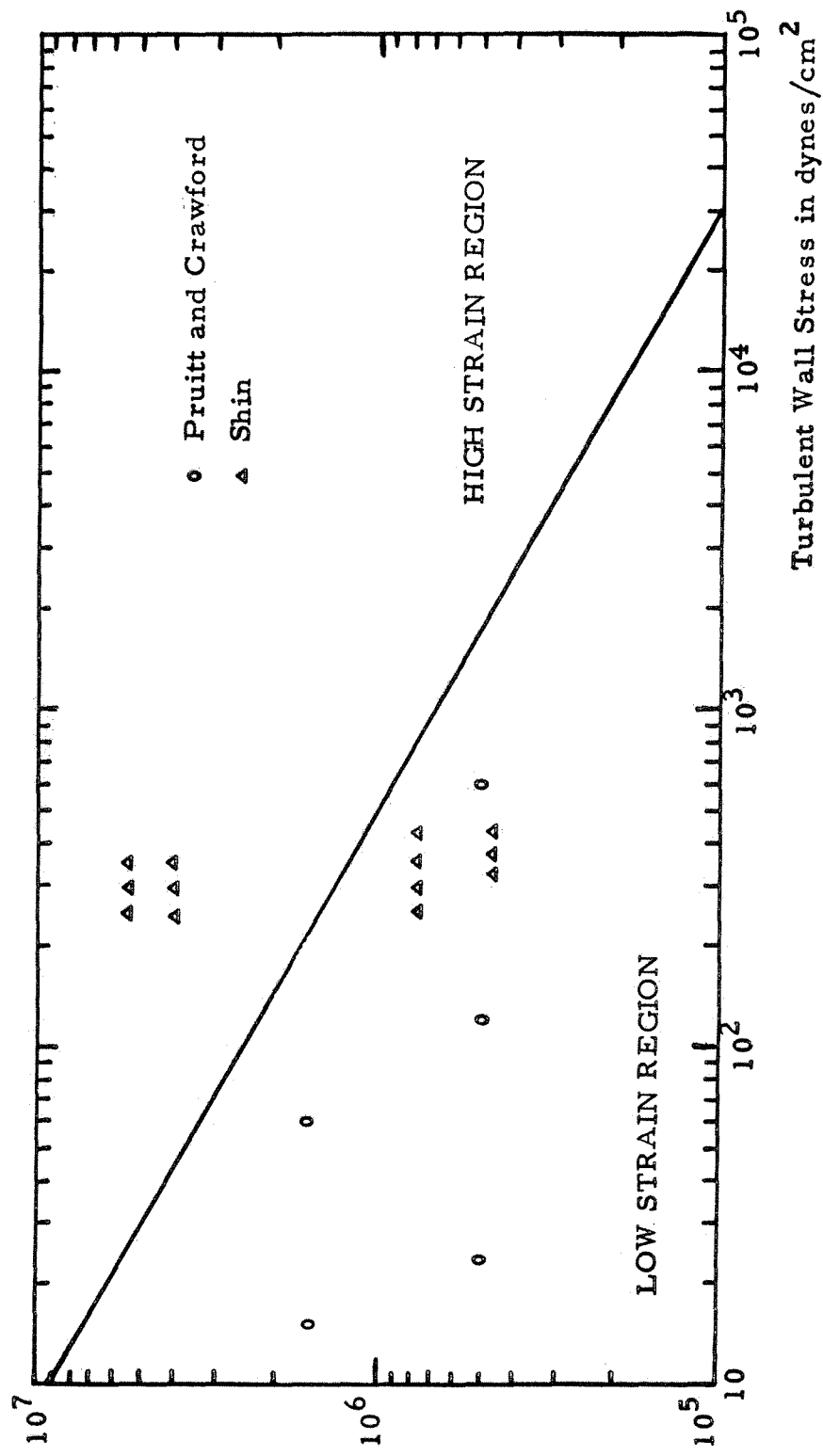
It should be further noted that H is very sensitive to the molecular weight of the sample used. Thus if a polymer sample is degraded or blended with another sample, the resulting molecular weight distribution must be known before H can be accurately determined.

This may be done as follows:

Consider a heterogeneous polymer in a solution so dilute that individual molecules can be considered to contribute to energy storage independently of one another. Then from (147)

$$H_i = \frac{8 c_i M_i [\eta]_i^2 \tau_w}{R T} \quad (i \text{ not summed}) \quad (151)$$

Molecular Weight of Polyox



Regions for the Toms Effect for Aqueous Polyox Solutions

Figure 8

where H_i , c_i , M_i and $[\eta]_i$ are the contribution to H , c , M and $[\eta]$ due to the i^{th} species. In general, it is experimentally observed that

$$[\eta]_i = K M_i^\alpha \quad (152)$$

where K and α are constants. (5) and (6) are specific examples of this general relationship. Substituting (152) into (151) and summing over i produces

$$H_{\text{actual}} = \left(\frac{8K^2 \tau_w}{RT} \right) \sum_i c_i M_i^{2\alpha+1} \quad (153)$$

However, H is usually calculated by taking the value of the intrinsic viscosity measured from a viscosity measurement and a value of the molecular weight measured using light-scattering, or the weight average molecular weight. Thus

$$H_{\text{calculated}} = \left(\frac{8\tau_w c}{RT} \right) \left(\frac{\sum M_i^\alpha c_i}{c} \right)^2 \left(\frac{\sum c_i M_i}{c} \right) \quad (154)$$

Thus dividing (154) into (153) produces the correction factor E where:

$$E = \frac{H_{\text{actual}}}{H_{\text{calculated}}} = \frac{\sum_i (c_i/c)(M_i/M_o)^{2\alpha+1}}{\left(\sum_i \left(\frac{c_i}{c} \right) (M_i/M_o)^\alpha \right)^2 \left(\sum_i (c_i/c)(M_i/M_o) \right)} \quad (155)$$

Here M_o is the molecular weight of the monomer, $(M_i/M_o) = i$ which equals the degree of polymerization and $(c_i/c) = w_i$ which equals the weight fraction of the sample with degree of polymerization i . Thus

$$\Xi = \frac{\sum_{i=1}^{\infty} w_i i^{2\alpha+1}}{\left(\sum_{i=1}^{\infty} w_i i^{\alpha}\right)^2 \sum_{i=1}^{\infty} w_i i} \quad (156)$$

Thus if w_i is known, Ξ may be evaluated using (156). In principle, for polymers formed by monomer addition without termination, poly(ethylene oxide) for example, (Flory, 1940)

$$w_i = \frac{\nu}{\nu+1} \frac{e^{-\nu} i \nu^{(i-2)}}{(i-1)!} \quad (157)$$

ν represents the number of monomers reacted per initiator. If (157) is substituted into (156), the sums may be exactly evaluated for $\alpha = 1$. Thus, for $\alpha = 1$,

$$\Xi = \frac{(\nu+1)^2}{\nu^2} \frac{(1/\nu + 25\nu + 15 + 10\nu^2 + \nu^3)}{(\nu + 3 + 1/\nu)^3} \quad (158)$$

For high-molecular weight polymers ν is typically large compared with 10^3 . Thus Ξ equals one and $H_{\text{calculated}}$ equals H_{actual} to an excellent approximation.

In practice, the idealized situation as represented by (157) is not realized unless great care is taken in the preparation and handling of solutions. Since it is current practice to examine the Toms Effect using aqueous Polyox solutions, it is relevant to examine the pitfalls inherent in the use of these solutions.

Union Carbide makes Polyox in a variety of molecular weights for industrial use.

The industrial specification is that a 5% solution by weight should, at a specified strain rate, have a viscosity between two specified values. If a batch does not meet specification, material

of different molecular weights is added until it does. From these blends, commercial samples are taken.

These samples have been used by experimenters to attempt to define the Toms Effect. Thus it is a matter of luck if an experimenter starts with a blend or with a heterogeneous sample.

As soon as a dilute solution is mixed, degradation begins. Polyox solutions are sensitive to chemical (see Appendix E), mechanical (see Chapter III), and perhaps biological degradation (see Appendix E). Thus as soon as the solutions are mixed, w_i begins to change. This can to some extent be prevented by using air-free distilled water, by not shaking the solutions, and by keeping the solutions under nitrogen in a cool, dark place.

Outdoor tanks and recirculating systems emphatically will not produce good results.

There is some reason to believe that the data presented in Table 1 and Figures 3 and 4 are for undegraded and unblended samples. Further there is reason to believe that, to date, no other data available in the literature is for undegraded polymer samples subjected to low strain rates.

Thus these data will be used for testing the theory.

V-2 Comparison of Theory with Experiment

Our theory predicts that the Toms Effect should become visible when H approaches $H_{critical}$, where $H_{critical}$ should be of the order of .01. From (147),

$$H_{critical} = \frac{8cM[\eta]^2\tau^*}{RT} \quad (159)$$

From (159) it is clear that if one onset wall stress and polymer concentration is known, then all other solutions formed using this polymer sample and solvent must obey the relation

$$c\tau^* = (c\tau^*)_{\text{known}} = \text{constant} \quad (160)$$

This result is in quantitative agreement with the experimental data in Table 1.

(160) explains why there is no "onset" stress for the 50 ppmw solution shown in Figure 2. For this case τ^* should have been 3 dynes/cm². Transition takes place at 6 dynes/cm². Thus transition and the Toms Effect take place simultaneously.

For each of the five solutions in Table 1, H_{critical} may be calculated. Thus for the first solution:

$$\begin{aligned} H_{\text{critical}} &= \frac{8(2 \times 10^{-6})(5 \times 10^5)(3 \times 10^2)^2(600)}{(8.3 \times 10^7)(300)} \\ &= 1.7 \times 10^{-2} \end{aligned} \quad (161)$$

The other values of H_{critical} may be calculated from the data in Table 1. They are shown in the right hand column of Table 1. The data, as they stand, indicate that H_{critical} equals .02. This is in excellent agreement with the theory.

Further excellent agreement is found if the data from Shin's thesis is plotted in terms of L and H. The computation procedure is quite straightforward. All of the data shown in Figures 3 and 4 are put in numerical form. There are thirty different points covering two different polymers in two different solvents, covering eight

different molecular weights and 30 different concentrations. The Reynolds numbers are also different.

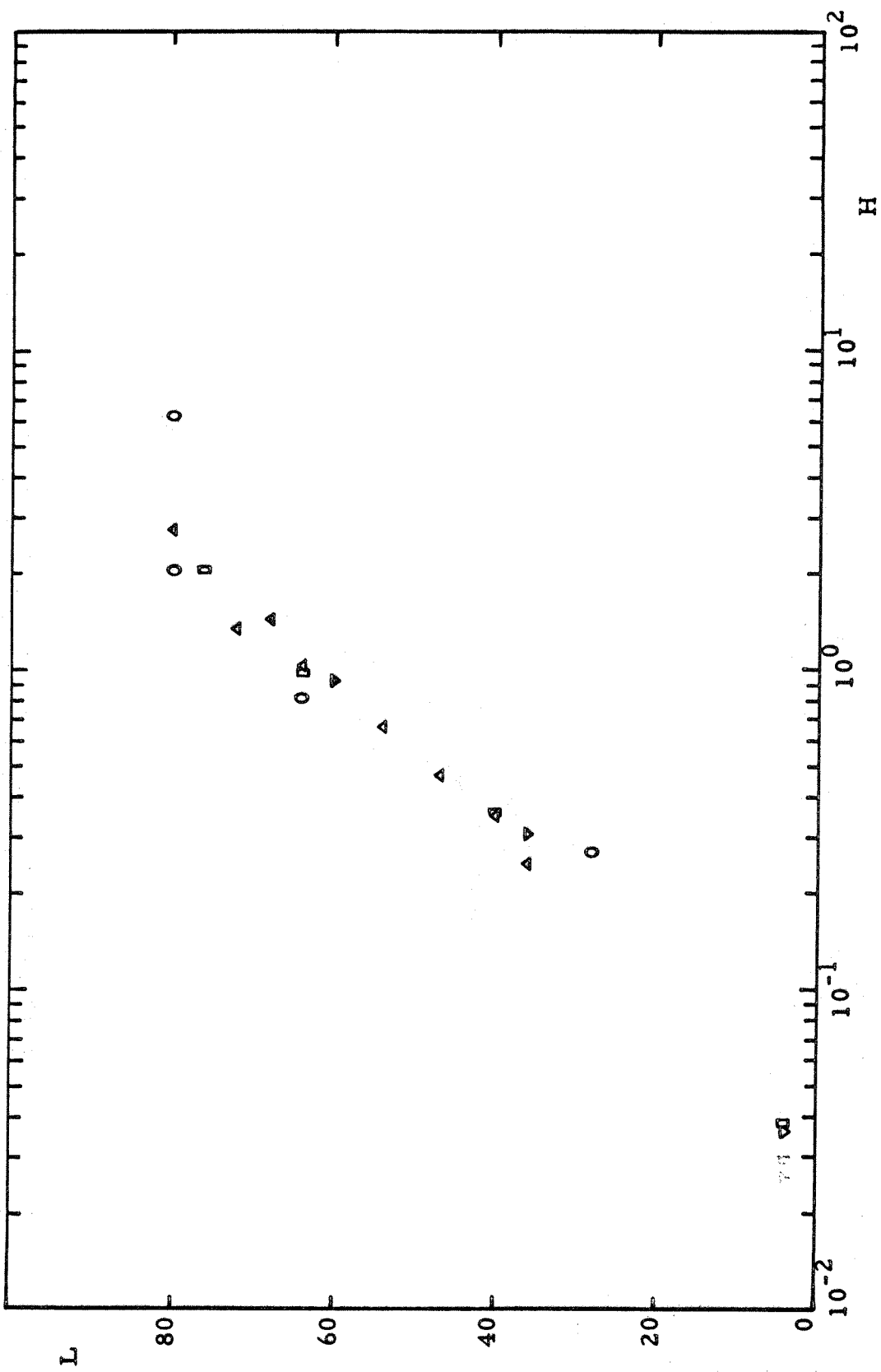
For each of these thirty points, H and L are calculated using (131) and (4). For our theory to be valid, this must produce a curve of the form shown in Figure 7.

Figure 9 presents the results of this calculation for the Polyox data shown in Figure 3. The remarkable superposition of Shin's Polyox data is strong evidence that the parameters, L and H , developed by this theory are the correct ones for describing the Toms Effect. It should be noted that the Toms Effect begins at $H \approx .02$, which is consistent with Pruitt and Crawford's data.

Figure 10 presents the results of this calculation for Shin's PIB data. The scatter here may result from uncertainties in the PIB data. It may also result from the defects inherent in the Rouse model.

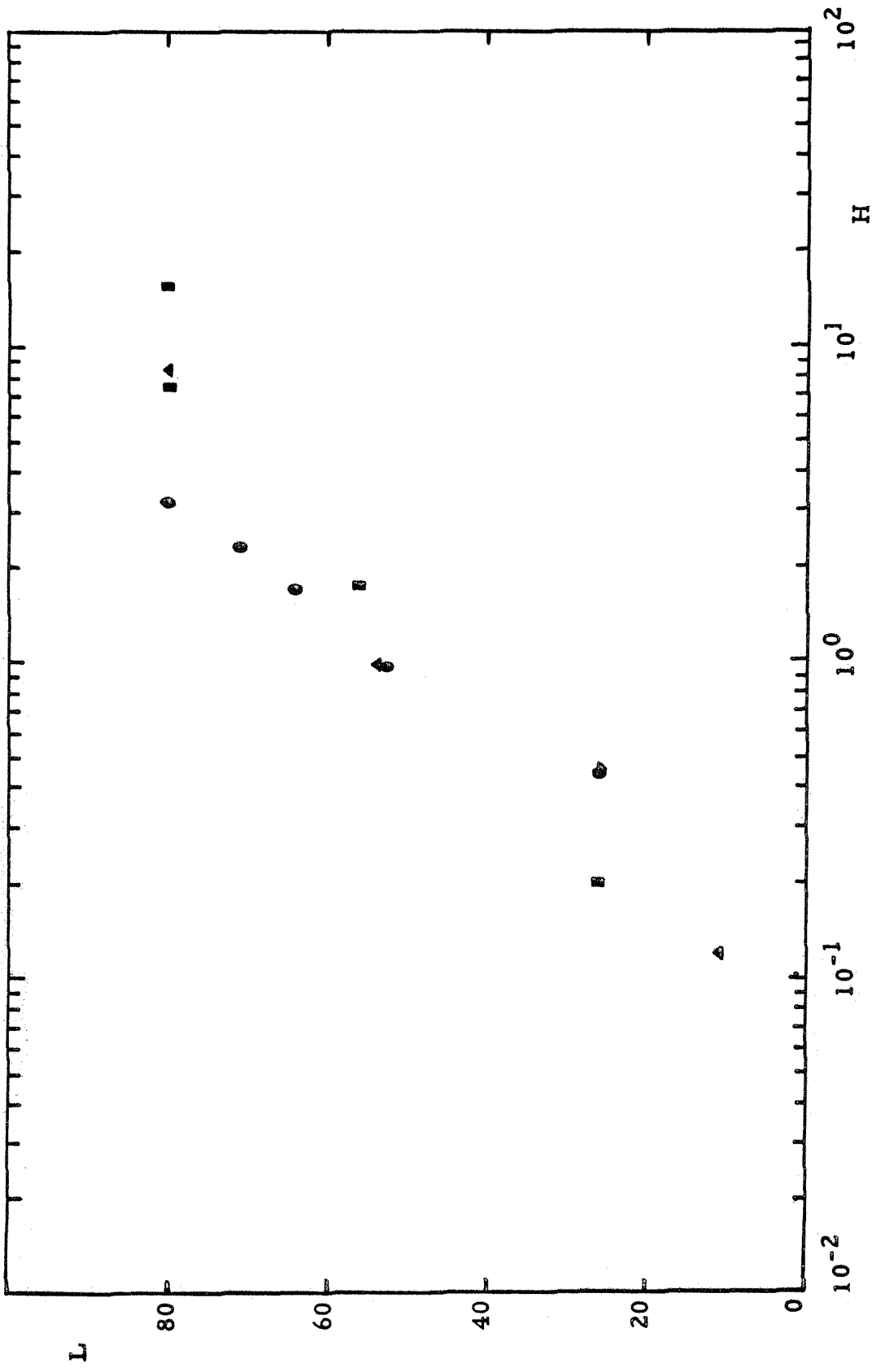
Figure 11 compares the data for Polyox in water and PIB in cyclohexane. The resulting differences may be due to errors inherent in the data (especially in the effects of molecular weight distribution).

It seems that high molecular weight polymers of ethylene oxide have broad molecular weight distributions in spite of the fact that the theory predicts otherwise (Flory, 1940). Elias (1961) experimentally found ratios of \overline{M}_w to \overline{M}_n in the range of 10 to 20. His work was done in water using the techniques of ultracentrifugation and osmometry.



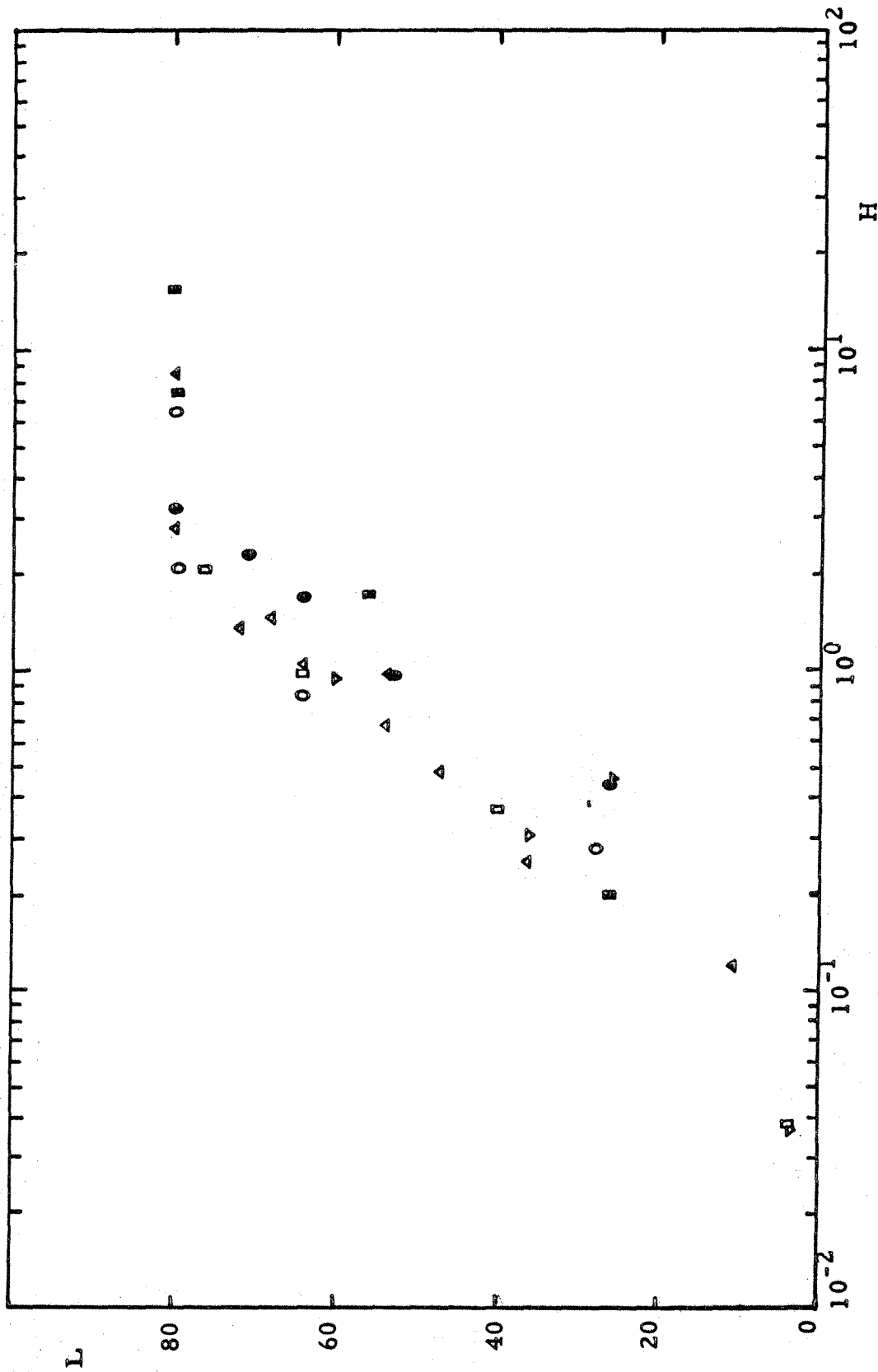
Relationship Between L and H from Shin's Polyox in Water Data

Figure 9



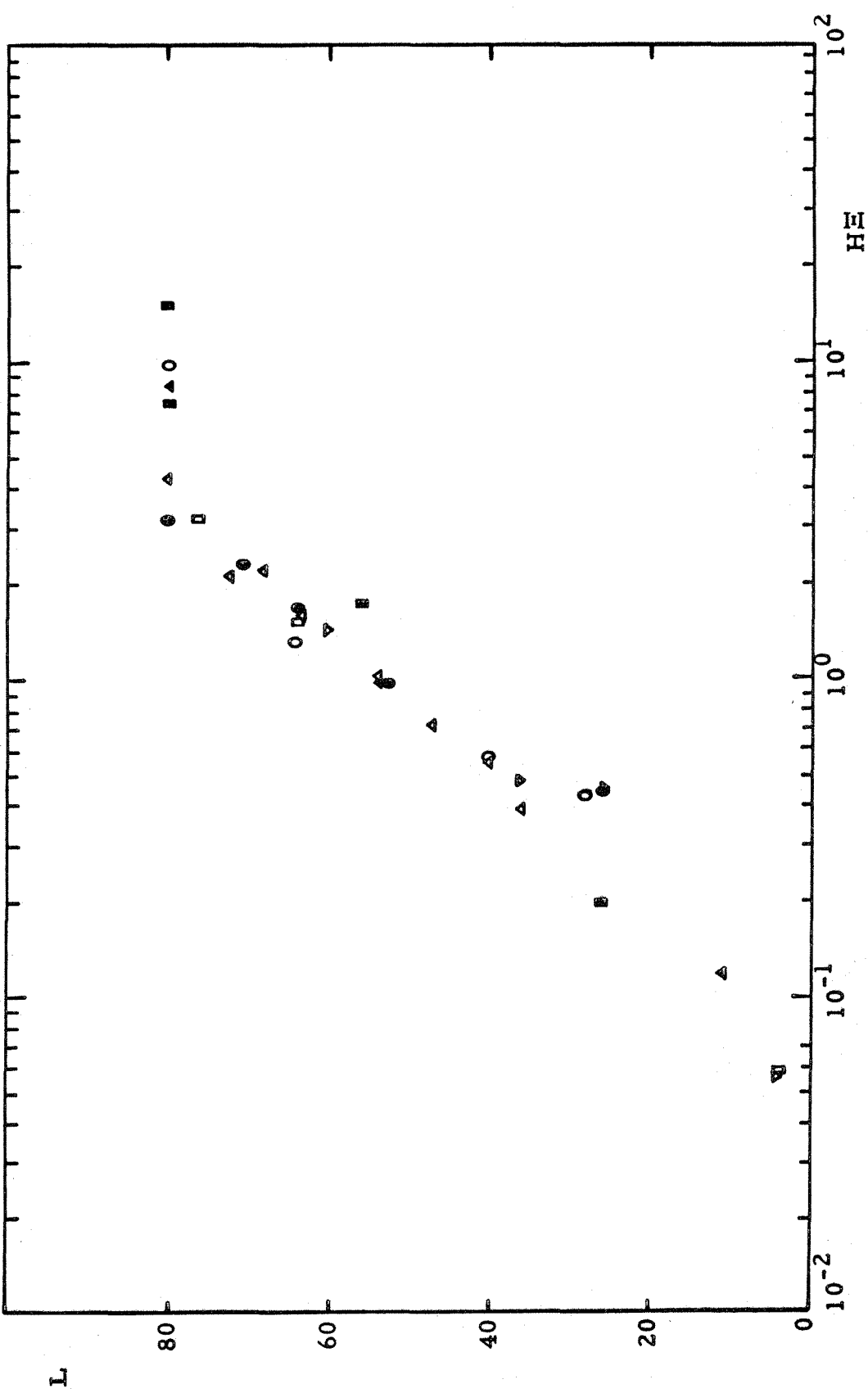
Relationship Between L and H for Shin's PIB in Cyclohexane Data

Figure 10



Relationship Between L and H for all of Shin's Data

Figure 11



Relationship Between L and $H\bar{E}$ for all of Shin's Data

Figure 12

Work done in Union Carbide laboratories (Koleske, 1966) is in general agreement with Elias's findings.

If Ξ is arbitrarily set equal to 1.52 for the Polyox data and 1.00 for the PIB data then the agreement is much better. The result is shown in Figure 12.

V-3 Conclusion

The major problem inherent in explaining the Toms Effect lies in reconciling two facts: first, momentum transport in wall turbulence is drastically reduced by polymer addition and, secondly, this reduction is accomplished without a significant change in either the solvent's density or viscosity.

This paradox may be resolved by realizing that the contribution of the polymer molecules should not be compared with the local energy dissipation, a relatively large quantity, but should be compared with the rate energy is diffusing from the sublayer towards the main flow. This latter quantity is small, but extremely influential. By altering it, the polymer molecules alter the structure of the turbulence and hence the wall stress.

The ratio of the contribution of the polymers to this small diffusion term is called H . One of the objects of this theory is to develop parameters for characterizing the Toms Effect. H and L are these parameters.

For the special case of low strain rate and dilute solution, we have demonstrated that H may be quantitatively estimated and that this estimate requires no arbitrary constants. Thus we are

able to predict the onset of Toms Effect quantitatively. Experimentally it appears to take place consistently where H equals .02.

The very nature of this explanation precludes the possibility of discovery of a Toms Effect in free turbulent flows. If the latter event is, in the future, observed for a single dilute solution, then our explanation for the Toms Effect must be incorrect.

VI. LARGE H

VI-1 Discussion of the Case for H Large Compared With One

In Chapter II we defined a dilute solution as one where

$$[\eta]c < 2.5 \times 10^{-2} \quad (3)$$

In Chapter V we pointed out that low strain rate means essentially that

$$\tau_w < \frac{10RT}{[\eta]M} \quad (162)$$

These two restrictions combine to restrict H as defined by (147) to values of less than 2. Thus when one is talking about large H, one is discussing an experiment which does not meet the restrictions developed in earlier chapters.

The simplest restriction to relax is that of low strain rate. For the full meaning of this and its effect on the Rouse model, the reader is referred to Chapter III. Essentially we now assume that the energy stored by the polymer molecules at high strain rate is

$$W \propto \frac{c[\eta]_\infty^2 \eta_o^2 M}{R T} \alpha_o^2 \quad (163)$$

Here the higher order terms in (163) are neglected. For the present (163) should be looked on as the simplest assumption which might be made, but not necessarily a valid one.

(163) is of the same form as (81). Thus the argument in Chapter IV is unaltered and we conclude that for high strain rate

$$H \propto \frac{cM[\eta]_\infty^2 \tau_w}{R T} \quad (164)$$

The proportionality constant in (164) is unknown since the Rouse theory certainly does not apply. Thus in the high strain case there is an arbitrary constant which must be determined by experiment.

VI-2 A Law of the Wall for a Viscoelastic Boundary Layer

On the basis of experience we assume that the mean flow in a smooth pipe, U , may be characterized by six independent variables, ρ , μ , a , y , τ_w and ℓ . Here a is the radius of the pipe and y is the distance from the wall. We assume that the effects of the molecules may be characterized by a length scale ℓ . Thus, in general,

$$\frac{U}{U_\tau} = \phi \left(\frac{U_\tau a}{\nu}, \frac{y}{a}, \frac{\ell}{a} \right) \quad (165)$$

We suspect that in a viscoelastic sublayer, the radius of the pipe enters in only in the elastic part of the profile determination. Thus tentatively we write for our law of the wall

$$\frac{U}{U_\tau} = H \left(\frac{U_\tau y}{\nu}, \frac{\ell y}{a^2} \right) \quad (166)$$

This is a special case of (165). In principle, there is no reason why (166) should be preferred over other possible choices. In practice, (166) might be tested with experiment if we knew what ℓ is physically.

Assume now that H for large strain-rate is of the form shown in (164) and that the proportionality constant is known. Thus it is meaningful to discuss H large compared to one.

By H large compared to one, we mean that the viscoelastic terms are greatly stabilizing the boundary layer and that it is getting

thicker. For large H we assume that viscosity is of secondary importance in determining the velocity profile throughout the pipe. Thus for large H we assume a law of the wall of the form

$$\frac{U}{U_\tau} = \psi \left(\frac{\ell y}{a} \right) \quad (167)$$

By examining the argument used to derive H in Chapter IV, we conclude that the viscoelastic length scale, ℓ , if it exists, must scale as

$$\ell^2 \propto \frac{c[\eta]_\infty^2 \eta_0^2 M}{\rho_0 R T} \quad (168)$$

for large H in dilute solutions. $[\eta]_\infty$ is the intrinsic viscosity of the solution at infinite strain rate.

VI-3 Velocity Defect Law for Large H

The difference between the maximum velocity U_m at the center of the pipe and the velocity anywhere else in the core is called the "velocity defect". $U_m - U$ will be determined by the turbulent fluctuations in the core which have been assumed independent of μ and ℓ for dilute solutions regardless of H . Thus the velocity defect law must be exactly the same as that for the turbulent pipe flow of the solvent, or

$$\frac{U_m - U}{U_\tau} = \frac{1}{\chi} \ln \left(\frac{a}{y} \right) \quad (169)$$

Here χ is independent of the nature of the wall conditions and is moreover a universal constant of turbulent flow. Experimentally it is found (Schlichting, 1961) that for both rough and smooth pipes

(169) becomes

$$\frac{U_m - U}{U_\tau} = 5.75 \log \left(\frac{a}{y} \right) \quad (170)$$

We shall assume that (170) is valid for the flow of dilute polymer solutions at large Reynolds number through pipes.

VI-4 Resistance Law for Large H

If there exists a region in the pipe where both (170) and (167) apply then in that region:

$$\frac{U_m}{U_\tau} - \psi \left(\frac{\ell y}{a^2} \right) = 5.75 \log \left(\frac{a}{y} \right) \quad (171)$$

Further if one assumes that the flow in the core is independent of direct effects of viscosity, (165) becomes

$$\frac{U}{U_\tau} = \Omega \left(\frac{y}{a} , \frac{\ell}{a} \right) \quad (172)$$

Thus

$$\frac{U_m}{U_\tau} = \Omega \left(1 , \frac{\ell}{a} \right) \quad (173)$$

$$= r \left(\frac{\ell}{a} \right) \quad (174)$$

Thus (171) becomes

$$r \left(\frac{\ell}{a} \right) - \psi \left(\frac{\ell y}{a^2} \right) = 5.75 \log \left(\frac{a}{y} \right) \quad (175)$$

Since ℓ , a and y are independent variables, (175) implies that in that region:

$$\frac{U_m}{U_\tau} = r \left(\frac{\ell}{a} \right) = 5.75 \log \left(\frac{\ell}{a} \right) + C_0 \quad (176)$$

$$\frac{U}{U_\tau} = \psi\left(\frac{ly}{2}\right) = 5.75 \log\left(\frac{ly}{2}\right) + C_0 \quad (177)$$

Here, C_0 is an arbitrary constant.

The velocity defect law, (169), may be integrated over the pipe's cross-sectional area to obtain

$$V = U_m - 3.75 U_\tau \quad (178)$$

V is the mean velocity of flow in the pipe. This equation will be fairly good provided the boundary layer remains fairly thin. Substituting (176) into (178):

$$\frac{V}{U_\tau} = 5.75 \log\left(\frac{l}{a}\right) + C_0 - 3.75 \quad (179)$$

The constant derived by integrating the profile now gets stuck in the arbitrary constant C_0 so that the final result becomes

$$\frac{V}{U_\tau} = 5.75 \log\left(\frac{l}{a}\right) + C \quad (180)$$

The definition of the friction factor, f , varies from author to author. We prefer:

$$f = \left(\frac{p_1 - p_2}{L}\right) \left(\frac{D}{\frac{1}{2} \rho V^2}\right) \quad (181)$$

Here $(p_1 - p_2)$ is the pressure difference between two static pressure taps a distance L apart on a pipe, D is the diameter of the pipe, ρ is the density of the solution and V is the mean flow velocity in the pipe. An equivalent definition is

$$f = 8 \left(\frac{U_\tau^2}{V}\right) \quad (182)$$

Thus our resistance law becomes

$$\frac{1}{\sqrt{f}} = 2.0 \log\left(\frac{2L}{D}\right) + \text{constant} \quad (183)$$

or more simply

$$\frac{1}{\sqrt{f}} = \log\left(\frac{\ell^2}{D^2}\right) + \text{constant} \quad (184)$$

Recalling that from (168)

$$\ell^2 \propto \left(\frac{c}{\rho_0}\right) \left(\frac{[\eta]_\infty^2 \eta_0^2 M}{R T}\right) \quad (168)$$

suggests that:

$$\frac{1}{\sqrt{f}} = \log\left(\frac{c}{\rho_0}\right) + \log\left(\frac{[\eta]_\infty^2 \eta_0^2 M}{D^2 R T}\right) + \text{constant} \quad (185)$$

This is a result which may be directly checked with experiment. The experiment would involve the use of a capillary tube because large wall stresses are required.

It would be desirable to use a single polymer sample initially. In this case, for a variety of dilute solutions:

$$\frac{1}{\sqrt{f}} = \log\left(\frac{c}{\rho_0}\right) + \text{constant} \quad (186)$$

This result is independent of Reynolds number, provided (168) is valid.

Many experimenters in the literature report their data in terms of "friction pressure drop", or $(p_1 - p_2)$ for a given L , versus

V. It is interesting to see what the effects of a viscoelastic boundary layer would look like in this coordinate system. A glance at (181) shows that in general

$$V = \left(\frac{1}{\sqrt{f}}\right) \left(\frac{2D}{\rho L}\right)^{\frac{1}{2}} (p_1 - p_2)^{\frac{1}{2}} \quad (187)$$

Thus for a given sample put through a given capillary tube, using (186),

$$V = k_1 \left(\log \left(\frac{c}{\rho_0}\right) + k_2\right) (p_1 - p_2)^{\frac{1}{2}} \quad (188)$$

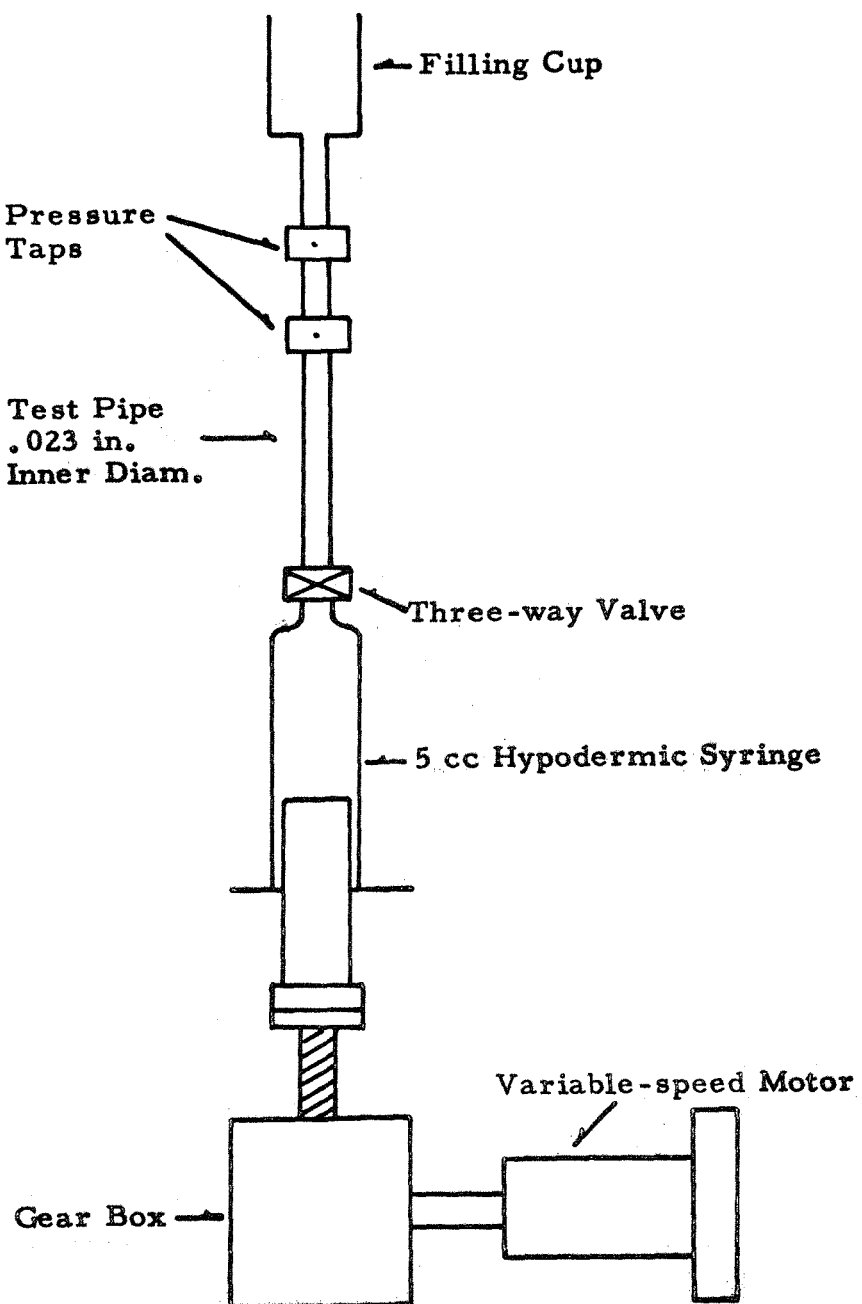
here k_1 and k_2 are held constant in the experiment. In general,

$$k_1 = \left(\frac{2D}{\rho L}\right)^{\frac{1}{2}} \quad (189)$$

VI-5 Comparison of Theory with Existing Data

White (1966) has performed experiments with some dilute Polyox WSR301 solutions in the test apparatus schematically shown in Figure 13.

Essentially this is a miniature pipeflow facility powered by a small D.C. motor whose speed can be continuously varied over a ten-to-one ratio. The motor in turn acts through a gear box and linear actuator to drive the plunger of a 5 cc hypodermic syringe at various preselected speeds. Fluid velocities from 6 ft/sec to 60 ft/sec can be obtained in the six-inch long test section. This corresponds to a water Reynolds number range of 1200 to 12,000 for the 0.023 of an inch inside diameter stainless-steel hypodermic tubing used in White's experiments. The two pressure taps are 3



White's Apparatus

Figure 13

inches apart and are connected to two separate strain gage pressure transducers whose outputs are recorded on an oscillograph. The exact fluid velocities are calculated from the time required for the plunger to move a measured distance near the end of its stroke. The filling cup at the top of the apparatus also acts as the receiving vessel when a test is in progress.

For White's experiment,

$$k_1 = (.114 \text{ psi}^{-1})^{\frac{1}{2}} \text{ ft/sec} \quad (190)$$

We arbitrarily set:

$$k_2 = 12.60 \quad (191)$$

If c is measured in ppmw, V in ft/sec and $p_2 - p_1$ in psi, we predict that for WSR301 in White's apparatus at 24°C ,

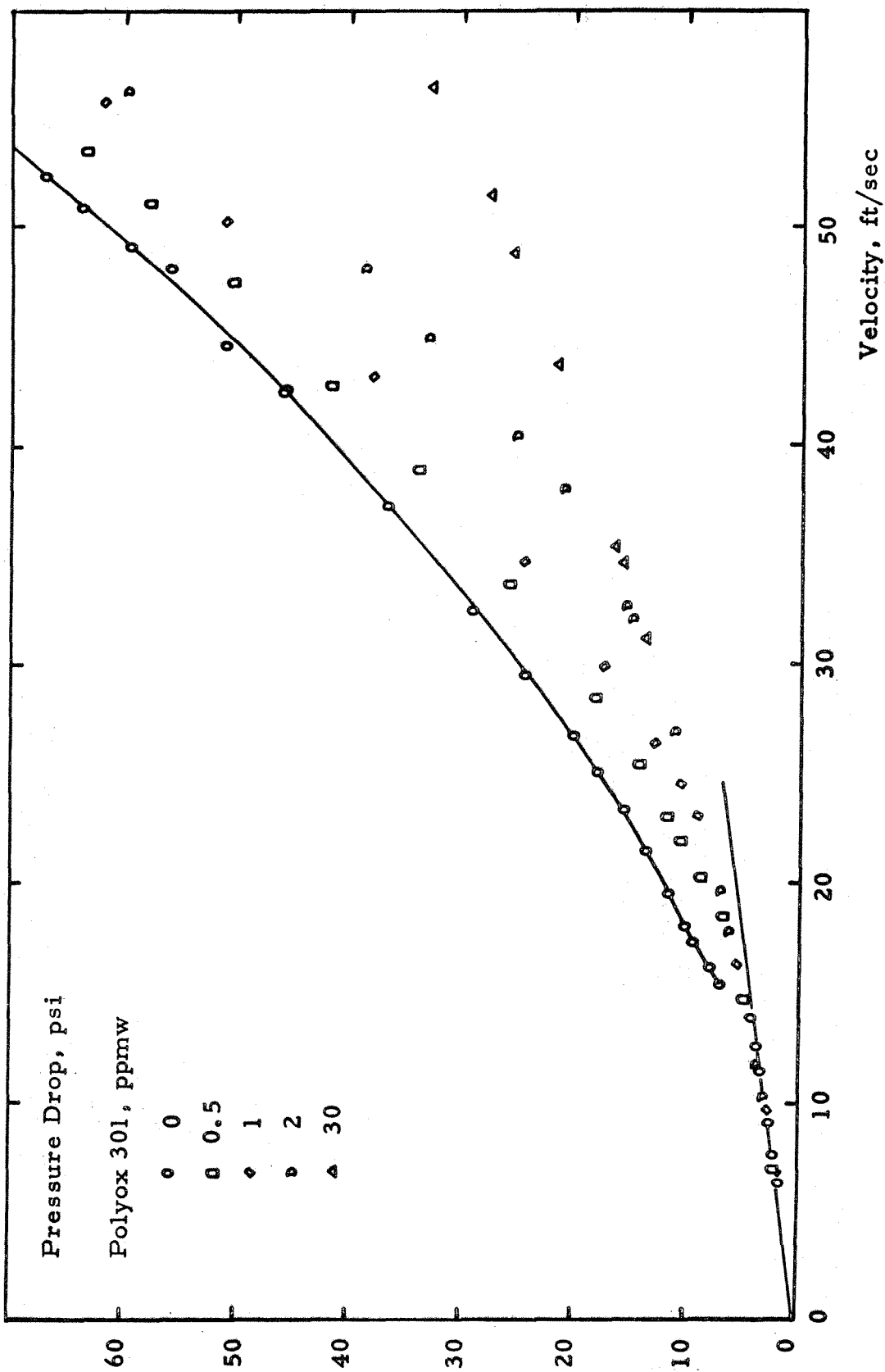
$$V = (\log c + 6.60) (.114 \Delta p)^{\frac{1}{2}} \quad (192)$$

From (192), the predicted values of V for $c = .5, 1, 2, 5, 10, 30$ ppmw for pressure drops ranging from 10 to 100 psi may be calculated. These values are shown in Table 2. Figure 14 shows White's actual data for $c = .5, 1, 2$, and 30 ppmw WSR301 solutions. Figure 15 compares the theoretically predicted dependence of V on c and Δp with White's data.

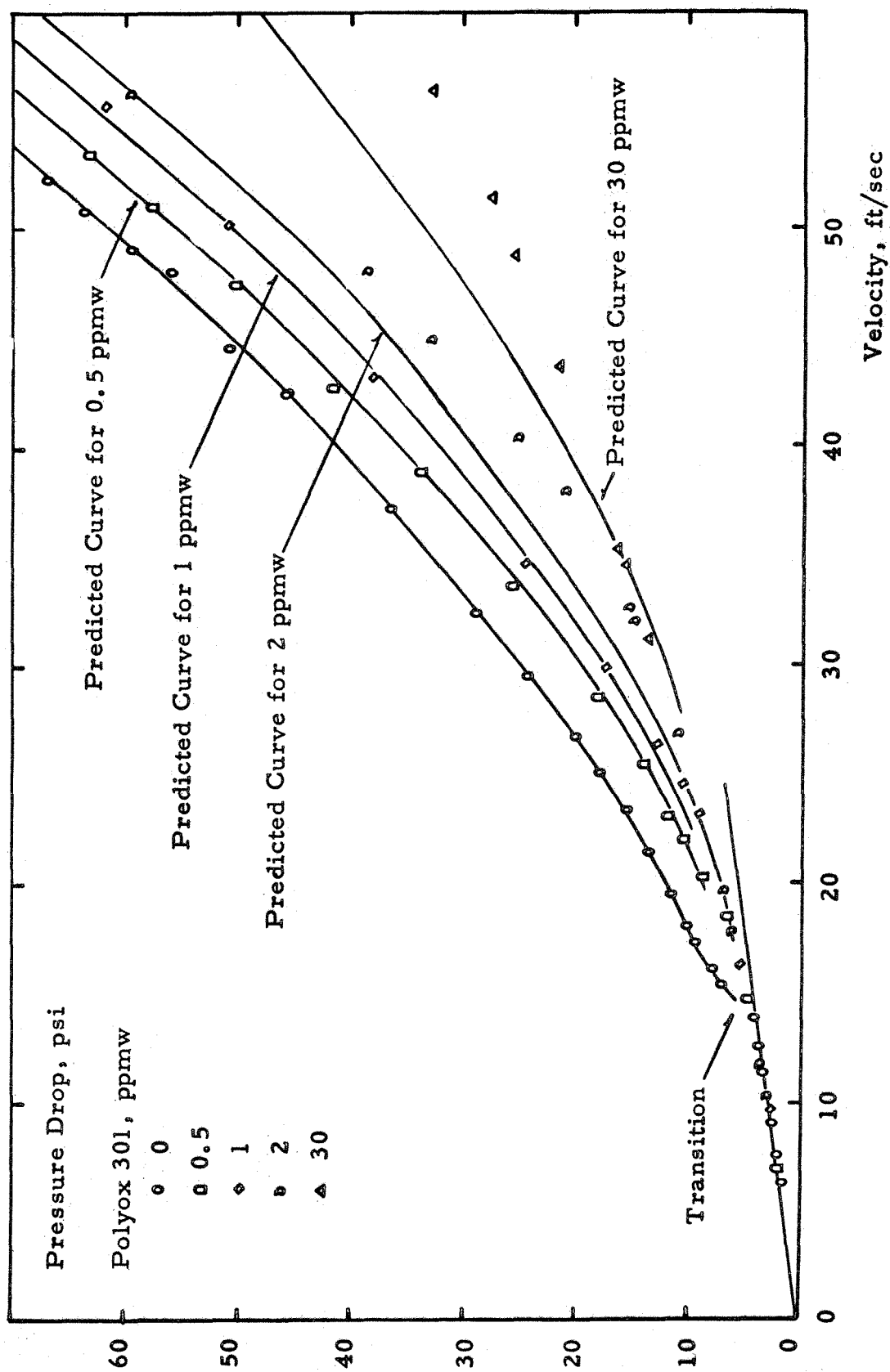
The agreement for the lower concentrations is excellent. As the solution starts to get concentrated, presumably the integrated velocity defect law begins to get altered by a serious thickening of the boundary layer.

TABLE 2
Calculated Values of the Velocity in ft/sec For White's Experiment
Pressure Drop in psi Between the Two Pressure Taps

Concentration in ppmw	10	20	30	40	50	60	70	80	90	100
.5	21.3	30.1	36.8	42.5	47.6	52.0	56.4	60.2	63.9	67.3
1	22.3	31.5	38.6	44.5	49.8	54.4	58.9	63.0	66.9	70.5
2	23.4	32.9	40.4	46.6	52.1	56.9	61.6	65.9	70.0	73.6
5	24.6	34.8	42.7	49.3	55.2	60.2	65.2	69.6	74.0	77.0
10	25.6	36.3	44.4	51.3	57.3	62.6	67.8	72.5	77.0	81.0
30	27.3	38.6	47.3	54.5	61.0	66.6	72.2	77.1	82.0	86.3
0	18.0	26.8	33.4	39.3	44.8	43.3	54.5	58.4	62.5	66.2



White's Data
Figure 14



Predicted Toms Effect for Large H Compared With White's Data

Figure 15

This agreement suggests that the Toms Effect will disappear at high strain rate. This has been observed but has previously been attributed solely to mechanical degradation of the molecules.

VII. THE TOMS EFFECT USING POLYELECTROLYTES

VII-1 An Experiment

It is well known (Katchalsky et al., 1951) that aqueous solutions of polymethacrylic acid, PMAA, possess the remarkable property that in the presence of dilute acid

$$[\eta] \propto M^{0.5} \quad (193)$$

while in a basic solution this dependence changes dramatically to

$$[\eta] \propto M^{2.0} \quad (194)$$

Physically in basic solutions sites on the molecular chain become ionized and repel one another. Thus the coil expands and turns into a rigid rod. In more real terms, changing the pH from 4 to 8 increases the intrinsic viscosity of an aqueous solution of 400,000 molecular weight PMAA 220 times.

A glance at (81) shows that this may have a dramatic effect on H and hence the Toms Effect. Further, since the pH can be changed reversibly, one should be able to switch on and off the Toms Effect by merely alternately adding acid and base to a dilute solution.

A sample of polymethacrylic acid, PMAA, was kindly donated by Dr. W. Peticolas of IBM. This sample was fractionated by the method described by Arnold and Overbeck (1950). The first two fractions were saved. The molecular weights of these fractions were determined as $4.8 \pm .5 \times 10^5$ and $4.0 \pm .5 \times 10^5$ using the viscosity-molecular weight relation of Katchalsky and Eisenberg

(1951).

Aqueous solutions of these fractions were mixed and forced through a stainless steel capillary tube, .046" in inner diameter. This pipe flow apparatus is essentially a larger version of that shown in Figure 12. The actual apparatus used is described in detail by Hoyt (1965). The pressure drops between two points on the pipe were measured. The velocity was held constant.

At 21.1°C, this device forces pure water through this tube at 12.65 meters/sec. This implies that for this device the Reynolds number for the flow of water is 15,100. Further,

$$\tau_o = 5.59 \times 10^3 \text{ dynes/cm}^2 \quad (195)$$

$$\tau_f = .85 \times 10^3 \text{ dynes/cm}^2 \quad (196)$$

for this case. From these numbers, L may be calculated for each of the solutions. Table 3 presents the data for the .40 million molecular weight material for pH less than 6 and for pH greater than 7. The solutions were made basic by adding a drop or two of conc NaOH.

From Table 3 it is clear that the Toms Effect may be produced by merely changing the pH of a dilute polyelectrolyte solution.

The viscosity of the basic solutions depends on strain rate. This is not surprising. However, for reasons which are not well understood (see Nature, Vol 176, Dec. 10, 1955, p. 1119) concentrated basic solutions of PMAA possess the interesting property that their viscosity appears to increase with strain rate.

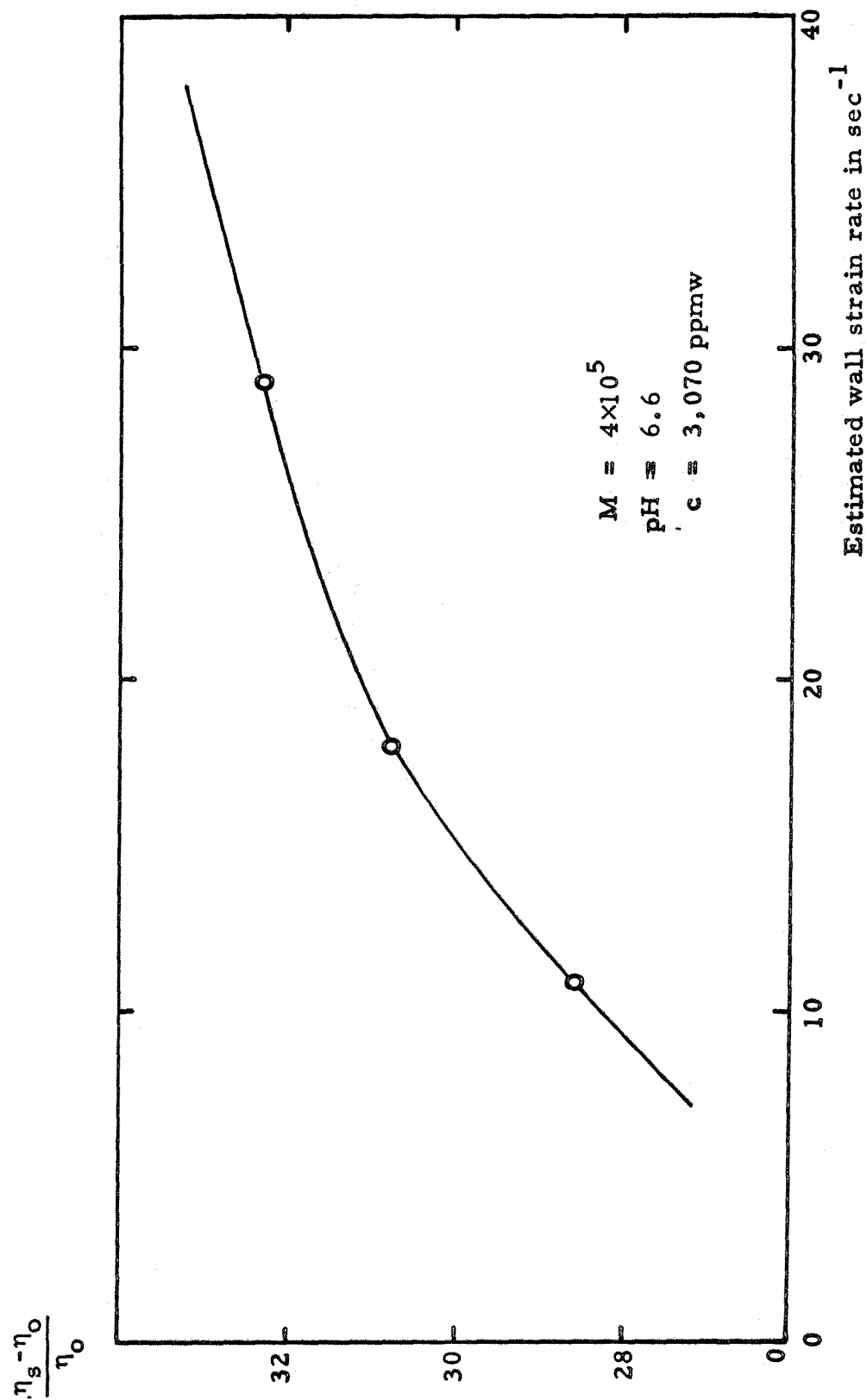
For example, the 3,070 ppmw solution with a pH of 6.6 was placed in a series of Ubbelohde viscometers. The strain rate at the wall (assuming a Newtonian fluid) can be estimated from the time it takes the sample to flow through the viscometer. It was found that $(\eta_s - \eta_o)/\eta_o$ decreased with decreasing strain rate for this particular solution. The exact results are shown in Figure 16.

This behavior is interesting because this same solution produces in turbulent flow an L of 65.0. Those who believe that "shear thinning" produces the Toms Effect might well study these concentrated solutions of PMAA.

For the 4.8×10^5 molecular weight material, similar results were found. These are tabulated in Table 4.

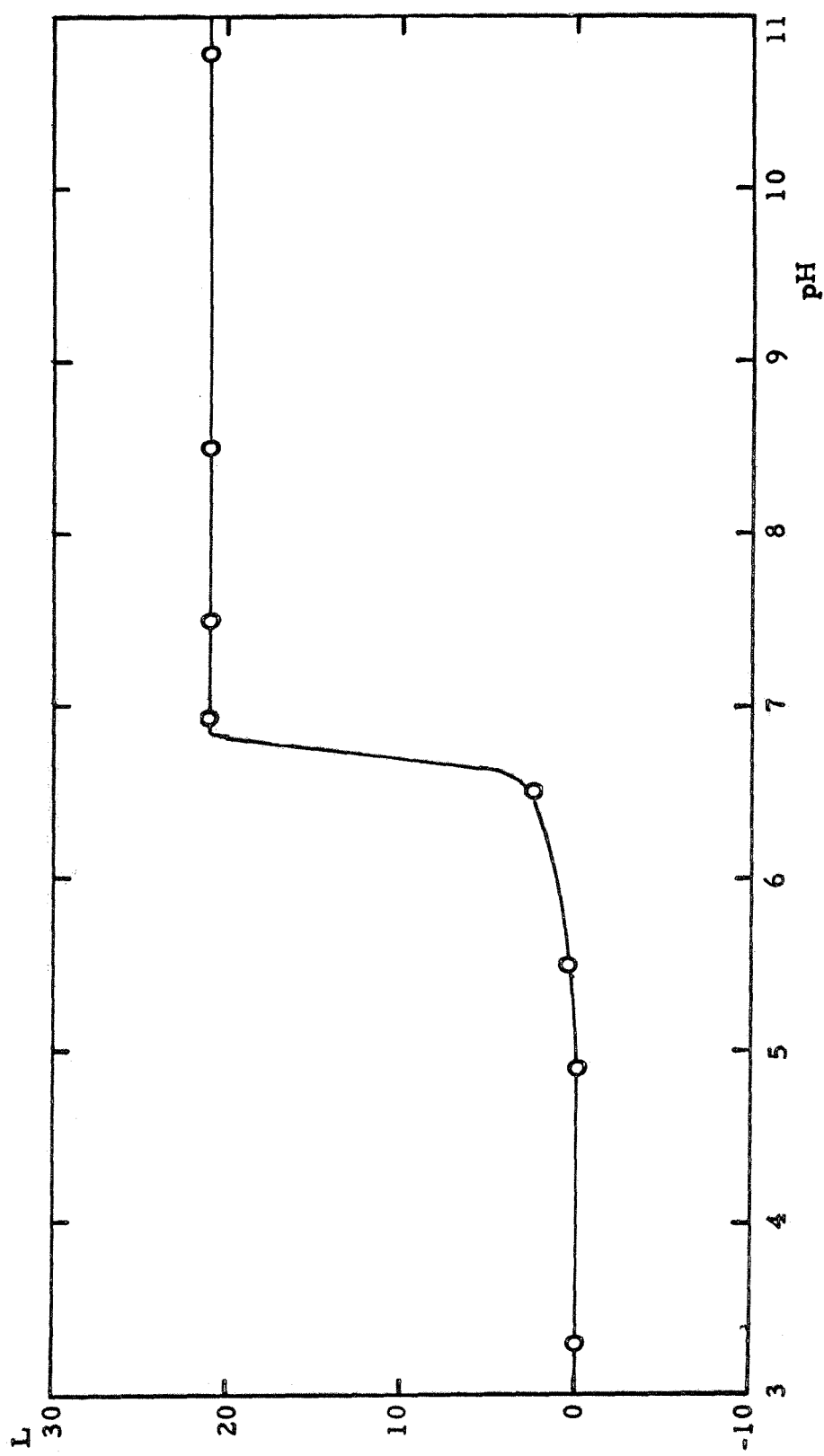
A more graphic demonstration of the effect of pH on solution may be seen in Figure 17. Here an unfractionated sample of PMAA is mixed with water to produce a large volume of 100 ppmw solution. The pH of this solution is 4.85. The pH of this solution was altered by adding small amounts of concentrated acid or base. These solutions were forced through Hoyt's turbulent flow rheometer and pH plotted versus L.

As expected the Toms Effect can be produced or removed at will merely by altering the pH of the solution.



Behavior of Concentrated Solution of PMAA

Figure 16



Effect of pH on the Toms Effect Using a Polyelectrolyte

Figure 17

TABLE 3
Data for Turbulent Pipe Flow of Dilute
Aqueous Solutions of 4.0×10^5 Molecular Weight PMAA

Concentration of Solution (ppmw)	L for pH < 6	L for pH > 7
12.1	0.0	1.9
12.3	0.0	1.3
36.3	0.0	7.0
36.9	0.0	5.1
60.6	0.0	10.8
61.4	0.0	10.2
121	0.0	17.0
123	0.0	17.0
242	0.0	26.3
246	0.0	27.8
378	0.0	32.2
384	0.0	34.6
758	0.0	42.4
766	0.0	46.8
3,034	0.0	59.4
3,070	0.0	65.0

TABLE 4
Data for The Turbulent Pipe Flow of Dilute
Aqueous Solutions of 4.8×10^5 Molecular Weight PMAA

Concentration of Solution (ppmw)	L for pH < 6	L for pH > 7
12.9	0.0	3.8
38.7	0.0	8.9
64.5	0.0	12.7
129	0.0	21.6
258	0.0	33.0
404	0.0	42.5
809	0.0	51.4

VIII. APPENDICES

A - The Rouse Matrix

The matrix R is well known. Hildebrand (1952) points out that it appears in the problem of determining the small deflections of a tightly stretched string due to a number of concentrated forces applied at equally spaced points along the string.

The eigenvalues of R may be calculated by solving the canonical equation by difference algebra. We denote the determinant of the $(l \times l)$ matrix $[R_{ij} - e_k \delta_{ij}]$ by the symbol D_l . ($1 \leq l \leq N$). Thus, for example, if l equals 3, D_3 equals the determinant of the matrix:

$$\begin{bmatrix} 2-e_k & -1 & 0 \\ -1 & 2-e_k & -1 \\ 0 & -1 & 2-e_k \end{bmatrix} \quad (197)$$

The various D_l are related to one another by the recursion relations:

$$D_l = (2-e_k)D_{l-1} - D_{l-2} \quad (198)$$

We define initial conditions as $D_0 = 1$ and $D_{-1} = 0$ and let

$$e_k = 2-2 \cosh \gamma_k = -4 \sinh^2 \frac{\gamma_k}{2} \quad (199)$$

The solution for the difference equation (198) becomes:

$$D_l = A_k e^{\ell \gamma_k} + B_k e^{-\ell \gamma_k} \quad (k \text{ not summed}) \quad (200)$$

The constants, A_k and B_k , may be determined for a given k by use of the initial conditions. Thus

$$D_\ell = \frac{\sinh(\ell+1)\gamma_k}{\sinh\gamma_k} \quad (201)$$

$1 \leq \ell \leq N$

D_N should be equated to zero in order to determine the eigenvalues of the $(N \times N)$ Rouse matrix.

Thus to insure that $D_N = 0$,

$$\gamma_k = \frac{\pi k \sqrt{-1}}{(N+1)} \quad (202)$$

Thus

$$e_k = 4 \sin^2 \left(\frac{\pi k}{2(N+1)} \right) \quad (37)$$

The coefficients of the matrix A must satisfy (38), namely,

$$(R_{ij} - e_k \delta_{ij}) A_{jk} = 0 \quad (38)$$

where k is not summed. This is equivalent to the set of recursion relations:

$$(2-e_k)A_{1k} - A_{2k} = 0$$

$$-A_{i-1,k} + (2-e_k)A_{ik} - A_{i+1,k} = 0 \quad (2 \leq i \leq N-1)$$

$$-A_{N-1,k} + (2-e_k)A_{N,k} = 0$$

(k not summed)

The normalized solution of these recursion relations is:

$$A_{jk} = \sqrt{\frac{2}{N+1}} \sin\left(\frac{jk\pi}{N+1}\right) \quad (39)$$

Thus the Rouse matrix possesses the unusual property that its normalized modal matrix A is symmetric.

B - Solution of (42)

Blatz (1966) was the first to note that (42) may be reduced to a first order partial differential equation by a 3N-iterated use of the two-sided Laplace transform. These transforms are defined as follows:

$$\Psi = \int_{-\infty}^{\infty} \dots \int_{-\infty}^{\infty} \Psi e^{-p_i \delta_i} \prod_{i=1}^N d\delta_i \quad (203)$$

$$\underline{\Psi} = \int_{-\infty}^{\infty} \dots \int_{-\infty}^{\infty} \underline{\Psi} e^{-q_i \epsilon_i} \prod_{i=1}^N d\epsilon_i \quad (204)$$

$$\underline{\underline{\Psi}} = \int_{-\infty}^{\infty} \dots \int_{-\infty}^{\infty} \underline{\underline{\Psi}} e^{-r_i \eta_i} \prod_{i=1}^N d\eta_i \quad (205)$$

These transforms may be readily inverted for the cases under consideration by the use of the identity shown in (206).

$$\exp(a^2 y^2 + by + c) =$$

$$1/2\sqrt{\pi} a \int_{-\infty}^{\infty} \exp \left[- \left(\frac{x}{2a} \right)^2 - \frac{bx}{2a^2} - yx - \left(\frac{b}{2a} \right)^2 + c \right] dx \quad (206)$$

$a \neq 0$

In terms of the 3N transform variables, p_i , q_i and r_i , and time, (42) becomes (207) where (207) is shown on the next page. Here use has been made of the facts that the fluid is incompressible and that the sum of all the eigenvalues of R is $2N$.

$$\begin{aligned}
 0 = & \tau \frac{\partial \Psi}{\partial t} + \sum_{i=1}^N e_i \left[p_i \frac{\partial \Psi}{\partial p_i} + q_i \frac{\partial \Psi}{\partial q_i} + r_i \frac{\partial \Psi}{\partial r_i} \right] \\
 & - \theta_{11} p_i \frac{\partial \Psi}{\partial p_i} - \theta_{12} r_i \frac{\partial \Psi}{\partial q_i} - \theta_{13} p_i \frac{\partial \Psi}{\partial r_i} \\
 & - \theta_{21} q_i \frac{\partial \Psi}{\partial p_i} - \theta_{22} q_i \frac{\partial \Psi}{\partial q_i} - \theta_{23} q_i \frac{\partial \Psi}{\partial r_i} \\
 & - \theta_{31} r_i \frac{\partial \Psi}{\partial p_i} - \theta_{32} r_i \frac{\partial \Psi}{\partial q_i} - \theta_{33} r_i \frac{\partial \Psi}{\partial r_i} \\
 & - \sum_{i=1}^N e_i \left[p_i^2 + q_i^2 + r_i^2 \right] \Psi
 \end{aligned} \tag{207}$$

The equations for the characteristics for (207) are given by the $3N+2$ set:

$$\frac{dt}{\tau} = \frac{dp_i}{(e_i - \theta_{11})p_i - \theta_{21}q_i - \theta_{31}r_i} = \frac{dq_i}{-\theta_{12}p_i + (e_i - \theta_{22})q_i - \theta_{32}r_i}$$

$$= \frac{dr_i}{-\theta_{13}p_i - \theta_{23}q_i + (e_i - \theta_{33})r_i} = \frac{d \ln \psi}{\sum_1^N e_i (p_i^2 + q_i^2 + r_i^2)}$$

(i is not summed) (208)

Here θ_{ij} are the nine dimensionless strain rates associated with this problem. They are in general only functions of time. We shall now consider two possible local flow fields. The first will be the Rouse flow field where:

$$\theta_{12} = \tau \alpha_0 \cos \omega \tau \quad (209)$$

All of the other θ_{ij} are set equal to zero.

The second will be the flow field where:

$$\theta_{11} = \frac{\tau \gamma_n}{2} = \theta_{33}$$

(210)

$$\theta_{22} = -\tau \gamma_n$$

Here γ_n is a constant and all the other θ_{ij} are set equal to zero.

Other flow fields may be chosen. These two were chosen for their simplicity.

For the first flow field, integration of the equation for the characteristics, (208), implies that:

$$p_i = P_i e^{t/2\tau_i}$$

$$q_i = Q_i e^{t/2\tau_i} - p_i \left(\frac{\alpha_0}{\omega}\right) \sin \omega t \quad (211)$$

$$r_i = R_i e^{t/2\tau_i}$$

where τ_i are the retardation times of the molecule as defined by (48). P_i , Q_i and R_i are integration constants along characteristics and are independent of time.

Thus from (208),

$$\frac{d \ln \underline{\Psi}}{dt} = \sum_{i=1}^N \frac{p_i^2 + q_i^2 + r_i^2}{2\tau_i} \quad (212)$$

(211) may be substituted into (212) and the resulting equation integrated with respect to time. The integration constant is evaluated using the result that as α_0 goes to zero, $\underline{\Psi}$ must approach $\underline{\Psi}_0$ where

$$\underline{\Psi}_0 = \exp \left[\frac{p_i^2 + q_i^2 + r_i^2}{2} \right] \quad (213)$$

The result of this integration as a function of p_i , q_i and r_i is:

$$\underline{\Psi} = \prod_{i=1}^N \exp \left[\frac{h_i p_i^2 + 2\epsilon_i p_i q_i + q_i^2 + r_i^2}{2} \right] \quad (214)$$

where

$$h_i = \epsilon_i^2 + \kappa_i^{-2} \quad (i \text{ not summed}) \quad (215)$$

and kappa and iota are defined in (46) and (47) respectively. (215) may be readily inverted by repeated use of (206). When this is done it is found that:

$$\psi = (2\pi)^{-3N/2} \prod_{i=1}^N \kappa_i \exp -\frac{1}{2} \left[\kappa_i^2 (\delta_i - \iota_i \epsilon_i)^2 + \epsilon_i^2 + \eta_i^2 \right] \quad (45)$$

For the second flow field, integration of the equations for the characteristics produces:

$$\begin{aligned} p_i &= P_i e^{(e_i - \theta_{11})t/\tau} \\ q_i &= Q_i e^{(e_i - \theta_{22})t/\tau} \quad (i \text{ not summed}) \\ r_i &= R_i e^{(e_i - \theta_{33})t/\tau} \end{aligned} \quad (216)$$

Thus from (208),

$$\tau \frac{d}{dt} \ln \underline{\psi} = \sum_{i=1}^N e_i (p_i^2 + q_i^2 + r_i^2) \quad (217)$$

Then we substitute (216) into (217), integrate with respect to the parameter t , evaluate the constant using (213), and then express the resulting $\underline{\psi}$ in terms of p_i , q_i and r_i . The result is that:

$$\underline{\psi} = \prod_{i=1}^N \exp \frac{1}{2} \left[\left(\frac{e_i}{e_i - \theta_{11}} \right) p_i^2 + \left(\frac{e_i}{e_i - \theta_{22}} \right) q_i^2 + \left(\frac{e_i}{e_i - \theta_{33}} \right) r_i^2 \right] \quad (218)$$

(218) may be inverted using (206). This produces using (206) and (72):

$$\begin{aligned} \psi &= (2\pi)^{-3N/2} \prod_{i=1}^N (1+2\theta_i)^{1/2} (1-\theta_i) \times \\ &\quad \exp -\frac{1}{2} [(1-\theta_i) \delta_i^2 + (1+2\theta_i) \epsilon_i^2 + (1-\theta_i) \eta_i^2] \end{aligned} \quad (71)$$

C - Evaluation of P_m

$$P_m = nkT\alpha_o \cos\omega t \prod_{j=1}^N \int_{-\infty}^{\infty} \int_{-\infty}^{\infty} \int_{-\infty}^{\infty} \psi \epsilon_i \frac{\partial}{\partial \delta_i} \ln \left(\frac{\psi}{\psi_o} \right) d\delta_j d\epsilon_j d\eta_j \quad (54)$$

In order to evaluate P_m it is useful to note that:

$$\int_{-\infty}^{\infty} x e^{-\frac{1}{2}x^2} dx = 0 \quad (219)$$

and

$$\int_{-\infty}^{\infty} x^2 e^{-\frac{1}{2}x^2} dx = \int_{-\infty}^{\infty} e^{-\frac{1}{2}x^2} dx = (2\pi)^{\frac{1}{2}} \quad (220)$$

Examination of (45) suggests that if we define a new coordinate system $(\delta'_j, \epsilon_j, \eta_j)$ such that

$$\delta'_j = (\delta_j - \epsilon_j \kappa_j) \kappa_j \quad (j \text{ not summed}) \quad (221)$$

then

$$\psi d\delta_j d\epsilon_j d\eta_j = \left[(2\pi)^{-3N/2} \prod_{i=1}^N \exp -\frac{1}{2}(\delta'_i)^2 + \epsilon_i^2 + \eta_i^2 \right] d\delta'_j d\epsilon_j d\eta_j \quad (j \text{ not summed}) \quad (222)$$

Further (45) implies that

$$\frac{\partial}{\partial \delta_i} \ln \frac{\psi}{\psi_o} = -\frac{1}{2} \frac{\partial}{\partial \delta_i} (\delta'_i)^2 - \delta_i^2 \quad (i \text{ not summed}) \quad (223)$$

which from (221) implies:

$$\epsilon_i \frac{\partial}{\partial \delta_i} \ln \frac{\psi}{\psi_o} = \sum_{i=1}^N \left[\epsilon_i^2 + \left(\frac{1}{\kappa_i} - \kappa_i \right) \epsilon_i \delta'_i \right] \quad (224)$$

According to (54) this sum is to be averaged over the configuration space. Consider just the i^{th} term of this sum. With the aid of (219), (220) and (45) its average is just v_i .

Thus

$$P_m = nkT \alpha_0 \cos \omega t \sum_{i=1}^N v_i \quad (225)$$

Using (47), (225) becomes:

$$P_m = \alpha_0^2 nkT \sum_{i=1}^N \frac{\tau_i (\cos^2 \omega t + \omega \tau_i \sin \omega t \cos \omega t)}{1 + \omega_i^2 \tau_i^2} \quad (55)$$

D - Evaluation of $\Delta \bar{F}$

The average energy storage per molecule arising from the entropy reduction produced by the flow of dilute solutions is in general:

$$\Delta \bar{F} = -kT \int_V \psi \ln \psi dV \quad (65)$$

where V is the configuration volume. In the $(\delta_j^!, \epsilon_j, \eta_j)$ space defined by (221):

$$dV = \prod_{j=1}^N d\delta_j^! d\epsilon_j d\eta_j = \prod_{j=1}^N \kappa_j^{-1} d\delta_j^! d\epsilon_j d\eta_j \quad (226)$$

For Rouse's flow field the distribution function ψ is:

$$\psi = (2\pi)^{-3N/2} \prod_{i=1}^N \kappa_i^{-1} \exp -1/2 (\delta_i^!{}^2 + \epsilon_i^2 + \eta_i^2) \quad (45)$$

Thus,

$$\ln \psi = -3N/2 \ln 2\pi + \sum_{i=1}^N \ln \kappa_i - 1/2 \sum_{i=1}^N (\delta_i^!{}^2 + \epsilon_i^2 + \eta_i^2)$$

Thus,

$$\bar{F}/kT = 1/2 (1 + 3N \ln 2\pi) + 1/2 \sum_{i=1}^N \ln \kappa_i^{-2} \quad (227)$$

(46) implies that when the solution is stagnant ($\alpha_o = 0$), κ_i^{-2} equals one. Thus the change in the mean Helmholtz free energy due to the deformation of the solution is $\Delta \bar{F}$, where:

$$\Delta \bar{F} = \bar{F} - \bar{F} \Big|_{\alpha_o=0} \quad (66)$$

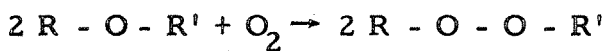
$$\Delta \bar{F} = kT/2 \sum_{i=1}^N \ln \kappa_i^{-2} \quad (67)$$

κ_i^{-2} is defined in (46).

E - Autoxidation and Biological Degradation

If a Polyox sample is neither aged nor subjected to excessive heat or light, it will remain stable. However, as soon as water is added, chemical degradation begins to take place. Schematically the reaction is as follows (McGary, 1960):

One of the oxygen-carbon bonds in the polymer chain is attacked by atmospheric oxygen present in the water. Thus:



Then this oxygen-oxygen bond is severed by catalytic decomposition due to certain metal ions, such as ferrous, copper and silver ions. Thus a cuprous ion is oxidized:



Then the resulting cupric ion is reduced:



The net result is to leave the polymer chain severed.

McGary (1960) observed that the quality of water used in the preparation of the polymer solution has a pronounced effect on the stability of the viscosity of the solution. For example, tap water, which contains chlorine and metallic salts, gives solutions having lower initial viscosities and poorer long-term stability. Distilled water stored in glass containers gives the most stable solutions.

Shin (1965) has observed that solutions may be stabilized by adding .38% formaldehyde. He suggested that the degradation was

due to "bacterial attack on the polymers". The formaldehyde, he claimed, killed the bacteria and hence prevented them from eating the Polyox. This conclusion is surprising in view of his evidence that the solution underwent a rapid followed by a relatively slow rate of degradation. For example, Shin found that "solutions of Polyox Coagulant normally had an intrinsic viscosity of between 20 and 28 dl/g immediately after preparation, the exact value depending upon the time of stirring". Within a week the intrinsic viscosity dropped to 18 dl/g. "Once it reached 18, the rate of degradation thereafter became relatively slow. For instance, in one case it took three months for the intrinsic viscosity to fall from 18 to 11.4 dl/g."

In our view, this evidence does not support the hypothesis of biological degradation. Presumably the bacteria continue to multiply until all their food is gone or the solution becomes toxic. In the former case the degradation rate should increase with time and the intrinsic viscosity should go quite rapidly to zero. In the latter case, the intrinsic viscosity should go to a constant value and remain there for long periods of time, much as the properties of "toxic" .38% aqueous formaldehyde solution remain constant for five weeks at a time. Neither of these predictions are supported by experiment.

Formaldehyde is one of the most reactive organic chemicals. Under alkaline conditions, silver, gold, cuprous, cupric and ferrous ions are all reduced to metals by formaldehyde. (Walker, 1953) Thus it is possible that the addition of formaldehyde reduces the metal ions in the solution to a form in which they are ineffective as

catalysts. Alternatively formaldehyde may be converted to formic acid by the atmospheric oxygen and thus actively compete for oxygen with the polyethylene oxide.

In either event, it is not clear from the evidence that the action of bacteria is important in the degradation of Polyox solutions.

REFERENCES

1. Black, T. J.: Some Practical Applications of a New Theory of Wall Turbulence. Proc. 1966 Heat Transfer and Fluid Mech. Inst., Stanford University Press, 366-386, June 1966.
2. Blatz, P. J.: Energy Storage in and Dissipation by Linear Polymer Molecules in Rubbery and Molten Phases and in Dilute Solution. Material Science CIT Polymer Science Report 66-5 (April 1966).
3. Boggs, F. W. and Tompson, J.: Flow Properties of Dilute Solutions of Polymers. Final Report for ONR Contract No. Nonr-3120(00), United States Rubber Company Research Center (February 1966).
4. Bueche, F.: The Viscoelastic Properties of Plastics. J. Chem. Phys. 22, 603-609 (1954).
5. Cerf, R.: La Dynamique des Solutions de Macromolecules dans un Champ de Vitesses. Fortschritte der Hochpolymeren-Forschung 1, No. 3, Springer-Verlag (1959).
6. Dodge, D. W. and Metzner, A. B.: Turbulent Flow of Non-Newtonian Systems. J. Am. Inst. Chem. Engrs. 5, 189-203 (1959).
7. Einstein, A.: New Determination of Molecular Dimensions. Ann. d. Physik, 19.2, 289-306 (1906).
8. Elias, H. G., Angew. Chem. 73, 209 (1961).
9. Eliassaf, J., Silberberg, A., and Katchalsky, A.: Negative Thixotropy of Aqueous Solutions of Polymethacrylic Acid. Nature, 176, p. 1119 (December 1955).

10. Ellis, A. T.: Private Communication. (1966).
11. Fabula, A. G.: The Toms Phenomenon in the Turbulent Flow of Very Dilute Polymer Solutions. Fourth International Congress on Rheology, Brown U., Providence, R. I., (26-30 August, 1963).
12. Fabula, A. G.: An Experimental Study of Grid Turbulence in Dilute High-Polymer Solutions. Report to the U. S. Bureau of Naval Weapons, Hydropropulsion Section, under Contract Nonr (G)-00043-65 (June 1966).
13. Flory, P. J., J. Am. Chem. Soc., 62, 1561 (1940).
14. Gadd, G. E.: Turbulence Damping and Drag Reduction Produced by Certain Additives in Water. Nature, 206, pp. 463-467 (May 1965).
15. Gadd, G. E.: Reduction of Turbulent Friction by Dissolved Additives. Nature, 212, 874-877 (1966).
16. Hildebrand, F. B., Methods of Applied Mathematics, Prentice Hall, New York (1952).
17. Hoyt, J. W. and Fabula, A. G.: The Effect of Additives on Fluid Flow. Fifth Symposium on Naval Hydrodynamics, Bergen, Norway (September 1964).
18. Hoyt, J. W.: A Turbulent Flow Rheometer. Symposium on Rheology, ASME, New York (1965).
19. Jackley, D. N.: Drag-Reducing Fluids in a Free Turbulent Jet. NavWep Report 9053, USNOTS, China Lake, California (April 1966).

20. Katchalsky, A. and Eisenberg, H.: Molecular Weight of Polyacrylic and Polymethacrylic Acid. *J. Polymer Sci.*, 6, pp. 145-153 (1951).
21. Koleske, J. V., Union Carbide Corp., Chemicals Division, South Charleston, West Virginia (December 1966). Private Communication.
22. Looney, W. R. and Blick, E. F.: Surface-Friction Coefficients of Compliant Surfaces in Turbulent Flow. *Jour. of Spacecraft and Rockets*, 3, pp. 1562-1564 (October 1966).
23. McGary, C. W., Jr.: Degradation of Polyethylene Oxide. *J. Polymer Sci.*, 46, 51-57 (1960).
24. Merrill, E. W. Private Communication to Shin (1965).
25. Merrill, E. W., Mickley, H. S., Ram, A. and Stockmayer, W.H. Upper Newtonian Regime in Polymer Solutions. *Trans. of the Soc. of Rheology*, 6, pp. 119-129 (1962).
26. Metzner, A. B. and Park, M. G.: Turbulent Flow Characteristics of Viscoelastic Fluids. *J. Fluid Mech.*, 20, Part 2, pp. 291-303 (October 1964).
27. Metzner, A. B. and Reed, J. C., A. I. Ch. E. Journal, 1, 4, 434 (1955).
28. Oldroyd, J. G.: A Suggested Method of Detecting Wall Effects in Turbulent Flow Through Pipes. *Proc. Int'l. Congress Rheology*, N. Holland Pub. Co., Amsterdam, Vol. II, pp. 131-134 (1948).
29. Pao, Y.: Theories for the Flow of Dilute Solutions of Polymers and of Nondiluted Liquid Polymers. *Jour. Polymer Sci.*, 61,

pp. 414-448 (1962).

30. Peterlin, A. and Copic, M., J. Appl. Phys., 27, 434 (1956).
31. Pruitt, G. T. and Crawford, H. R.: Effect of Molecular Weight and Segmental Constitution on the Drag Reduction of Water Soluble Polymers. Final Report Contract No. 4306(00), David Taylor Model Basin, Washington, D. C. (April 1965).
32. Ripken, J. F. and Pilch, M.: Studies of the Reduction of Pipe Friction with the Non-Newtonian Additive CMC. St. Anthony Falls Hydraulic Laboratory Technical Paper 42, Series B (April 1963).
33. Rouse, P. E., Jr.: A Theory of the Linear Viscoelastic Properties of Dilute Solutions of Coiling Polymers. J. Chem. Phys. 21, 1272-1280 (1953).
34. Rouse, P. E., Jr. and Sittel, K.: Viscoelastic Properties of Dilute Polymer Solutions. Jour. of Appl. Phys., 24, pp. 690-696 (June 1953).
35. Savins, J. G.: Drag Reduction Characteristics of Solutions of Macromolecules in Turbulent Pipe Flow. Symposium on Non-Newtonian Fluid Mechanics, 56th Annual Meeting, A. I. Ch. E., Houston, Texas (1963).
36. Schlichting, Hermann, Boundary Layer Theory, McGraw-Hill (1960).
37. Sharman, L. J., Sones, R. H., and Cragg, L. H.: Effects of Rate of Shear on Inherent and Intrinsic Viscosities of Polystyrene Fractions. Jour. of Appl. Physics, 24, pp. 703-711 (June 1953).

38. Shaver, R. G. and Merrill, E. W.: Turbulent Flow of Pseudo-plastic Polymer Solutions in Straight Cylindrical Tubes. Am. Inst. Chem. Engr. J., 5, pp. 181-204 (June 1959).
39. Shin, H.: Reduction of Drag in Turbulence by Dilute Polymer Solutions. Sc. D. Thesis, M. I. T. (1965).
40. Spriggs, T. W., Huppler, J. D., and Bird, R. B.: An Experimental Appraisal of Viscoelastic Models. Trans. of the Society of Rheology, 10, pp. 191-213 (1966).
41. Staudinger, H. and Heuer, W., Ber., 63, 222 (1930).
42. Takemura, T., J. Polymer Sci., 27, 549 (1958).
43. Toms, B. A.: Some Observations on the Flow of Linear Polymer Solutions Through Straight Tubes at Large Reynolds Numbers. Proc. 1st Int. Congress Rheol., Holland II, 135-141 (1948).
44. Townsend, A. A., The Structure of Turbulent Shear Flow. Cambridge U. Press (1956).
45. Treloar, L. R. G., The Physics of Rubber Elasticity. Clarendon (1958).
46. Tulin, M. P.: Hydrodynamic Aspects of Macromolecular Solutions. 6th Naval Hydrodynamics Symposium, Washington, D. C. (1966).
47. Walker, J. F., Formaldehyde, Reinhold (1953).
48. White, William D., USNOTS, Pasadena, California (1966).
Private Communication.

49. Wiederhorn, N. M. and Brown, A. R.: Viscosity-Molecular Weight Relation for Polymethacrylic Acid in Methanol. J. Polymer Sci., 8, pp. 651-656 (1951).

50. Zimm, B. H.: Dynamics of Polymer Molecules in Dilute Solution: Viscoelasticity, Flow Birefringence and Dielectric Loss. J. Chem. Phys., 24, 269-278 (1956).